NASA Technical Memorandum 78438

(NASA-TM-78438) LOW-SPEED AERODYNAMIC CHARACTERISTICS OF A 0.08-SCALE YF-17 AIRPLANE MODEL AT HIGH ANGLES OF ATTACK AND SIDESLIP (NASA) 118 p HC A06/MF A01 CSCL 01A G3/02
N78-22025
Unclas 15663

Low-Speed Aerodynamic Characteristics of a 0.08-Scale YF-17 Airplane Model at High Angles of Attack and Sideslip

Daniel N. Petroff, Stanley H. Scher, and Carl E. Sutton

April 1978

NASA
National Aeronautics and Space Administration

NASA Technical Memorandum 78438

Low-Speed Aerodynamic Characteristics of a 0.08-Scale YF-17 Airplane Model at High Angles of Attack and Sideslip

Daniel N. Petroff
Stanley H. Scher
and
Carl E. Sutton, Ames Research Center, Moffett Field, California

NASA
National Aeronautics and
Space Administration

Ames Research Center
Moffett Field, California 94035

TABLE OF CONTENTS

LOW-SPEED AERODYNAMIC CHARACTERISTICS OF A 0.08-SCALE YF-17 AIRPLANE MODEL AT HIGH ANGLES OF ATTACK AND SIDESLIP

Daniel N. Petroff, Stanley H. Scher, and Carl E. Sutton*

Ames Research Center

SUMMARY

A 0.08-scale model of the YF-17 airplane was tested in the Ames 12-Foot Pressure Wind Tunnel at a Mach number of 0.2 and Reynolds numbers of 0.2 to 2.3 million based on a fuselage forebody depth of 0.128 m (0.42 ft). Angles of attack ranged from 0° to 90°, and the angle of sideslip ranged from −10° to 30°. Data were obtained with and without the nose boom and with several strake configurations; data were also obtained for various control surface deflections.

Analysis of the results revealed that selected strake configurations adequately provided low Reynolds number simulation of the high Reynolds number characteristics. The addition of the boom in general tended to reduce the Reynolds number effects.

INTRODUCTION

Reynolds number effects caused by the crossflow over the fuselage ahead of an airplane wing's leading edge in a spin can cause appreciably different side forces and yawing moments on a small-scale model from those obtained at the same attitudes on the full-scale configuration (refs. 1 and 2). These effects usually occur in the angle of attack range between 40° and 90°. In the course of conducting investigations in the spin tunnel at Langley Research Center on necessarily small-scale models, the Reynolds number effects for some configurations have been so marked that model spin and recovery characteristics are not representative of the full-scale airplane.

Normally, a wind tunnel Reynolds number investigation is conducted on a given design to determie if spin tunnel results could be significantly altered by Reynolds number effects. When such effects are discovered, various strake configurations are tested on the nose of the model in an attempt to eliminate the differences. Then, the selected strake configuration that most closely duplicates the side-force and yawing moment characteristics of the full-scale airplane is placed on the spin tunnel model.

*Project Engineer, ARO, Inc., Moffett Field, Calif. 94035.

For some designs, the effects of Reynolds number at low angles of attack are also of interest in connection with (1) wind-tunnel model tests at angles of attack up to the aerodynamic stall, (2) spin entry tests conducted with radio-controlled models dropped from a helicopter, and (3) theoretical analysis.

In the investigation reported in this paper, a 0.08-scale YF-17 lightweight fighter airplane model was tested in the Ames 12-Foot Wind Tunnel to determine static longitudinal and lateral directional aerodynamic characteristics over a range of Reynolds number from subcritical to supercritical. The angle of attack ranged from 0° to 90° and the angle of sideslip ranged from -10° to 30°.

Since Reynolds number effects sufficient to affect spin tunnel results were present for the basic configuration, a number of strake configurations were evaluated at model angles of attack from 40° to 90°. Whereas the flight vehicle will be equipped with the nose boom and boom-compatible strake, for the purpose of this investigation, the basic configuration was taken to be without the boom and strake.

Included in this investigation were tests at both high and low Reynolds numbers to determine the separate and combined effects of a nose boom and of a faired boom-compatible pair of strakes. These tests were performed at angles of attack ranging from 0° to 90°. Also, for both high and low Reynolds numbers, lateral and longitudinal control deflection effects were measured at angles of attack from 10° to 60°.

The data are presented with minimum discussion.

NOMENCLATURE

The axis systems and sign conventions are shown in figure 1. Data are presented in the body axis coordinate system. Because the data were computer-plotted, the corresponding plot symbol, where used, is given together with the conventional symbol.

Symbol	Plot symbol	Definition
b	BREF	wing reference span
$\bar{c}$	LREF	wing reference chord
C_A	CA	body axes axial force coefficient
C_D	CD	stability axes drag coefficient
C_L	CL	stability axes lift coefficient

Symbol	Plot symbol	Definition
$C_{\ell,b}$	CBL	body axes rolling-moment coefficient
C_m	CLM	body and stability axes pitching-moment characteristics
C_N	CN	body axes normal force coefficient
C_n	CBN	body axes yawing-moment coefficient
$C_{n,s}$	CLN	stability axes yawing-moment coefficient
C_Y	CY	body and stability axes side-force coefficient
L/D	L/D	lift-to-drag ratio
M_∞	MACH	free-stream Mach number
q	Q(PSF)	dynamic pressure
RN	RN	Reynolds number, based on a fuselage forebody depth of 0.128 m
S	SREF	wing reference area
α	ALPHA	angle of attack, deg
β	BETA	angle of sideslip, deg
δ_a	AIL	aileron, total aileron deflection angle, deg, positive with trailing edge down
i_H	HOR	horizontal tail incidence, deg, positive with trailing edge down

Model Notation

B_4	body
C_1	canopy
D_6	duct
H_1	horizontal
V_2	vertical tail
W_2	wing (3% camber)

Symbol	Plot symbol	Description
a_1		aileron
d_1		dorsal
g_5		gutter
h_4		aileron actuator fairing without P_2 pylon
h_7	LH7	vertical tail tip pod with V_2 vertical
h_{10}		wing tip missile launchers
i_1		nose boom
n_1	N1	leading-edge flap with hinge line at 7.5 and 20% local chord
n_3	N3	leading-edge flap with hinge line at 20% local chord
r_2		rudder with V_2 vertical
$\bar{r}_3$		ramp
s_x		strake with B_4 body (x designates strake geometry)
s_1'		strake
s_2'		strake
s_3'		strake
s_4'		strake
s_5'		strake
s_6'		strake
s_3		S_2 strake terminated at model station 8.80
s_4		S_2 strake terminated at model station 10.05
w_1		AIM-9E missile
X_1		B_4 C_1 D_6 W_2 d_1 g_5 h_4 h_{10} $\bar{r}_3$ w_1
X_2		B_4 C_1 D_6 W_2 d_1 g_5 h_4 h_{10} $\bar{r}_3$
X_3		B_4 C_1 D_6 W_2 d_1 g_5 h_4 h_{10} $\bar{r}_3$ + grit

TEST FACILITY

The Ames 12-Foot Pressure Wind Tunnel is a variable-density, low-turbulence wind tunnel that operates in the Mach number range of 0.1 to 0.94. The wind tunnel is powered by a two-stage, axial flow fan driven by electric motors totaling 12,000 horsepower. Airspeed in the test section is controlled by variation of the fan's rotative speed. Eight fine-mesh screens in the settling chamber, together with a contraction ratio of 25:1, provide an airstream of exceptionally low turbulence.

MODEL DESCRIPTION

The model was a 0.08-scale version of the YF-17 airplane. The geometry of the model is given in table 1, strake configurations in table 2, installation drawings and model drawings in figures 2 and 3, respectively, and installation photographs in figure 4.

The YF-17 airplane is a twin-engine jet fighter aircraft with a wing leading edge sweep back of 26.6°, under-wing inlets, twin canted vertical tails, and an all-movable differential horizontal tail.

All airfoils are NACA 65A, modified with a sharp leading edge. The wing camber is 3% and the thickness is 5% at the root, decreasing linearly to 4% at 65% semispan and the remaining being constant 4% to the tip. The highly swept leading-edge extension has a total exposed area of 4.27 m^2 (46 ft^2). The horizontal tails have symmetrical sections and are 5.5% thick at the root, tapering linearly to 3% at the tip. The twin vertical tails have symmetrical sections, are canted outboard 20°, and are 5% thick at the root, tapering linearly to 3% at the tip.

The model was fitted with variable position leading-edge flaps (LEF) having hinge-lines at both the 7.5 and 20% chord lines. Flap positioning was manually accomplished using brackets. Horizontal tail deflections were also manually accomplished using brackets.

The aft end of the model, between the vertical tails, was distorted to accept the model support sting.

TESTING AND PROCEDURE

The investigation was performed at Mach number 0.20 and over a range of fuselage forebody depth based Reynolds number from 0.2 million to 2.3 million. Data were obtained at angles of attack from 10° to 90° and at angles of sideslip of -10° to 30°. To insure boundary-layer transition to turbulent conditions, for selected configurations a 0.254 cm (0.1 in.) wide strip of grit having a nominal diameter of 0.0140 cm (0.0055 in.) was placed 3.68 cm

(1.45 in.) aft (streamwise) of all leading edges. Grit size was conservatively selected to be one sieve size larger than needed, as indicated in reference 3. The trip effectiveness for these tests was not verified.

Forces and moments were sensed by an internally mounted six-component strain-gage balance. Model cavity pressure was sensed by two transducers connected to tubes on the left- and right-hand side of the sting. No axial force corrections were applied from these measurements. An angle transducer mounted on the support system was used to measure model angles of attack.

For angles of attack to 40°, the LEF were deflected 25° at the 20% chord line. At angles of attack above 40°, the LEF were deflected to 30° at the 7.5% chord line and 15° at the 20% chord line.

The effects of control surface deflections were investigated. The horizontal tails were deflected, both together and differentially, from -15° to 10°. The ailerons were deflected differentially from -30° to 30°.

DATA REDUCTION

The six-component force and moment data were reduced about the model moment reference center in both the body and stability axes systems. The axes systems are defined in figure 4 and the moment reference center was assumed to be at the 30% m.a.c. The base and cavity pressure were measured but were not used as correction factors on axial force or drag. The angle of attack and the angle of sideslip were corrected for sting deflections in the longitudinal and lateral planes. The angle of attack and the appropriate aerodynamic coefficients were corrected for tunnel-wall interference effects (ref. 4). The additive wall correction increments are as follows:

$$\Delta\alpha = 0.15733447\ C_L$$

$$\Delta C_D = 0.0025903\ C_L$$

$$\Delta C_m(\text{tail off}) = -0.00590325\ C_L$$

$$\Delta C_m(\text{tail on}) = -0.00496259\ C_L$$

Tunnel static pressure was measured in the plenum surrounding the test section and no blockage corrections were applied. A prior calibration of the 12-ft wind tunnel at these test conditions with large blockage models showed plenum pressure to be essentially identical to free-stream static pressure. Consequently, this pressure is currently being used as the basis of free-stream pressure for all high altitude tests.

Data repeatability for the test was estimated by reviewing repeat runs and repeat points within a run and is as follows:

$C_L = \pm 0.002$ $C_\ell = \pm 0.0010$

$C_D = \pm 0.0002$ $\alpha = \pm 0.05°$

$C_Y = \pm 0.0006$ $\beta = \pm 0.05°$

$C_m = \pm 0.008$ $M = \pm 0.005$

$C_n = \pm 0.0012$ $RN = \pm 0.0025 \times 10^6$

RESULTS AND DISCUSSION

For the basic configuration, the variation of aerodynamic characteristics with Reynolds number for given angles of attack and angles of sideslip are presented in figure 5. Boom-on and boom-off data at high and low Reynolds number are presented in figures 6 and 7. Boom-compatible strake-configuration data obtained at high and low Reynolds number without the boom installed are presented in figures 8 and 9, and with the boom installed in figures 10 and 11. Data from low Reynolds number tests of eight strake configurations on the basic model are presented in figure 12. The effects of control deflections at high and low Reynolds number are shown in figures 13 and 14. See table 3 for a listing of the data figures.

Analysis of the data indicates that maximum Reynolds number effects occurred on the basic model at an angle of attack of 60° (e.g., see C_n data in fig. 5, pp. 44-47 and in fig. 6, p. 54). Some smaller effects of Reynolds number were also present at angles of attack higher and lower than 60°.

As may be seen in figure 6, pages 52-54, the main effect of adding the boom to the basic configuration was the reduced Reynolds number effect in the yawing-moment coefficient C_n at angles of attack of 40°, 50°, and 60°.

The results of tests of the model with strakes installed indicated that through use of some of the strake configurations, the Reynolds number effects found on the basic model were eliminated or reduced significantly. (For example, see fig. 8, p. 67, and fig. 12, p. 101.)

Other strake configurations tested did not provide the needed corrections.

CONCLUDING REMARKS

A 0.08-scale YF-17 airplane model has been tested at Mach number 0.2 in the Ames 12-Foot Wind Tunnel at high and low Reynolds numbers at angles of attack of 10° to 90° and angles of sideslip of -10° to 30°. Longitudinal and lateral-directional characteristics were investigated with and without horizontal tail and aileron deflections.

Reynolds number effects of significance were found to be present. The Reynolds number effects were eliminated or significantly reduced through the addition of selected forebody strake configurations.

REFERENCES

1. Neilhouse, Anshal I.; Klinar, Walter J.; and Scher, Stanley H.: Status of Spin Research for Recent Airplane Designs. NASA TR R-57, 1960. (Supersedes NACA RML 57F12.)

2. Polhaums, Edward C.: Effect of Flow Incidence and Reynolds Number on Low-Speed Aerodynamic Characteristics of Several Noncircular Cylinders with Applications to Directional Stability and Spinning. NASA TR-29, 1959.

3. Braslow, Albert L.; and Knox, Eugene C.: Simplified Method for Determination of Critical Height of Distributed Roughness Particles for Boundary Layer Transition at Mach Numbers from 0 to 5.0. NACA TN-4363, 1958.

4. Sivells, James; and Salmi, Rachel: Jet-Boundary Corrections for Complete and Semispan Swept Wings in Closed Circular Wind Tunnels. NACA TN-2454, 1951.

TABLE 1.- MODEL GEOMETRY

(a) Model component: wing (W_2)

Total data	Full-scale		Model-scale	
Area				
Planform	325,160 cm^2	50,400 in.^{2}	2081 cm^2	322.6 in.^{2}
Wetted				
Span (equivalent)	1066.8 cm	420 in.	85.344 cm	33.6 in.
Aspect ratio	3.5	3.5	3.5	3.5
Rate of taper				
Taper ratio	0.3483	0.3483	0.3483	0.3483
Dihedral angle, deg	-5	-5	-5	-5
Incidence angle, deg	0	0	0	0
Aerodynamic twist, deg	0	0	0	0
Toe-in angle	---	---	---	---
Cant angle	---	---	---	---
Sweep-back angles, deg				
Leading edge	26.660	26.660	26.660	26.660
Trailing edge	-2.881	-2.881	-2.881	-2.881
0.25 element line	20	20	20	20
Chord				
Root (wing sta. 0.0)	452.12 cm	178.0 in.	36.17 cm	14.240 in.
Tip (equivalent)	157.48 cm	62.0 in.	12.598 cm	4.960 in.
MAC	328.534 cm	129.344 in.	26.281 cm	10.349 in.
Fus. sta. of 0.25 MAC	1152.04 cm	453.56 in.	92.161 cm	36.284 in.
W.P. of 0.25 MAC	10.980 cm	4.323 in.	0.876 cm	0.345 in.
B.L. of 0.25 MAC	222.880 cm	87.748 in.	17.828 cm	7.019 in.
Airfoil section Root Tip	NACA65A modified with sharp leading edge, 3% camber, 5% thick at root tapering linearly to 4% at 65% span, constant 4% to tip			
Exposed data				
Area	212,748 cm^2	32,976 in.^{2}	1361 cm^2	211 in.^{2}
Span (equivalent)	---	---	---	---
Aspect ratio	3.5	3.5	3.5	3.5
Taper ratio	--	--	--	--
Chords				
Root	---	---	---	---
Tip	---	---	---	---
MAC	---	---	---	---
Fus. sta. of 0.25 MAC	---	---	---	---
W.P. of 0.25 MAC	---	---	---	---
B.L. of 0.25 MAC	---	---	---	---
Leading-edge extension (LEX)	42,735 cm^2	6624 in.^{2}	273.5 cm^2	42.39 in.^{2}

TABLE 1.- MODEL GEOMETRY - Continued

(b) Model component: vertical (V_2)

Data per side	Full-scale		Model-scale	
Area				
Planform	48,419 cm^2	7505 in.^{2}	309.4 cm^2	47.95 in.^{2}
Wetted	---	---	---	---
Span (equivalent)	241.30 cm	95.00 in.	19.304 cm	7.600 in.
Aspect ratio	1.2	1.2	1.2	1.2
Rate of taper	---	---	---	---
Taper ratio	0.394	0.394	0.394	0.394
Dihedral angle, deg	---	---	---	---
Incidence angle, deg	0	0	0	0
Aerodynamic twist, deg	0	0	0	0
Toe-in angle L.E. (outboard)	1	1	1	1
Cant angle outboard	20	20	20	20
Sweep-back angles, deg				
Leading edge	41.320	41.320	41.320	41.320
Trailing edge	9.278	9.278	9.278	9.278
0.25 element line	35	35	35	35
Chords				
Root (wing sta. 0.0)	287.02 cm	113.00 in.	22.962 cm	9.04 in.
Tip (equivalent)	114.30 cm	45.00 in.	9.144 cm	3.60 in.
MAC	213.042 cm	83.875 in.	17.043 cm	6.710 in.
Fus. sta. of 0.25 MAC	1477.986 cm	581.8837 in.	118.239 cm	46.5507 in.
W.P. of 0.25 MAC	135.207 cm	53.2312 in.	10.817 cm	4.2585 in.
B.L. of 0.25 MAC	124.952 cm	49.194 in.	9.996 cm	3.9355 in.
Airfoil section Root Tip	NACA65A with modified sharp leading edge, no camber, root thickness of 5%, varying linearly to 3% thickness at the tip			
Exposed data per side				
Area	48,309 cm^2	7488 in.^{2}	308.4 cm^2	47.81 in.^{2}

TABLE 1.- MODEL GEOMETRY - Continued

(c) Model component: body (B_4)

	Full-scale		Model-scale	
Length	1825.307 cm	718.625 in.	146.025 cm	57.49 in.
Max. width	213.995 cm	84.25 in.	17.120 cm	6.74 in.
Max. depth	202.248 cm	79.625 in.	16.180 cm	6.37 in.
Fineness ratio	---	---	---	---
Area				
Max. cross-sectional	29,738 cm^2	4609.375 $in.^2$	190 cm^2	29.50 $in.^2$
Planform	241,249 cm^2	37,393 $in.^2$	1544 cm^2	239.32 $in.^2$
Wetted	---	---	---	---
Base	13,891 cm^2	2153.125 $in.^2$	88.9 cm^2	13.78 $in.^2$
Profile	208,325 cm^2	32,290.56 $in.^2$	1333 cm^2	206.64 $in.^2$

TABLE 1.- MODEL GEOMETRY - Concluded

(d) Model component: horizontal stabilizer (H_1)

Total data	Full-scale		Model-scale	
Area				
Planform	60,096 cm^2	9314.93 in.^{2}	384.62 cm^2	09.62 in.^{2}
Wetted	---	---	---	---
Span (equivalent)	675.1 cm	265.8 in.	54.01 cm	21.26 in.
Aspect ratio	1.5	1.5	1.5	1.5
Rate of taper	---	---	---	---
Taper ratio	0.6	0.6	0.6	0.6
Dihedral angle, deg	-2.0	-2.0	-2.0	-2.0
Incidence angle, deg	0	0	0	0
Aerodynamic twist, deg	0	0	0	0
Toe-in angle	---	---	---	---
Cant angle	---	---	---	---
Sweep-back angles, deg				
Leading edge	40.846	40.846	40.846	40.846
Trailing edge	27.979	27.979	27.979	27.979
0.25 element line	38.000	38.000	38.000	38.000
Chords				
Root (wing sta. 0.0)	234.493 cm	92.32 in.	18.760 cm	7.386 in.
Tip (equivalent)	121.920 cm	48.00 in.	9.754 cm	3.840 in.
MAC	165.946 cm	65.33 in.	14.736 cm	5.802 in.
Fus. sta. of 0.25 MAC	1644.65 cm	647.50 in.	131.572 cm	51.800 in.
Z.P. of 0.25 MAC	-3.715 cm	1.4625 in.	0.297 cm	0.117 in.
B.L. of 0.25 MAC	150.939 cm	59.425 in.	12.075 cm	4.754 in.
Airfoil section	NACA65A modified with sharp leading edge, no camber, 5-1/2% thick at root varying linearly to 3% at the tip			
Exposed data				
Area	39,483.8 cm^2	6120 in.^{2}	252.7 cm^2	39.17 in.^{2}
Span (equivalent)	243.84 cm	96.00 in.	19.507 cm	7.680 in.
Aspect ratio	1.5	1.5	1.5	1.5
Taper ratio	0.6	0.6	0.6	0.6
Chords				
Root	203.2 cm	80.00 in.	16.256 cm	6.400 in.
Tip	121.92 cm	48.00 in.	9.754 cm	3.840 in.
MAC	165.956 cm	65.327 in.	13.276 cm	5.227 in.
Fus. sta. of 0.25 MAC	1687.386 cm	664.325 in.	134.991 cm	53.146 in.
W.P. of 0.25 MAC	-56.198 cm	-22.125 in.	-4.496 cm	-0.177 in.
B.L. of 0.25 MAC	205.677 cm	80.975 in.	16.454 cm	6.478 in.

TABLE 2.- NOSE STRAKE IDENTIFICATION

Strake designation	Strake length, cm	Strake width, cm	Strake thickness, cm	Strake angle, deg	Strake L.E. fuselage station, cm	Strake pivot F.S., cm	Strake pivot vertical location, cm	Port			Starboard		
								1	2	3	1	2	3
S_1	18.999	0.533	10° wedge	-2 fwd	12.598	15.850	-0.610	off	off	off	off	off	off
S_2	18.161			3.58 aft	14.351	14.351	-0.686						
S_3	8.001			3.58									
S_4	11.176												
S_1'	15.24	1.016	0.159	3.80	27.922	26.111	FRP	on	on		on	on	
S_2'								off	off				
S_3'								on	on		off	off	
S_4'					20.32			off	on	on		on	on
S_5'	7.62				27.992					off			off
S_6'					35.524			on	off		on	off	

TABLE 3.- INDEX OF DATA FIGURES

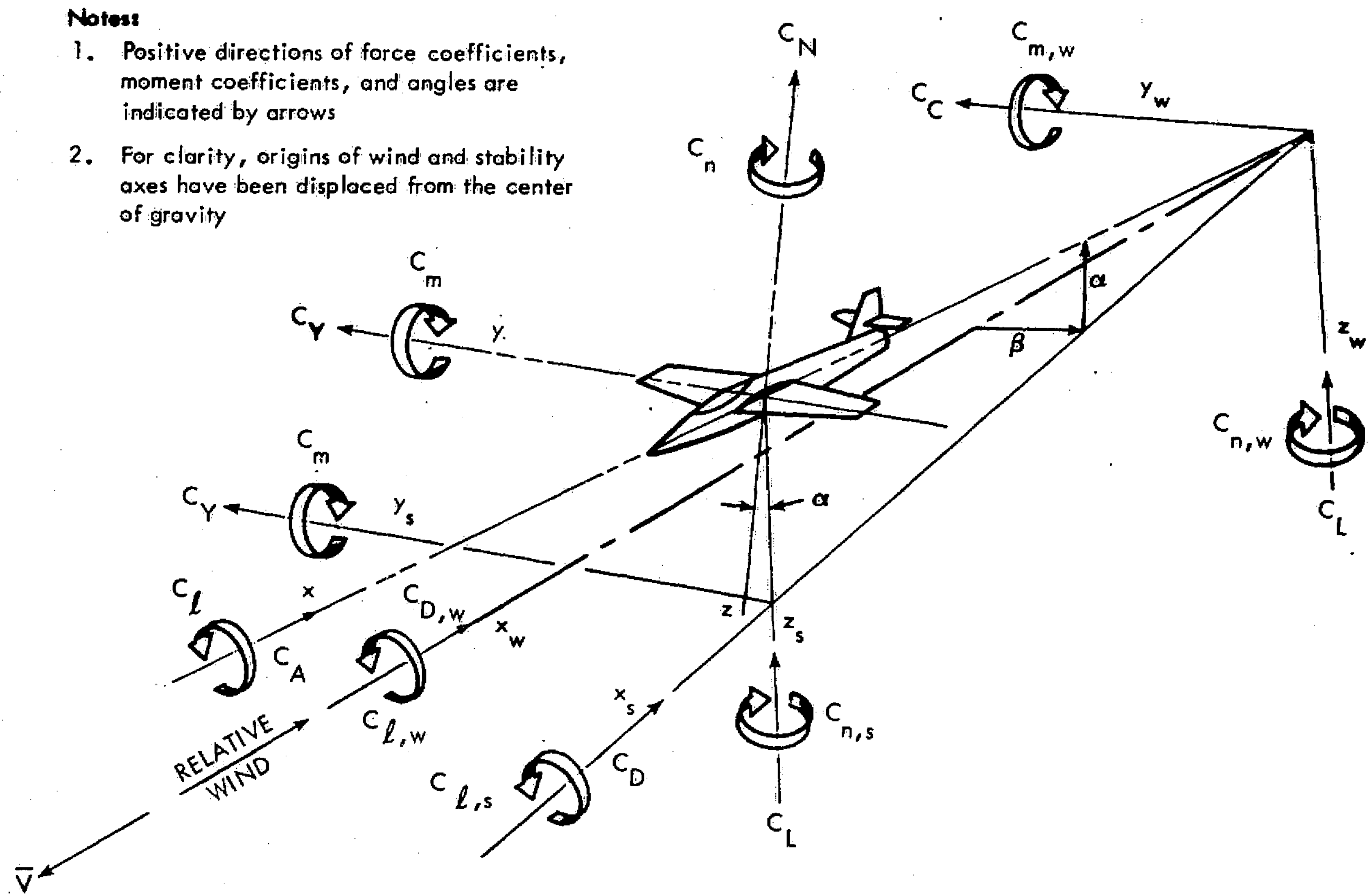

Figure 1.- Orientation of force and moment coefficients about body, wind, and stability axes.

All dimensions are model scale cm(in.)

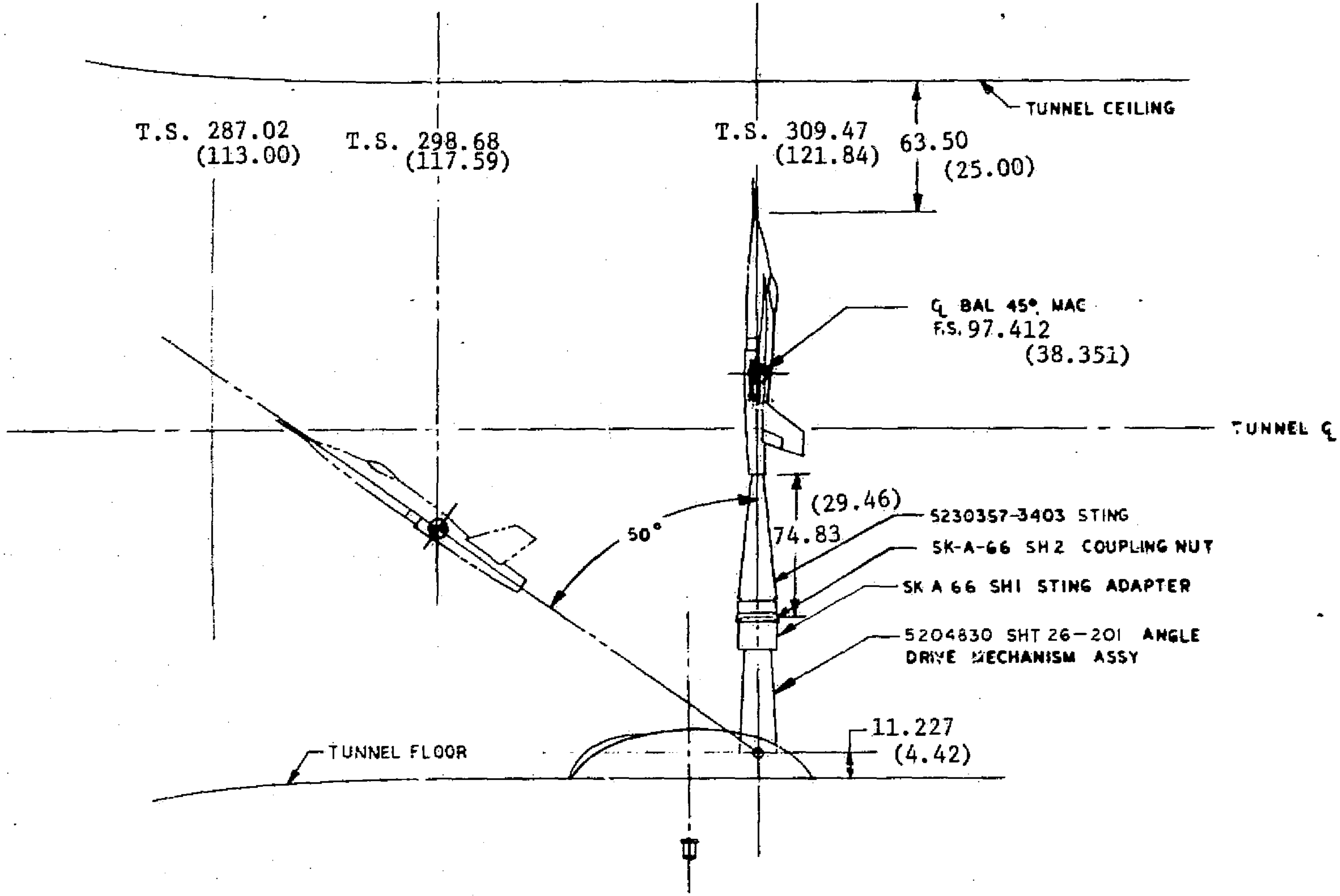

(a) 12-foot 40°-90° cannon support.

Figure 2.- Installation drawings.

All dimensions are model scale cm(in.)

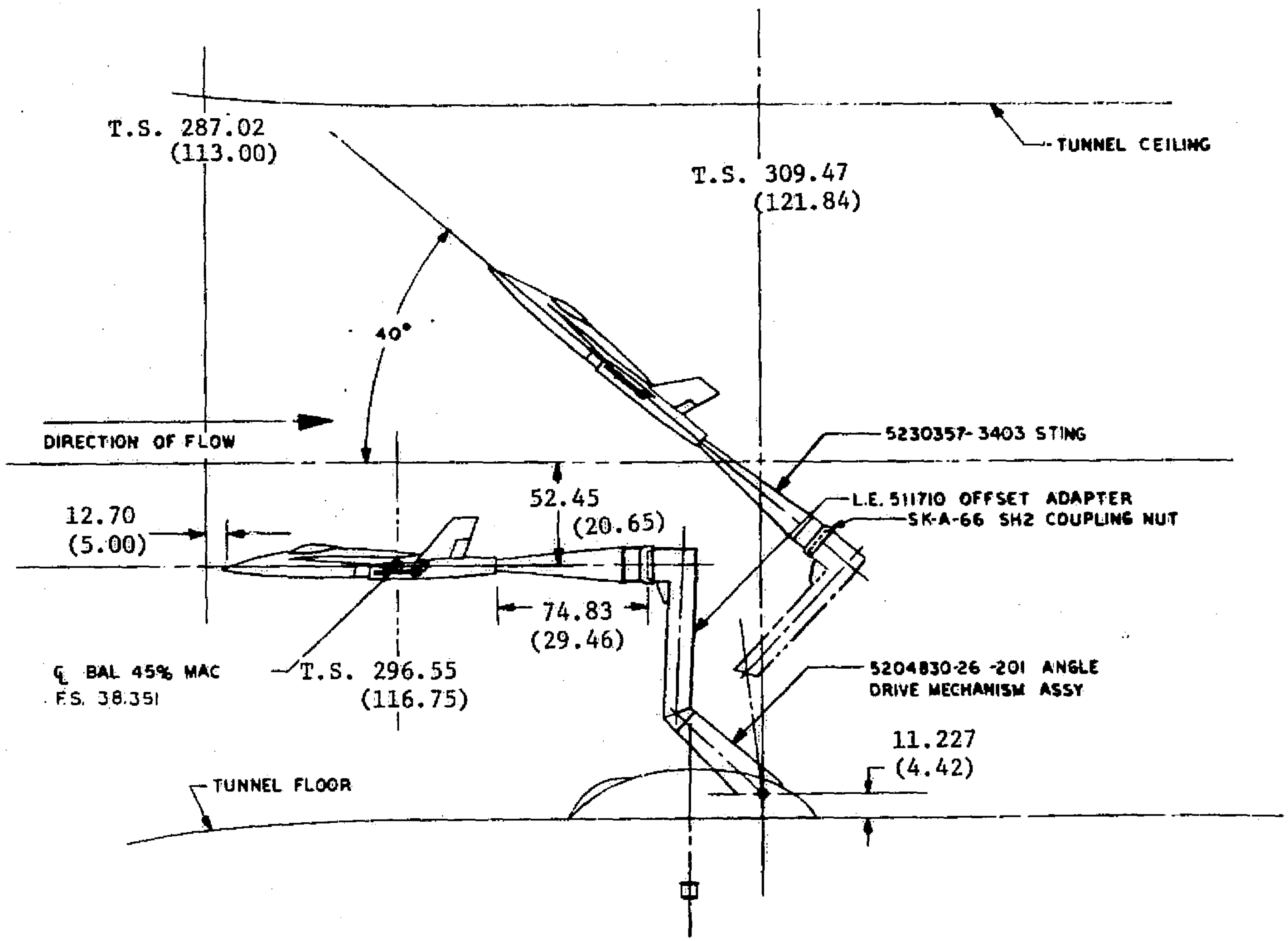

(b) 12-foot 0°-40° cannon support.

Figure 2.- Concluded.

All dimensions are model scale cm(in.)

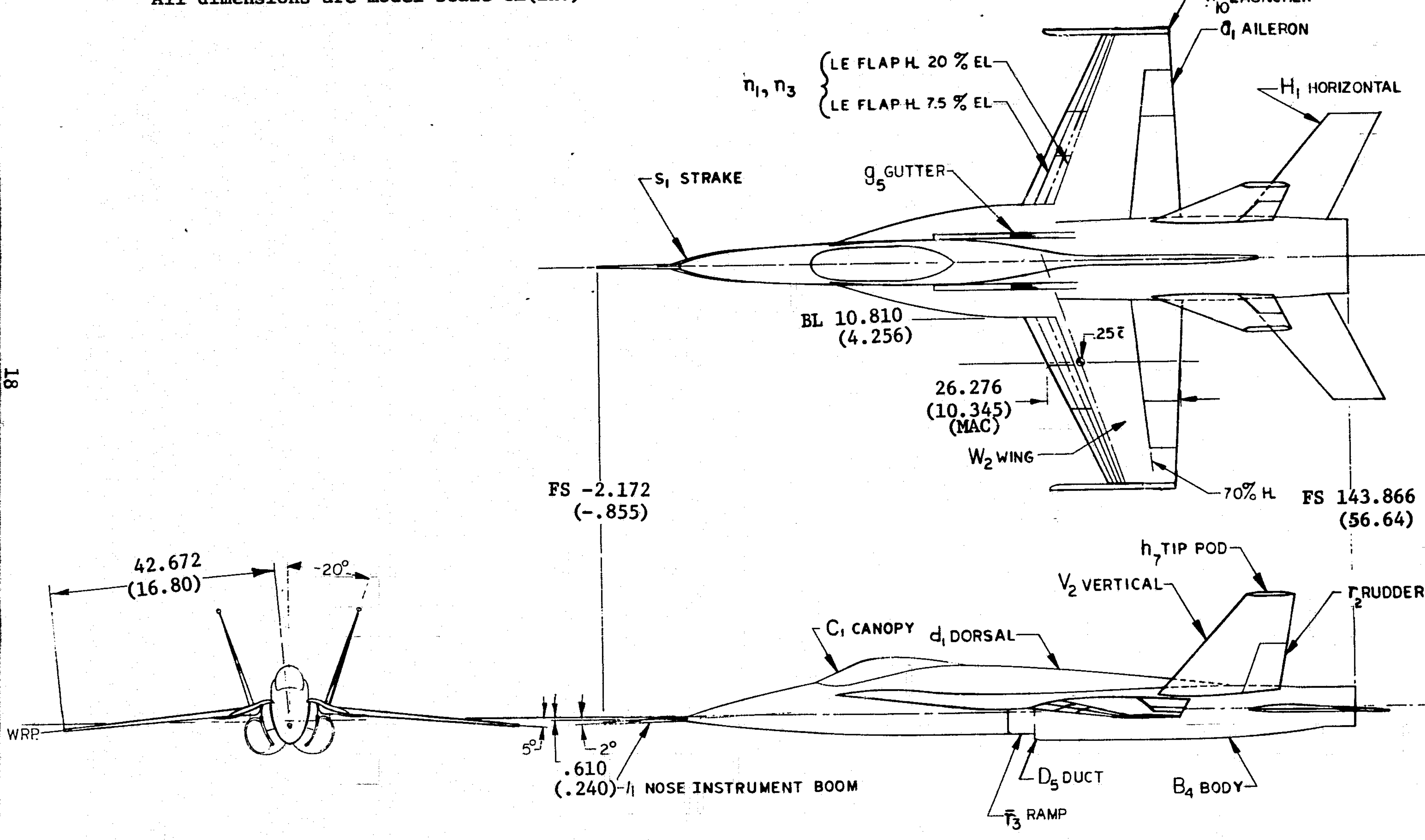

(a) Three view with launchers.

Figure 3.- Model drawings.

All dimensions are model scale cm(in.)

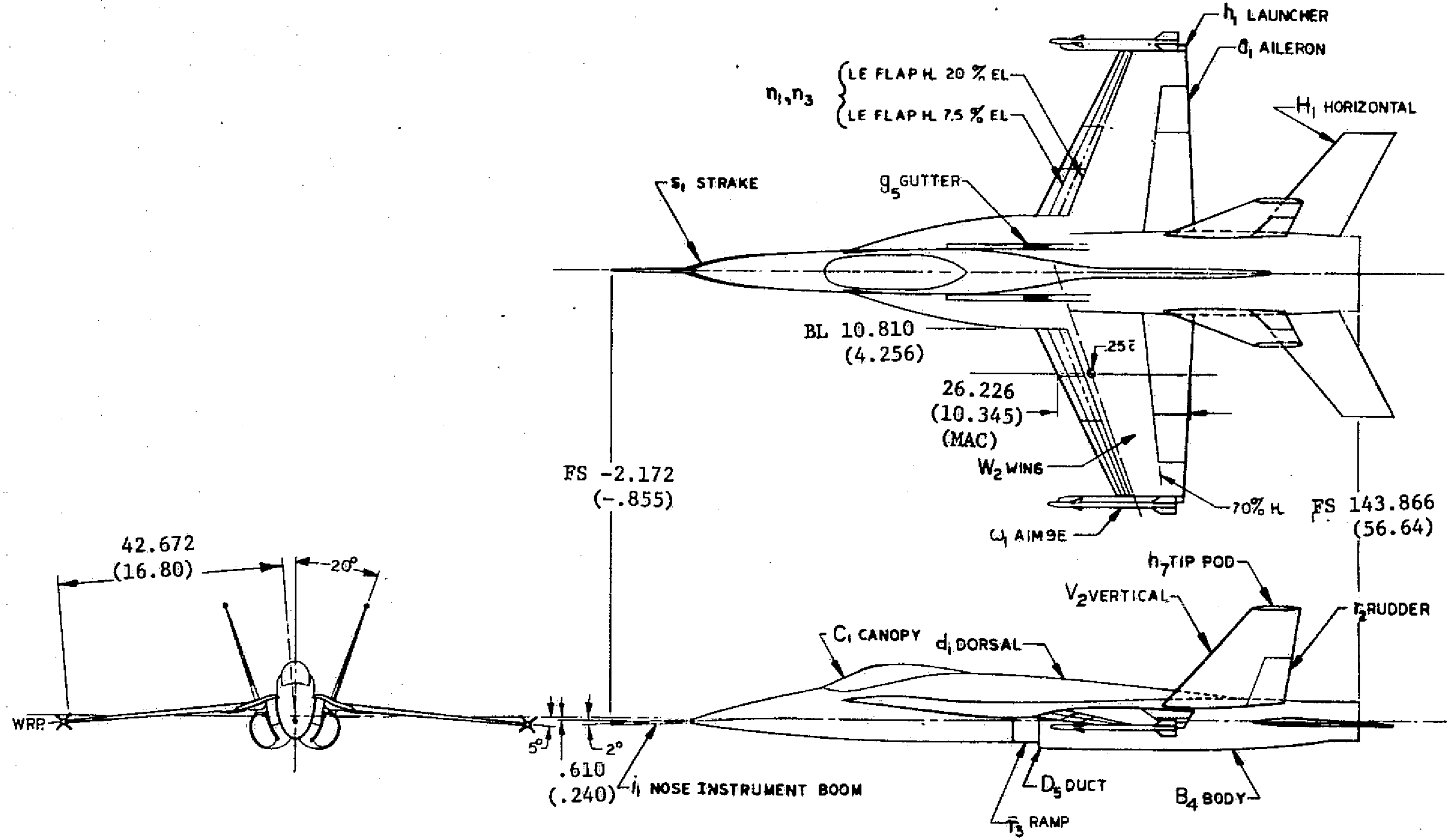

(b) Model 3-view with missiles.

Figure 3.- Continued.

All dimensions are model sclae cm(in.)

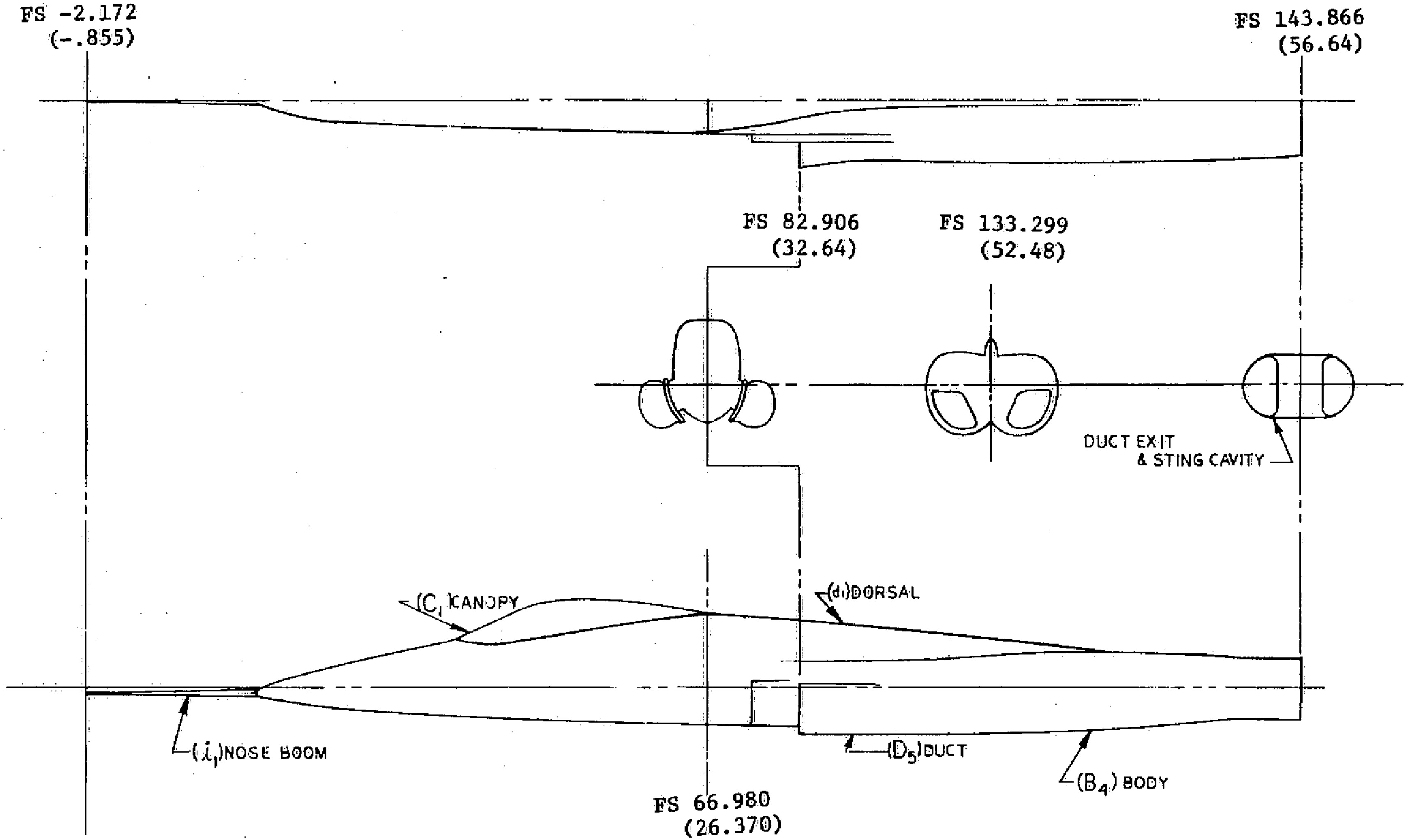

(c) Fuselage.

Figure 3.- Continued.

All dimensions are model scale cm(in.)

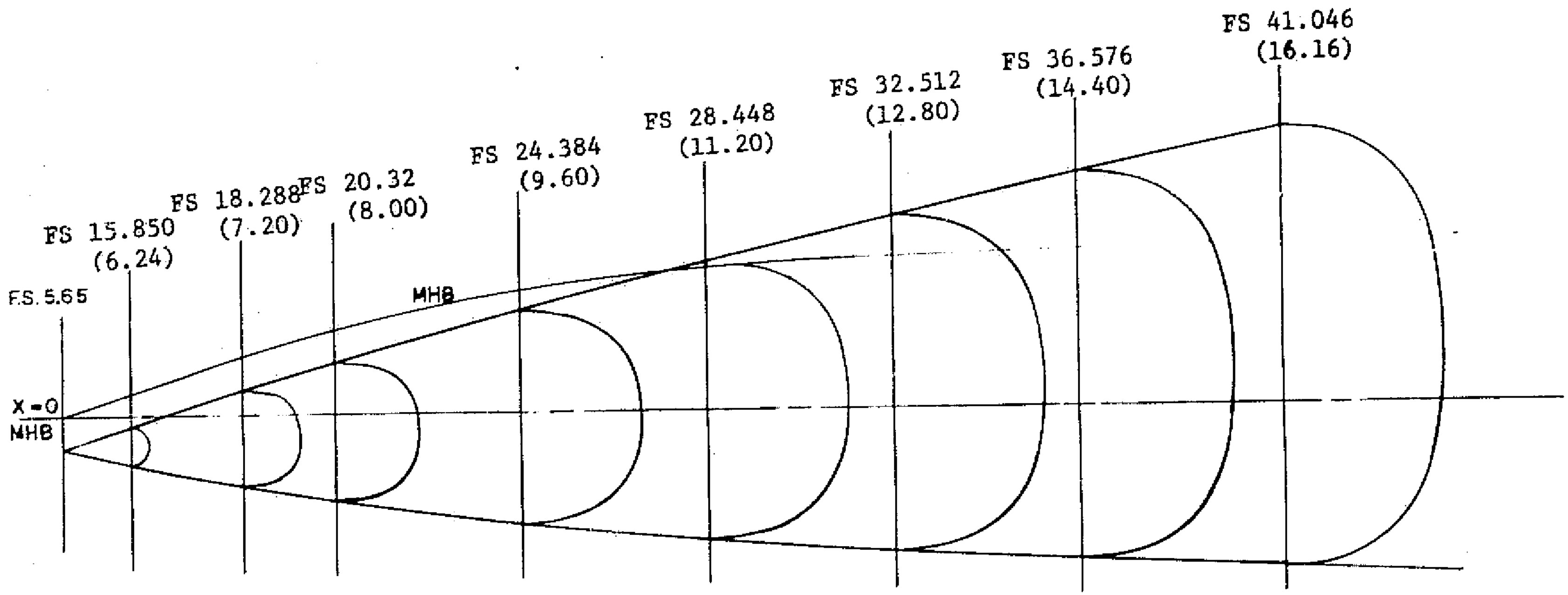

(d) Fuselage nose sections.

Figure 3.- Continued.

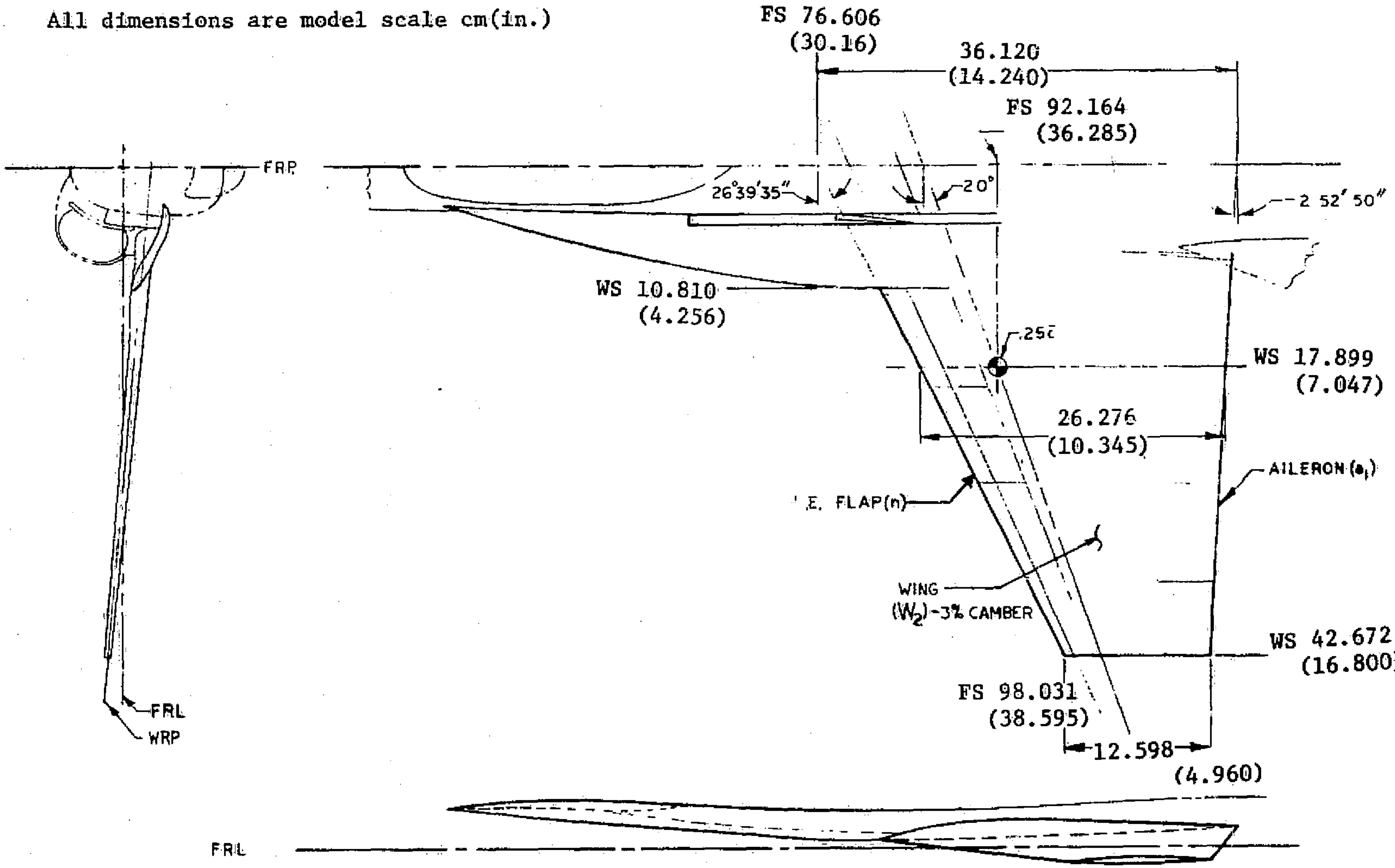

(e) W_2 wing with LEX.

Figure 3.- Continued.

All dimensions are model scale cm(in.)

δ_n (SINGLE DROOP)

B	
15%	20%
—	25°

δ_n (DOUBLE DROOP)

A	B	
7.5%	15%	20%
30°	—	15°

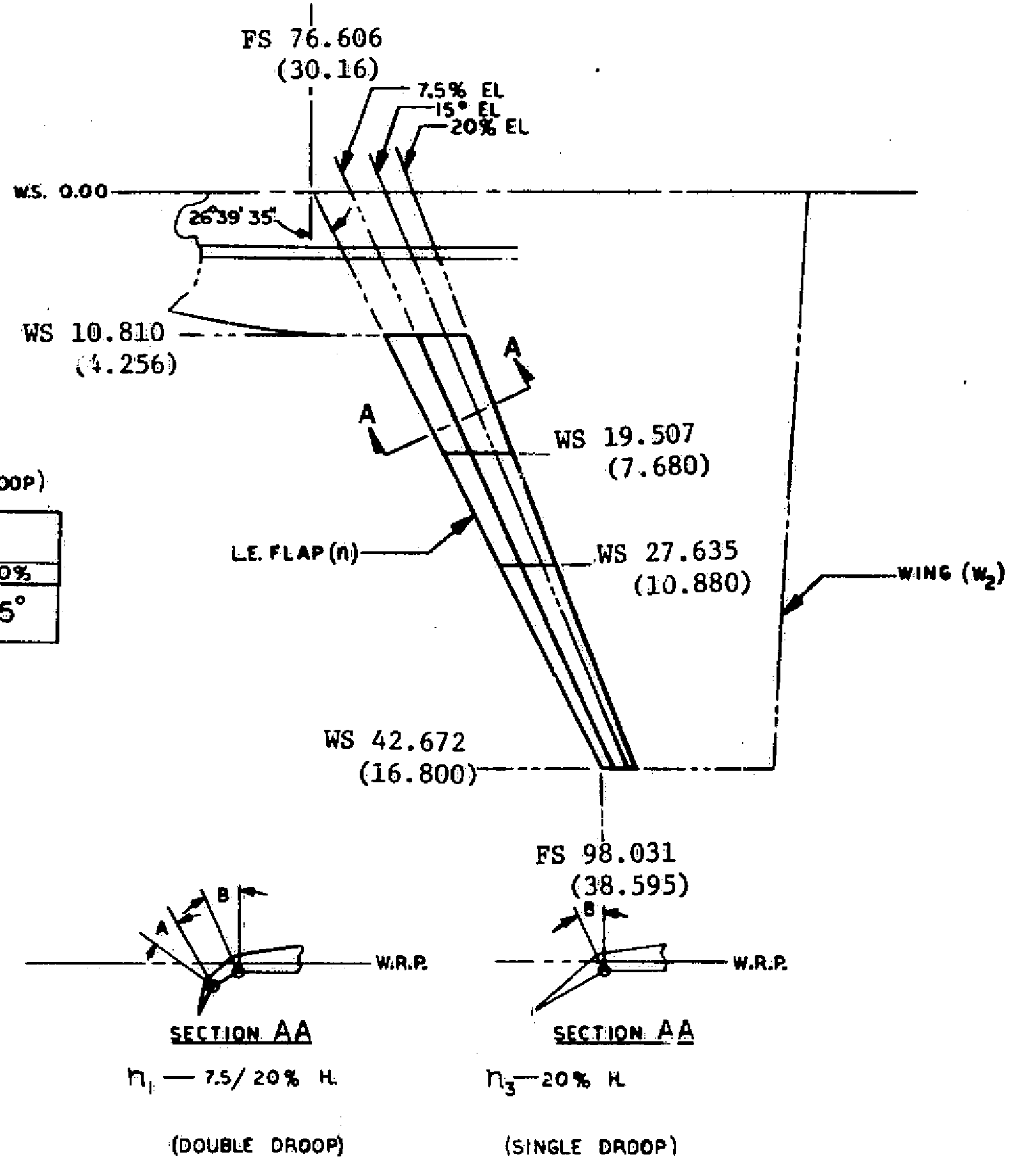

(f) Leading-edge flap detail.

Figure 3.- Continued.

All dimensions are model scale cm(in.)

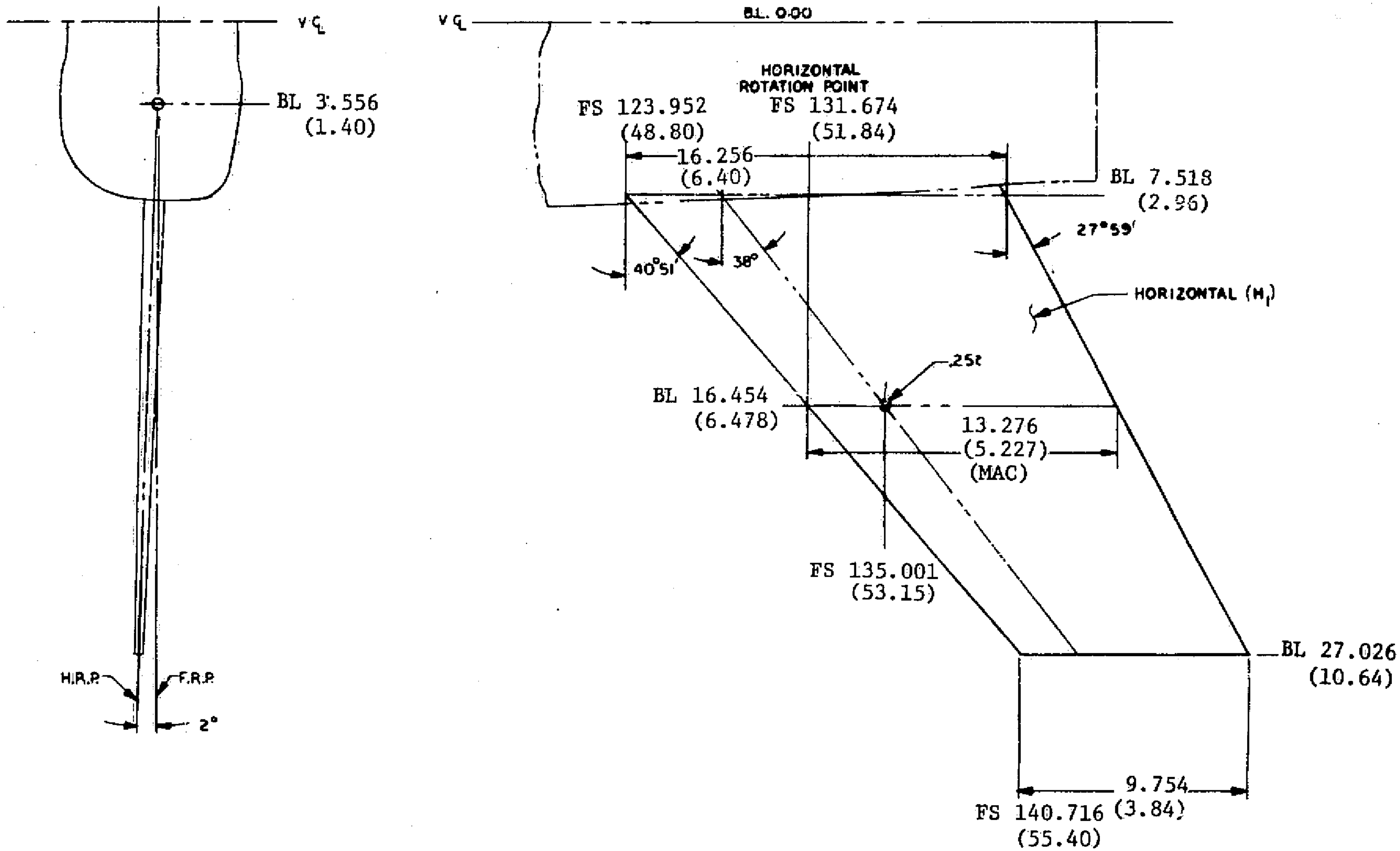

(g) Horizontal H_1.

Figure 3.- Continued.

All dimensions are model scale cm(in.)

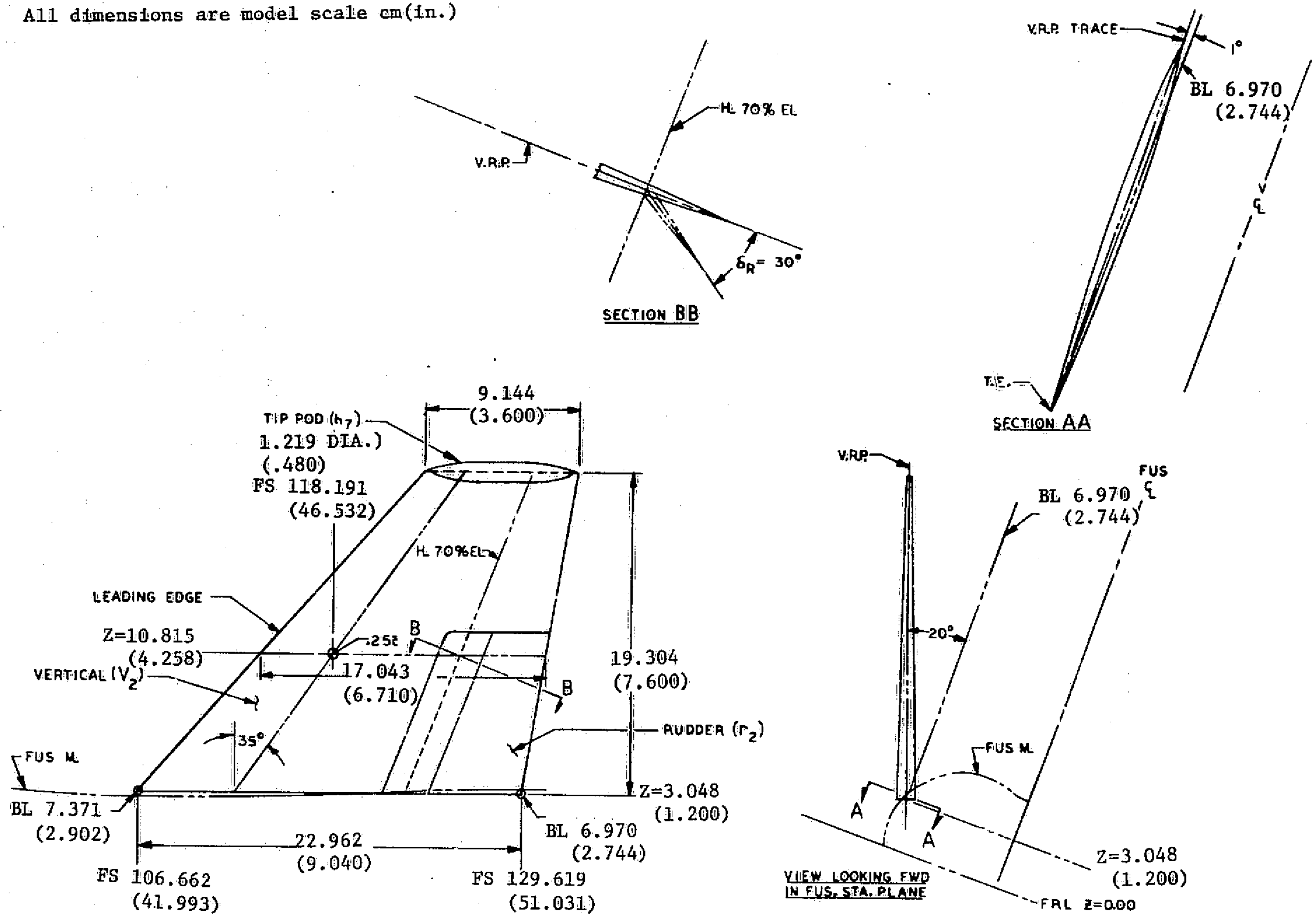

(h) V_2 (0.3982 taper ratio).

Figure 3.- Continued.

All dimensions are model scale cm(in.)

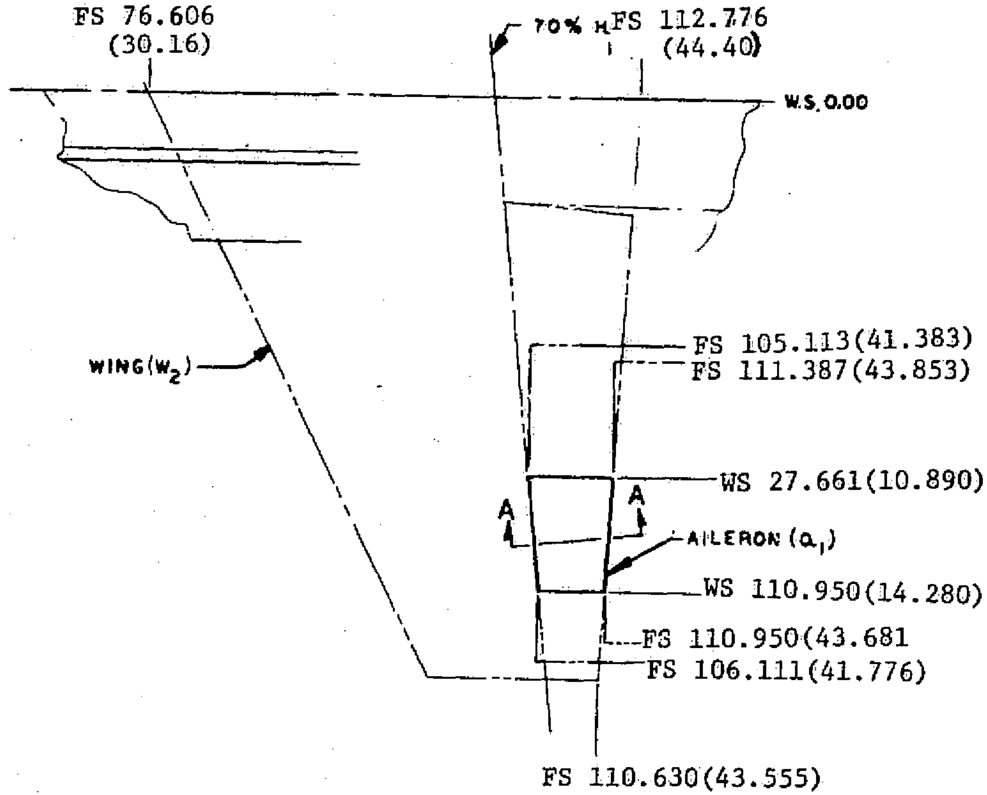

δ_a
0°
10°
20°
30°
−10°
−20°
−30°

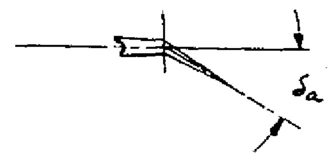

SECTION AA

(i) Aileron.

Figure 3.- Continued.

All dimensions are model scale cm(in.)

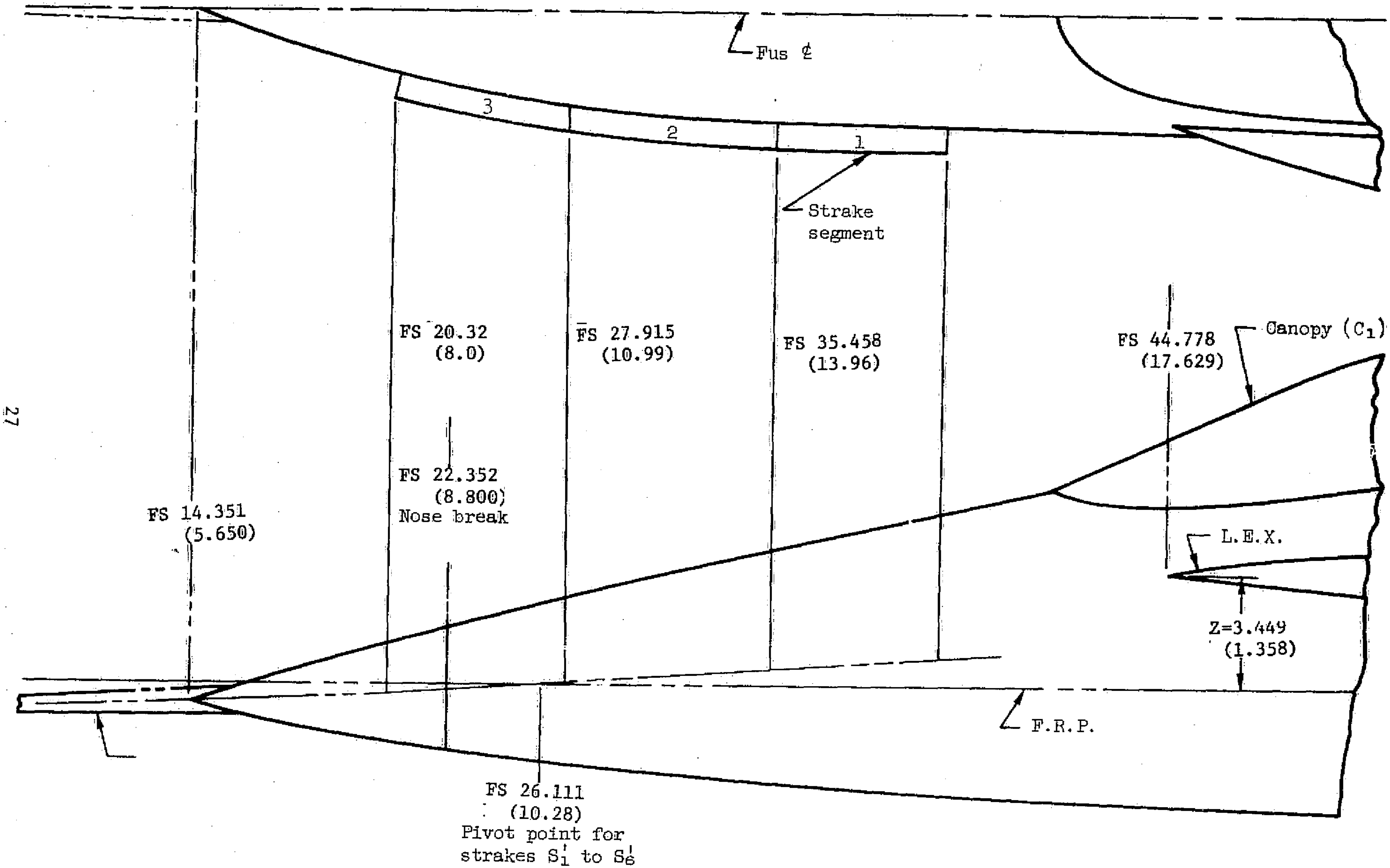

(j) S' strakes.

Figure 3.- Continued.

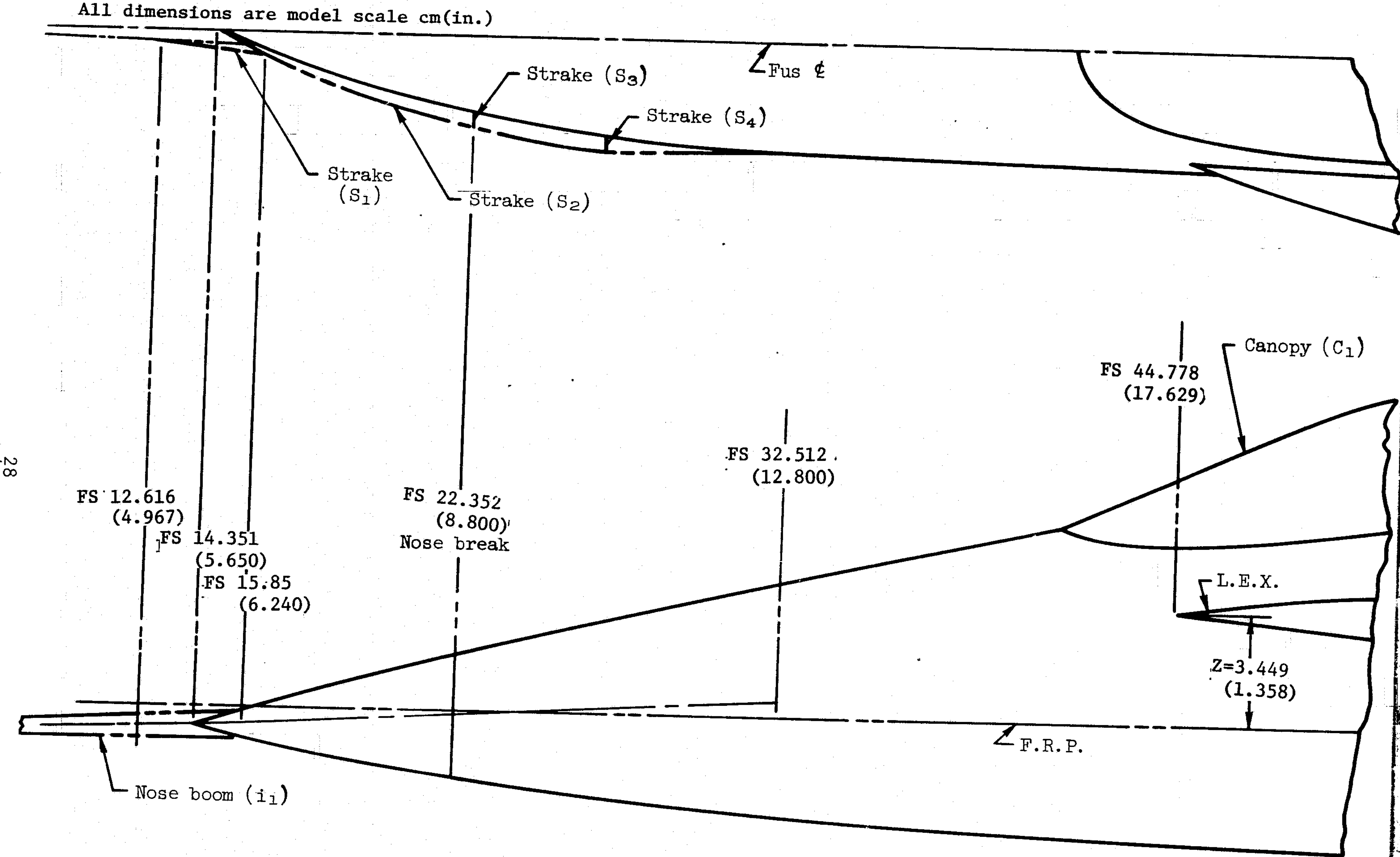

(k) Nose boom compatible strakes.

Figure 3.- Continued.

All dimensions are model scale cm(in.)

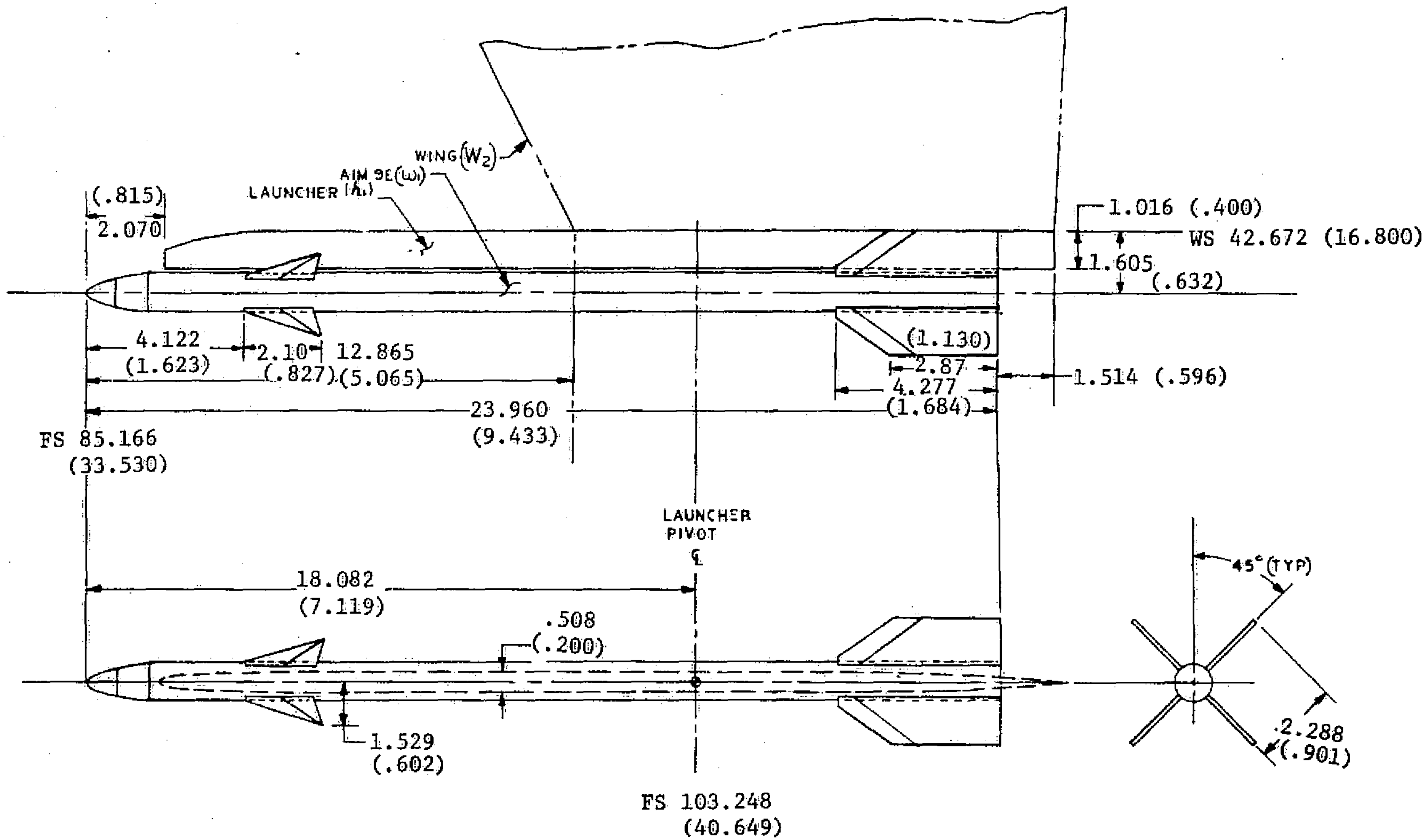

(1) AIM-9E missile.

Figure 3.- Concluded.

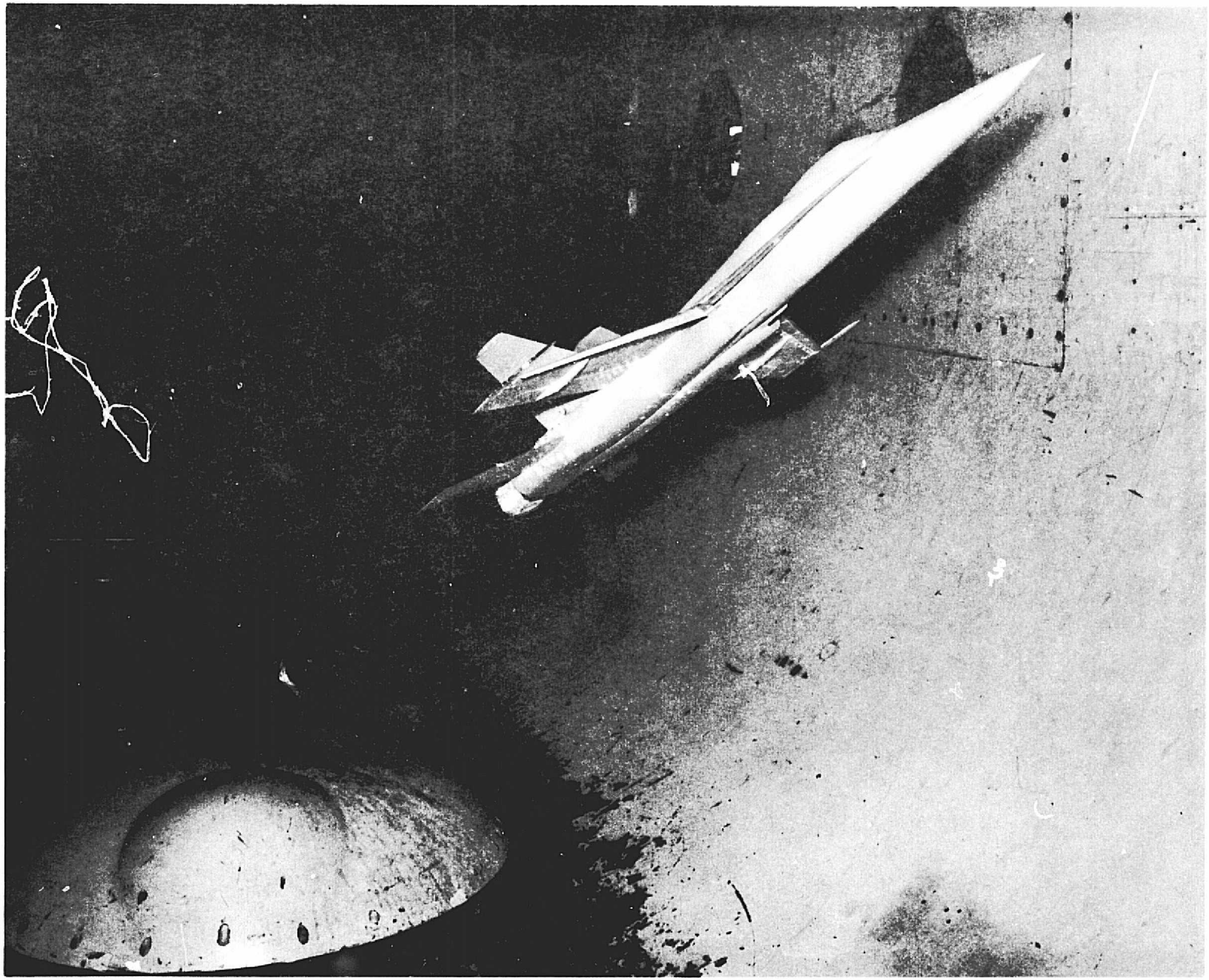

(a) One-quarter front view.

Figure 4.- Model installation photographs.

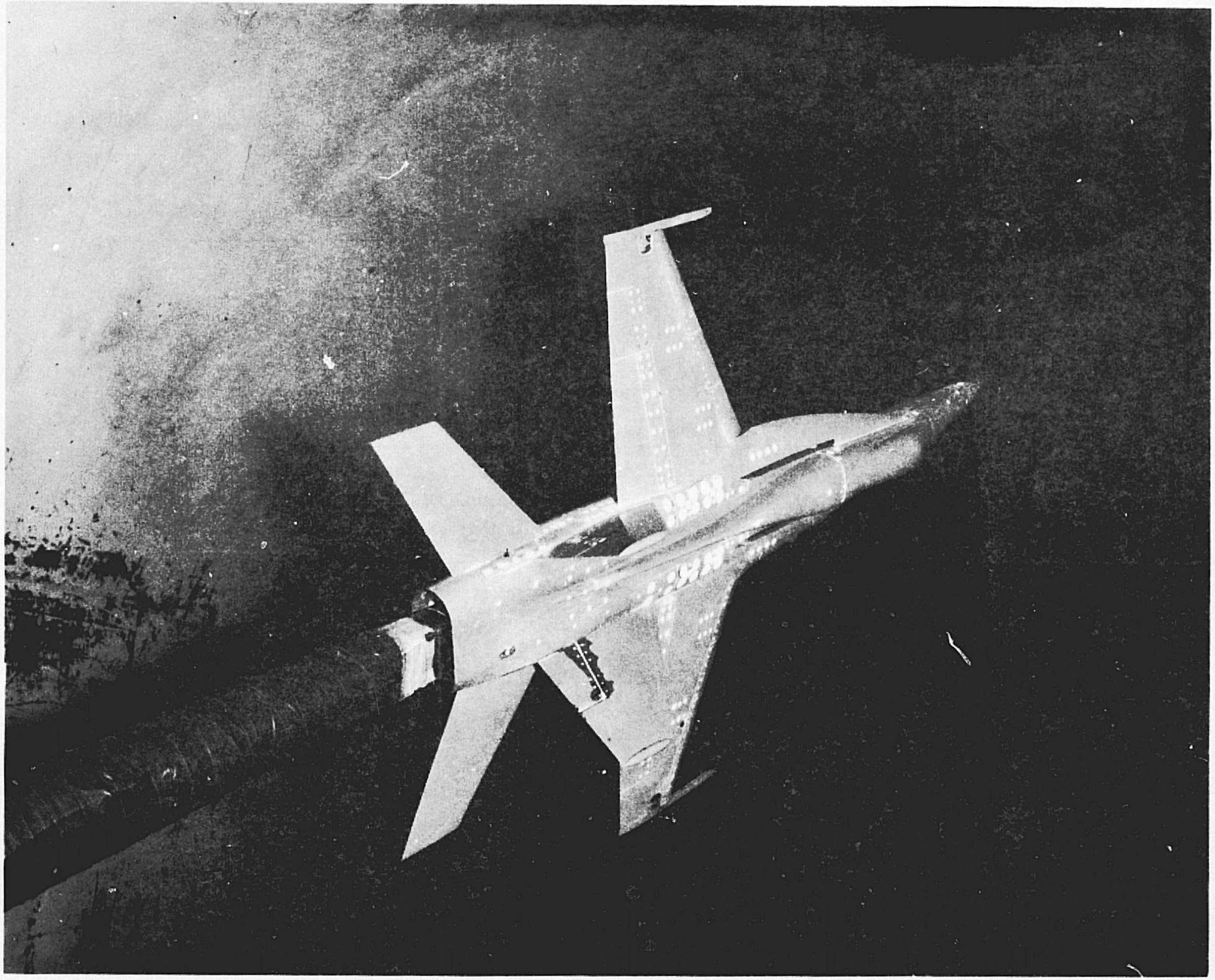

(b) One-quarter rear view.

Figure 4.- Concluded.

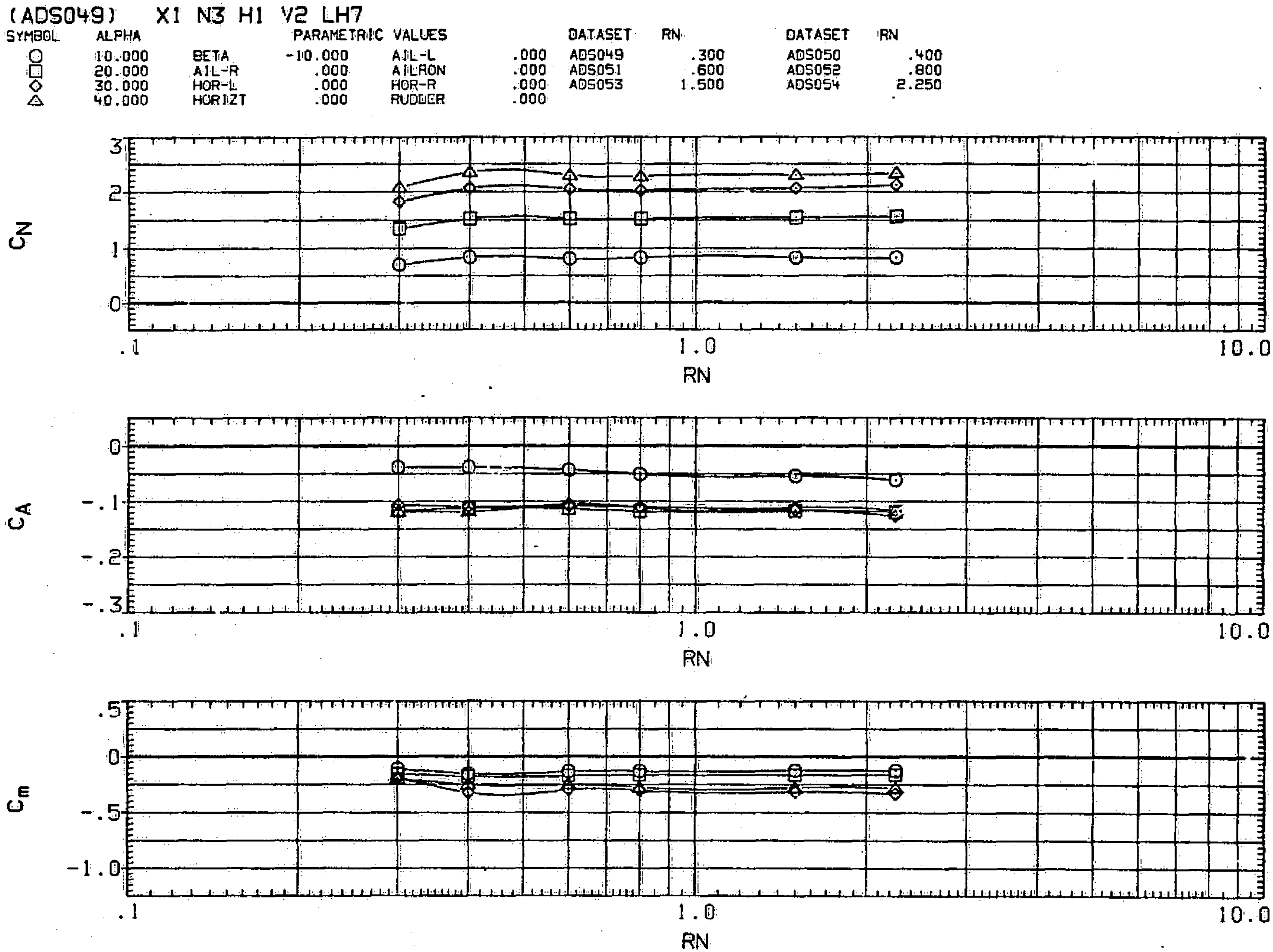

FIG.5 LONGITUD. AND LATERAL-DIRECT. AERO CHARAC. VARIATION WITH REYNOLDS NUMBER

(ADS049) X1 N3 H1 V2 LH7

SYMBOL	ALPHA	PARAMETRIC VALUES				DATASET	RN	DATASET	RN
○	10.000	BETA	.000	AIL-L	.000	ADS049	.300	ADS050	.400
□	20.000	AIL-R	.000	AILRON	.000	ADS051	.600	ADS052	.800
◇	30.000	HOR-L	.000	HOR-R	.000	ADS053	1.500	ADS054	2.250
△	40.000	HORIZT	.000	RUDDER	.000				

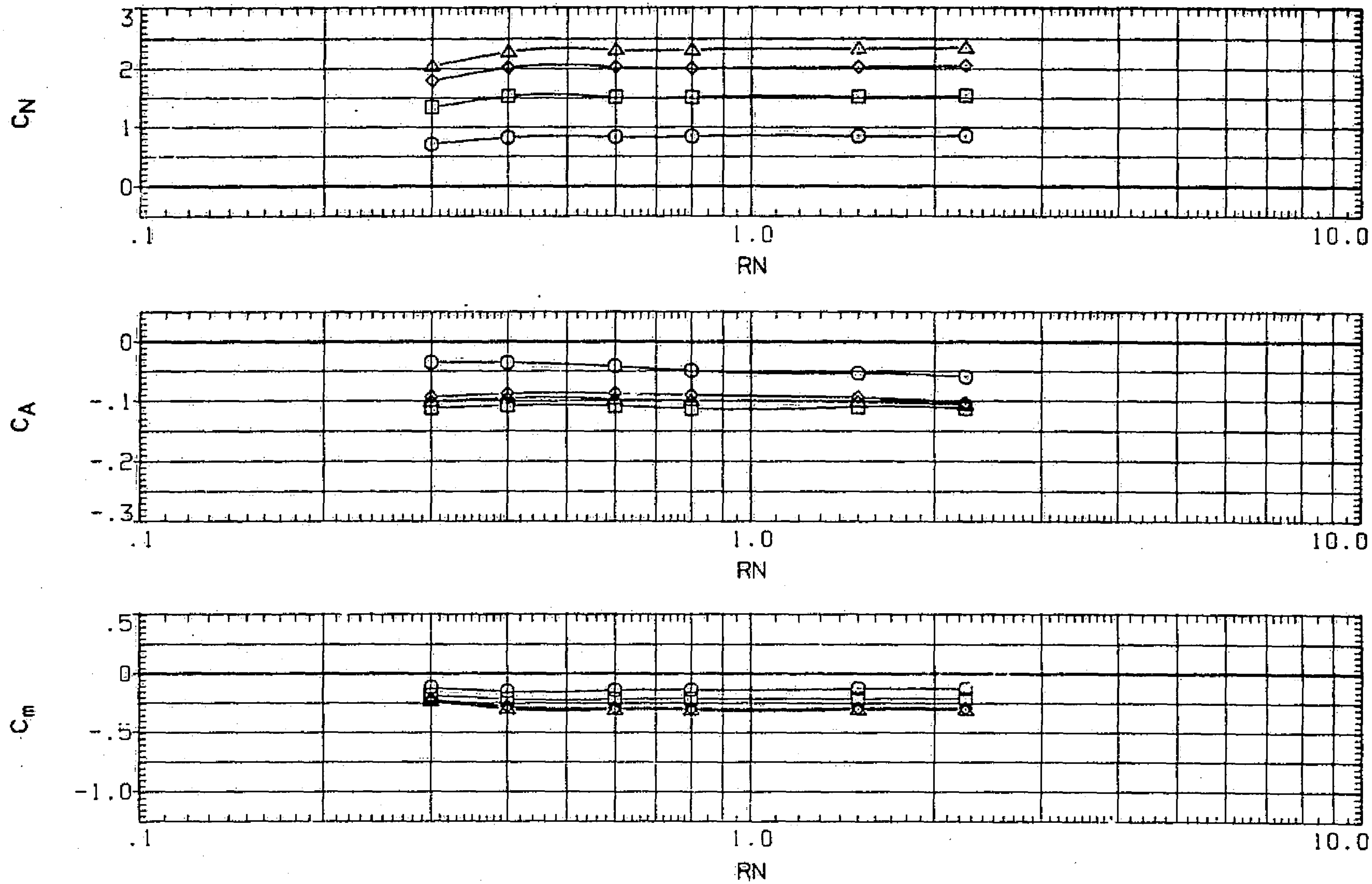

FIG.5 LONGITUD. AND LATERAL-DIRECT. AERO CHARAC. VARIATION WITH REYNOLDS NUMBER

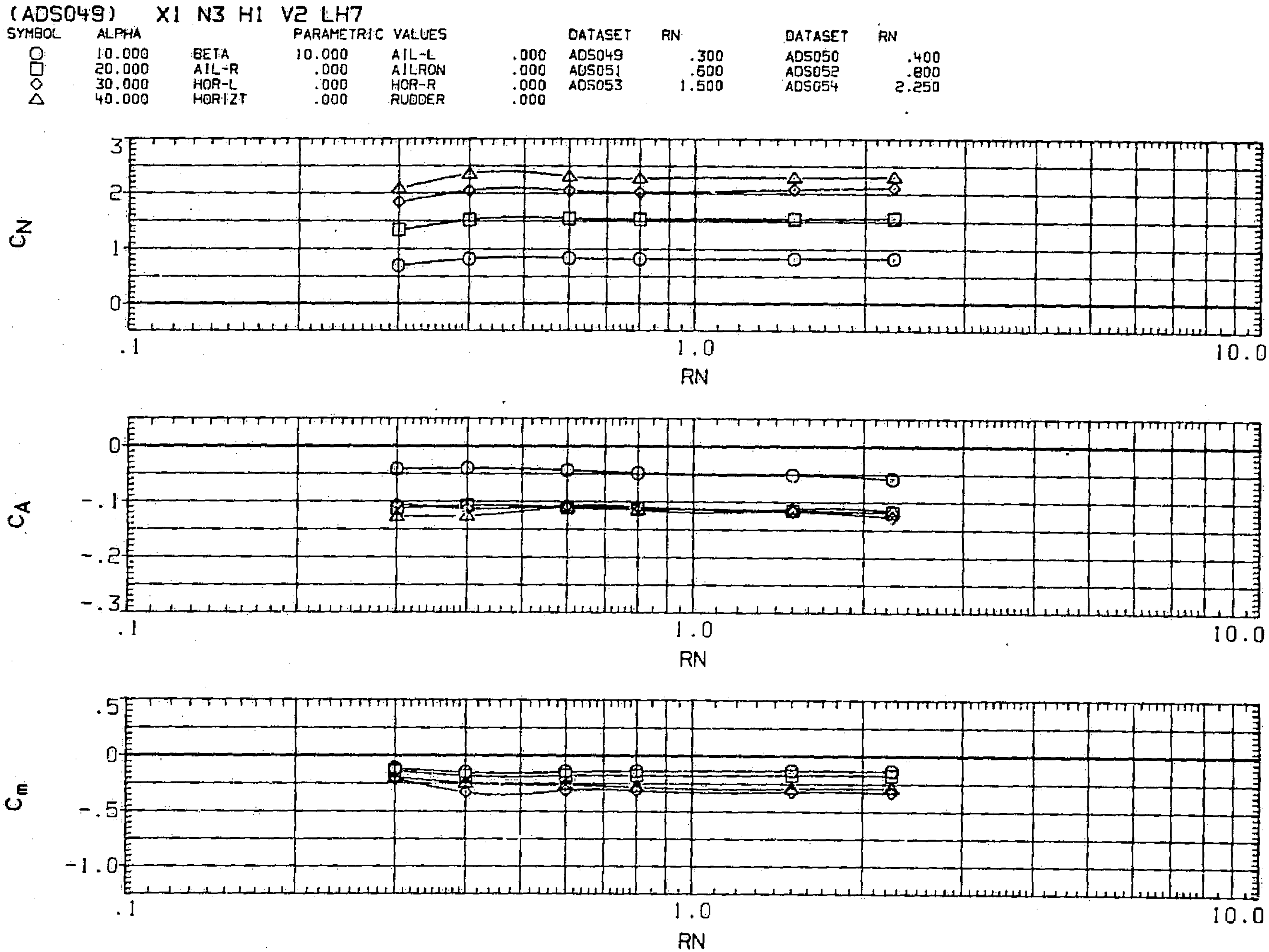

FIG.5 LONGITUD. AND LATERAL-DIRECT. AERO CHARAC. VARIATION WITH REYNOLDS NUMBER

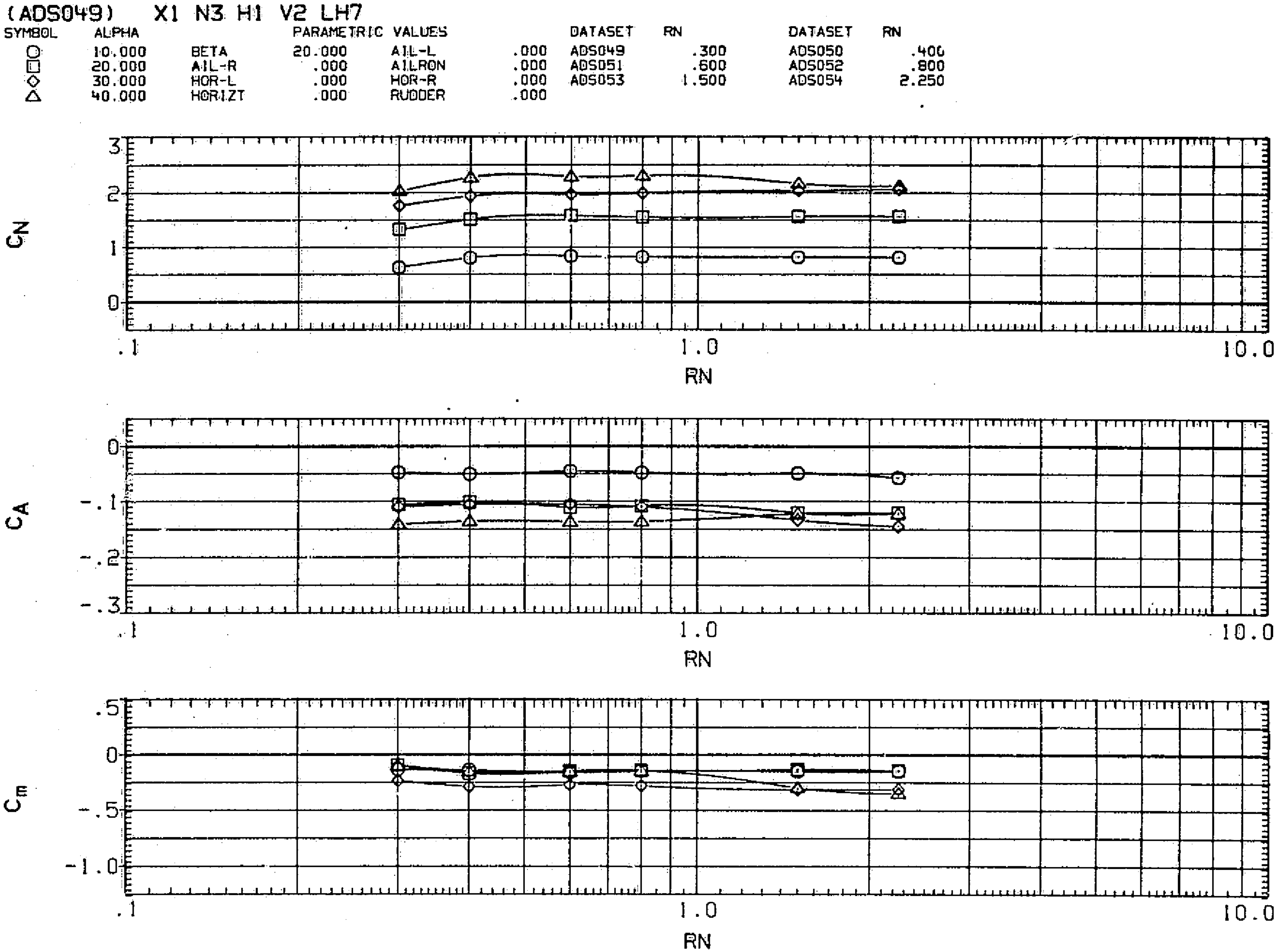

FIG.5 LONGITUD. AND LATERAL-DIRECT. AERO CHARAC. VARIATION WITH REYNOLDS NUMBER

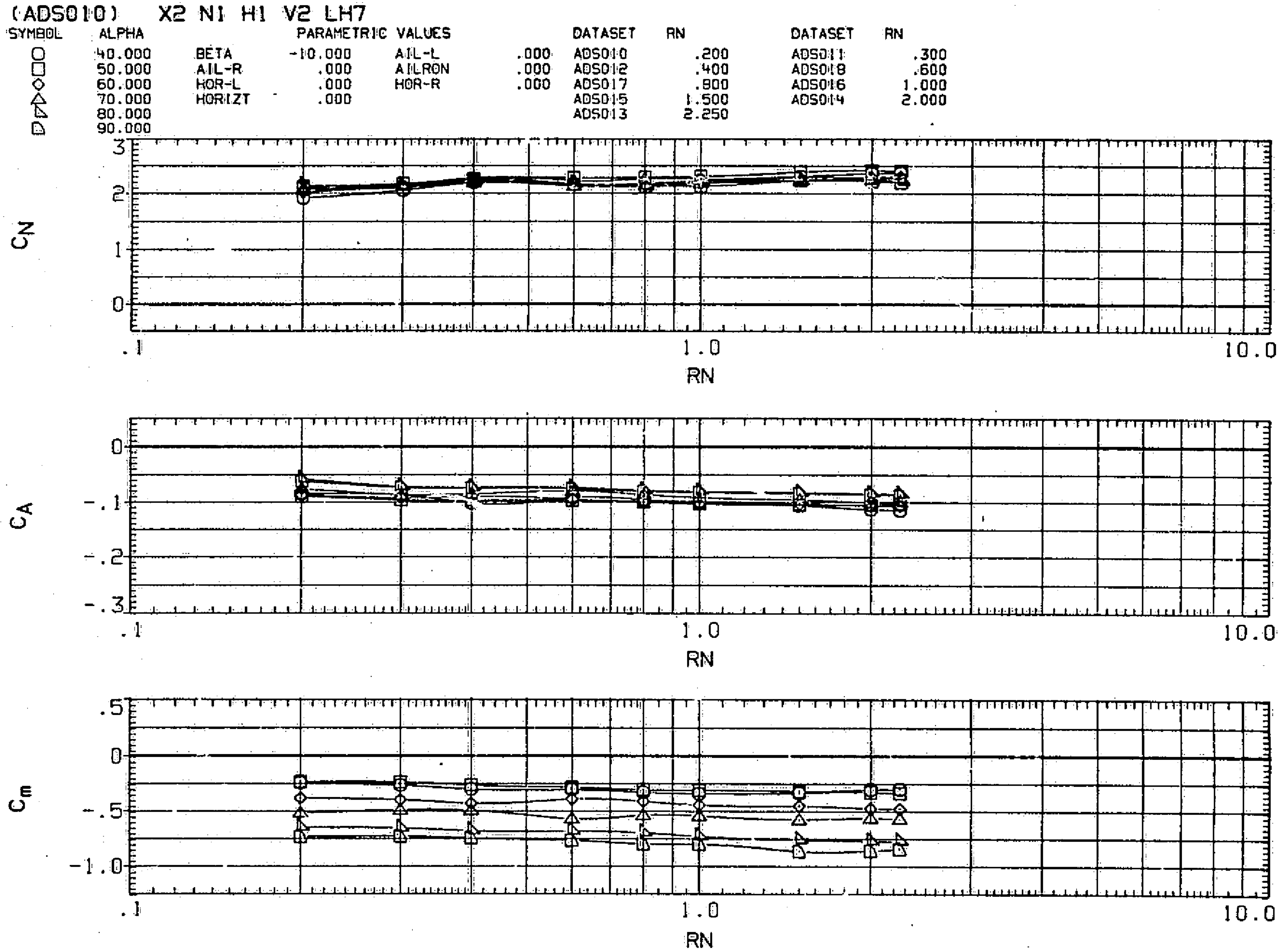

FIG.5 LONGITUD. AND LATERAL-DIRECT. AERO CHARAC. VARIATION WITH REYNOLDS NUMBER

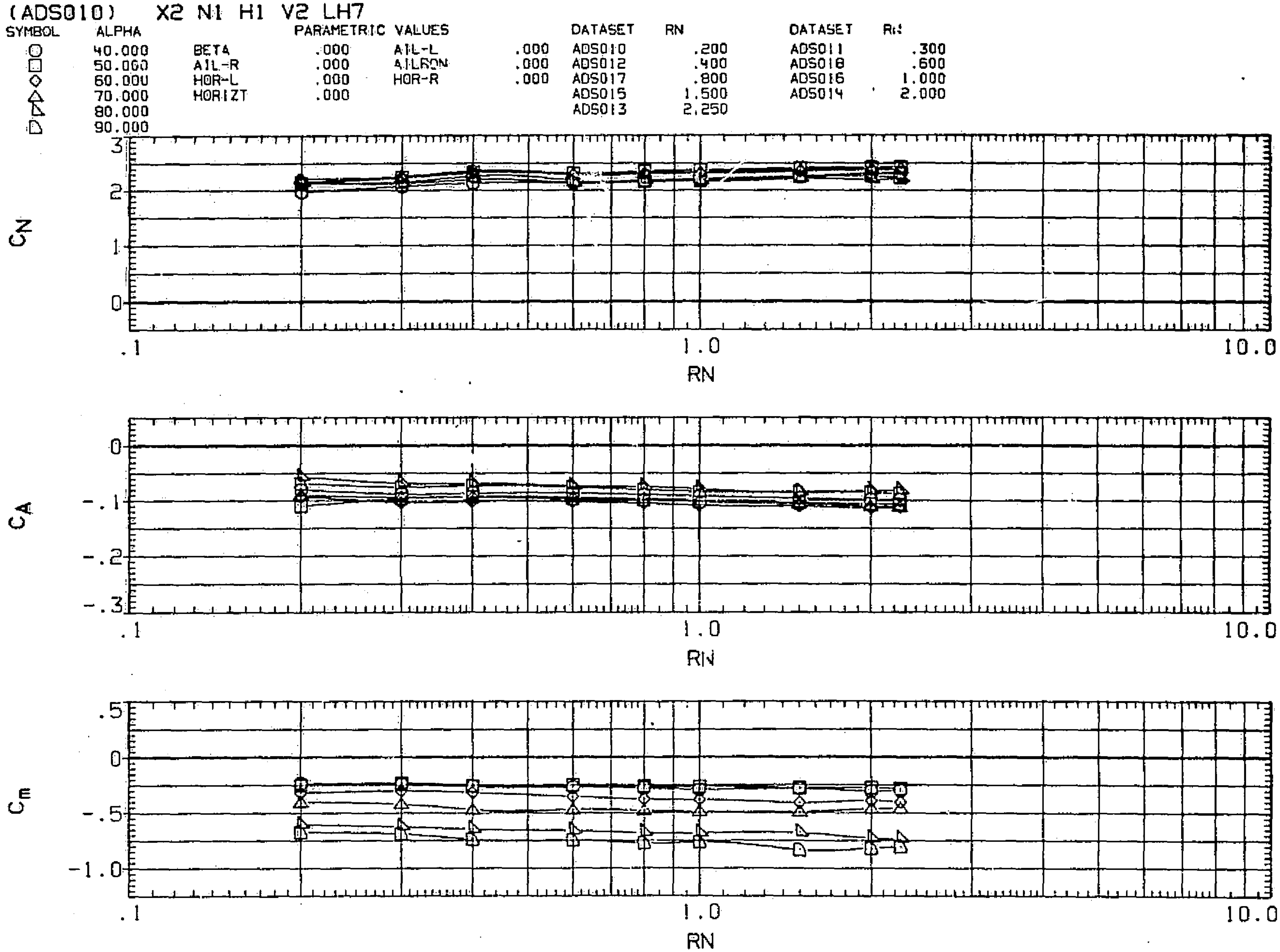

FIG.5 LONGITUD. AND LATERAL-DIRECT. AERO CHARAC. VARIATION WITH REYNOLDS NUMBER

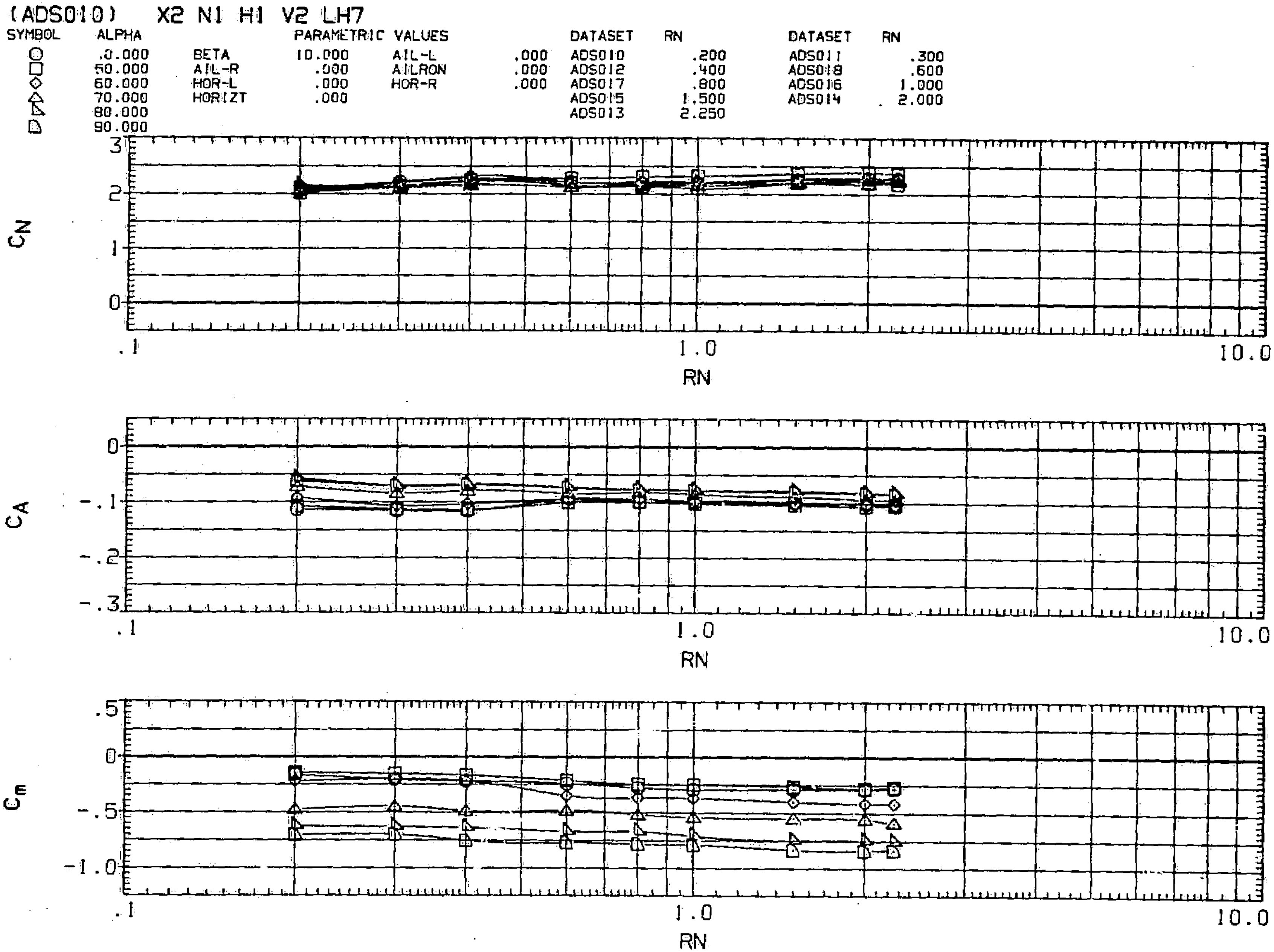

FIG.5 LONGITUD. AND LATERAL-DIRECT. AERO CHARAC. VARIATION WITH REYNOLDS NUMBER

(ADS010) X2 N1 H1 V2 LH7

SYMBOL	ALPHA	PARAMETRIC VALUES				DATASET	RN	DATASET	RN
○	40.000	BETA	20.000	AIL-L	.000	ADS010	.200	ADS011	.300
⊡	50.000	AIL-R	.000	AILRON	.000	ADS012	.400	ADS018	.600
◇	60.000	HOR-L	.000	HOR-R	.000	ADS017	.800	ADS016	1.000
△	70.000	HORIZT	.000			ADS015	1.500	ADS014	2.000
◺	80.000					ADS013	2.250		
D	90.000								

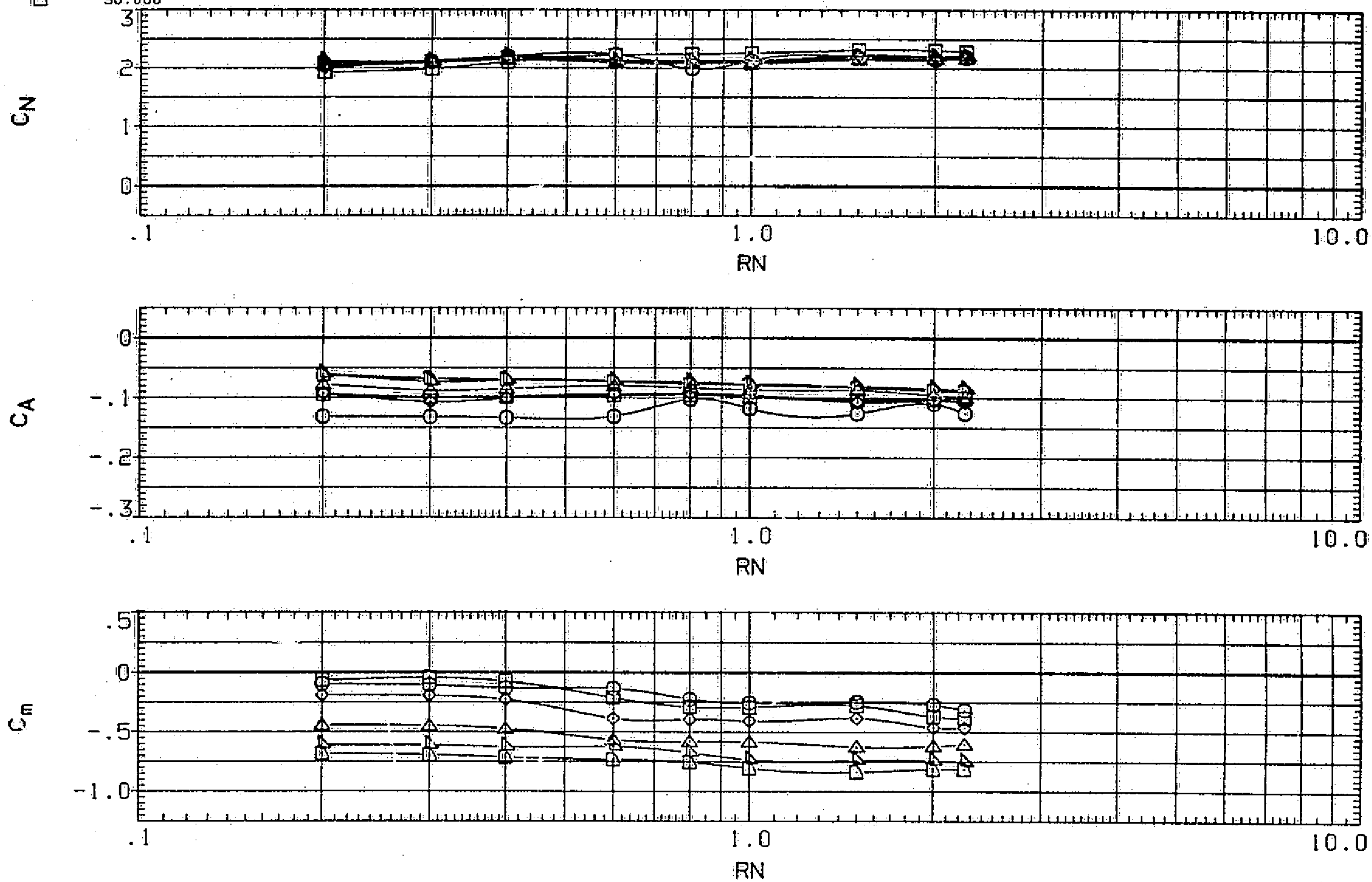

FIG.5 LONGITUD. AND LATERAL-DIRECT. AERO CHARAC. VARIATION WITH REYNOLDS NUMBER

(ADS049) X1 N3 H1 V2 LH7

SYMBOL	ALPHA	PARAMETRIC VALUES				DATASET	RN	DATASET	RN
○	10.000	BETA	-10.000	AIL-L	.000	ADS049	.300	ADS050	.400
□	20.000	AIL-R	.000	AILRON	.000	ADS051	.600	ADS052	.800
◇	30.000	HOR-L	.000	HOR-R	.000	ADS053	1.500	ADS054	2.250
△	40.000	HORIZT	.000	RUDDER	.000				

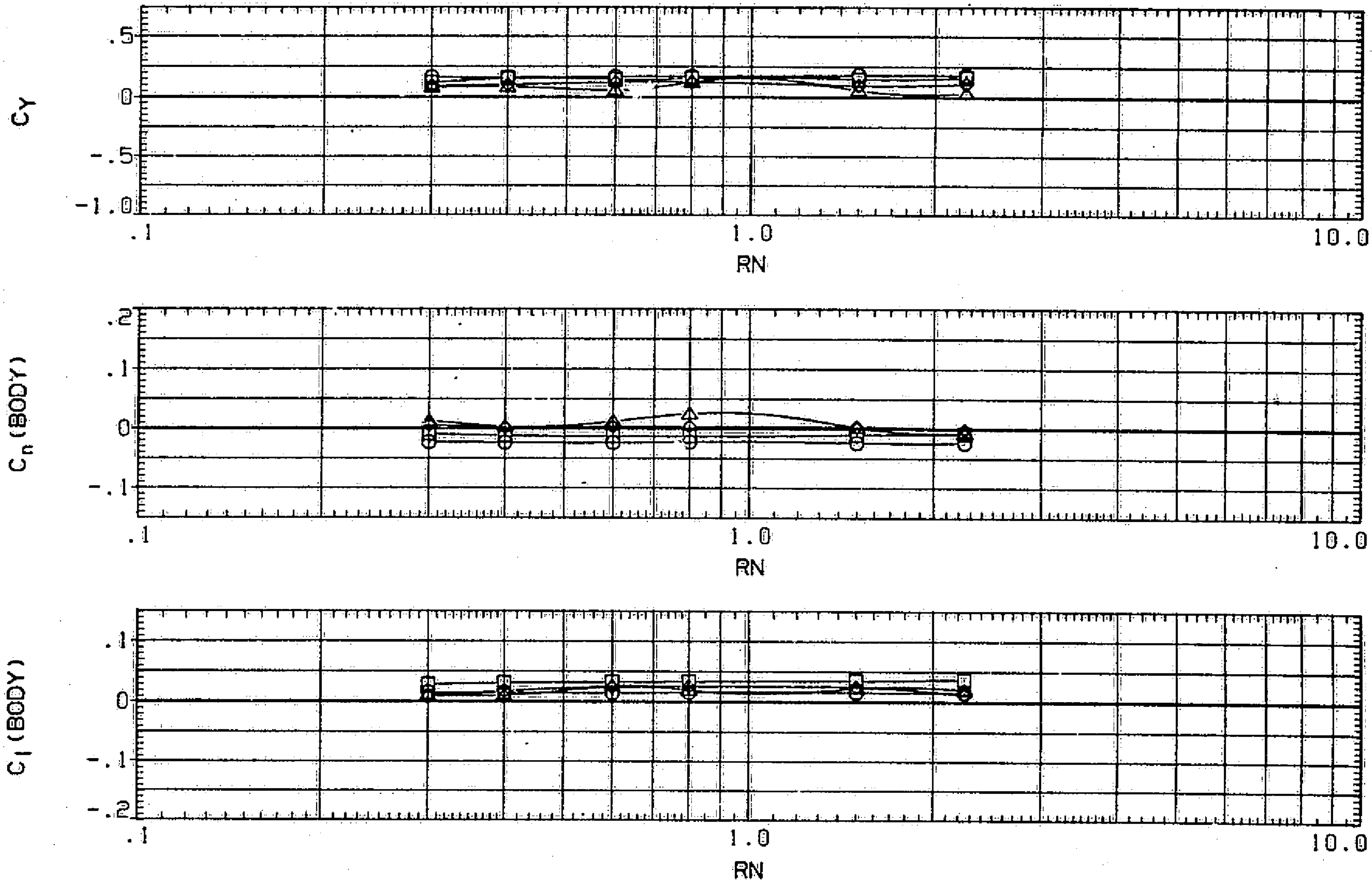

FIG.5 LONGITUD. AND LATERAL-DIRECT. AERO CHARAC. VARIATION WITH REYNOLDS NUMBER

(ADS049) X1 N3 H1 V2 LH7

SYMBOL	ALPHA	PARAMETRIC VALUES				DATASET	RN	DATASET	RN
○	10.000	BETA	.000	AIL-L	.000	ADS049	.300	ADS050	.400
□	20.000	AIL-R	.000	AILRON	.000	ADS051	.600	ADS052	.800
◇	30.000	HOR-L	.000	HOR-R	.000	ADS053	1.500	ADS054	2.250
△	40.000	HORIZT	.000	RUDDER	.000				

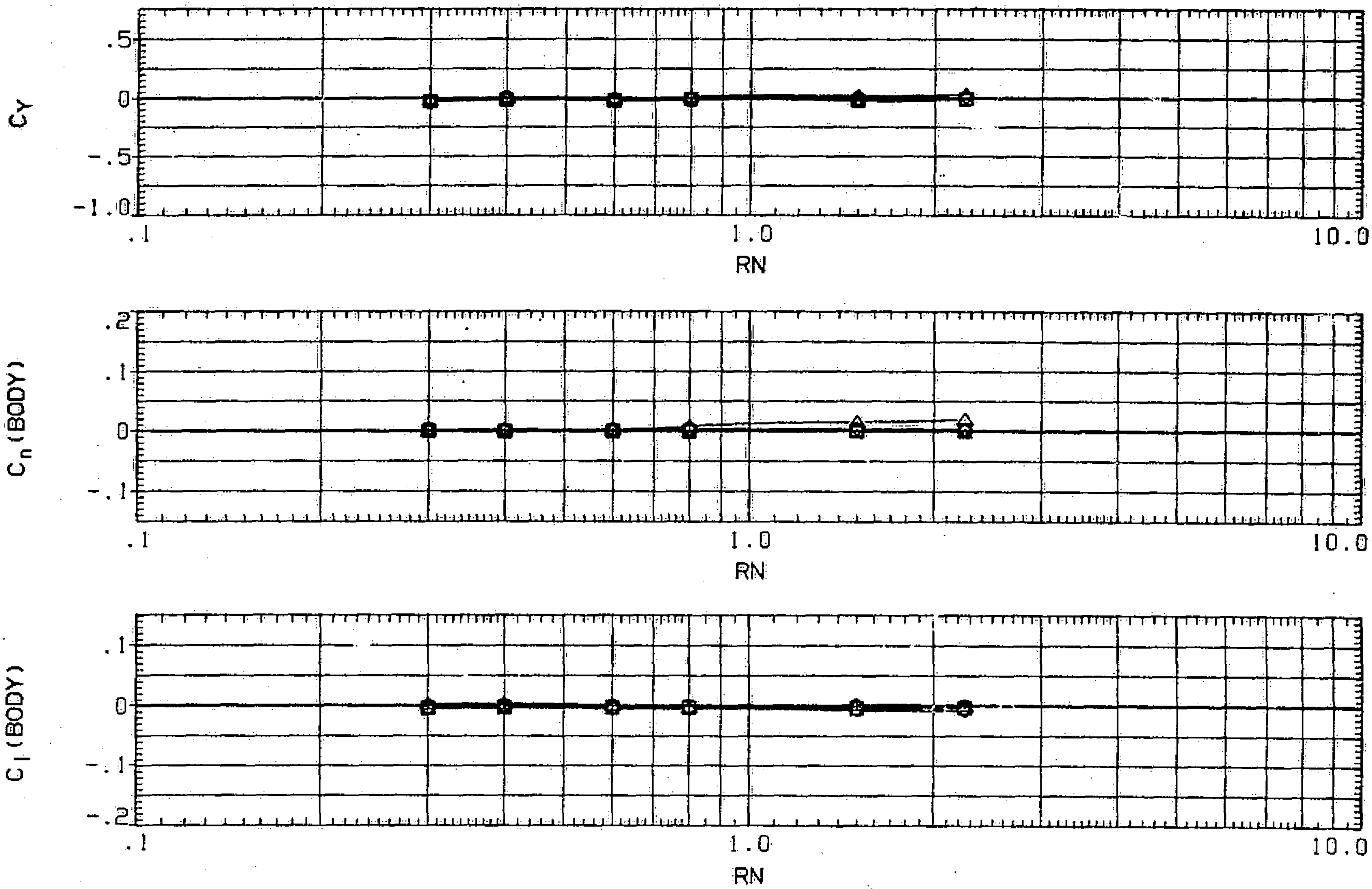

FIG.5 LONGITUD. AND LATERAL-DIRECT. AERO CHARAC. VARIATION WITH REYNOLDS NUMBER

(ADS049) X1 N3 H1 V2 LH7

SYMBOL	ALPHA	PARAMETRIC VALUES				DATASET	RN	DATASET	RN
○	10.000	BETA	10.000	AIL-L	.000	ADS049	.300	ADS050	.400
□	20.000	AIL-R	.000	AILRON	.000	ADS051	.600	ADS052	.800
◇	30.000	HOR-L	.000	HOR-R	.000	ADS053	1.500	ADS054	2.250
△	40.000	HORIZT	.000	RUDDER	.000				

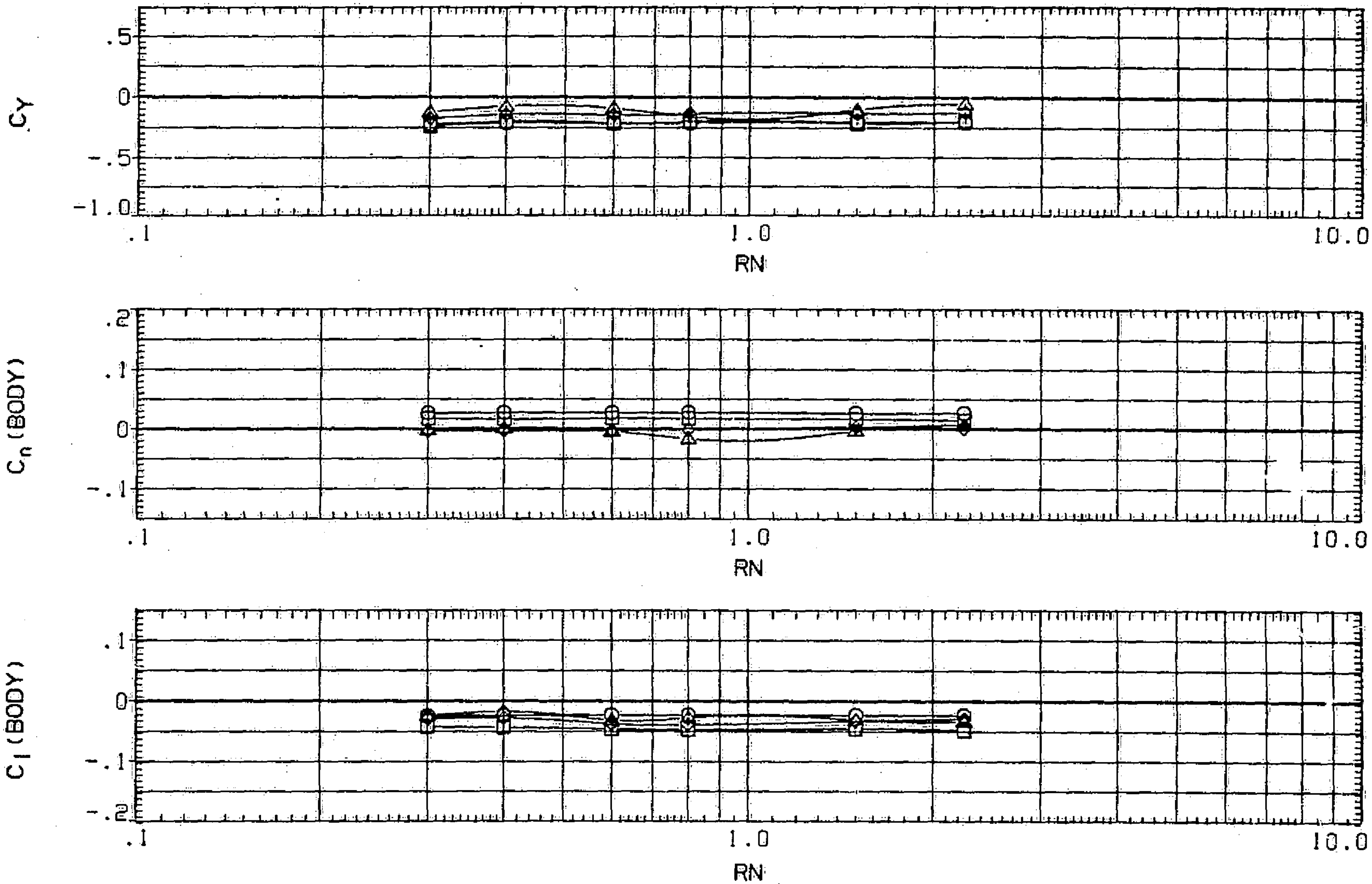

FIG.5 LONGITUD. AND LATERAL-DIRECT. AERO CHARAC. VARIATION WITH REYNOLDS NUMBER

(ADS049) X1 N3 H1 V2 LH7

SYMBOL	ALPHA	PARAMETRIC VALUES				DATASET	RN	DATASET	RN
○	10.000	BETA	20.000	AIL-L	.000	ADS049	.300	ADS050	.400
□	20.000	AIL-R	.000	AILRON	.000	ADS051	.600	ADS052	.800
◇	30.000	HOR-L	.000	HOR-R	.000	ADS053	1.500	ADS054	2.250
△	40.000	HORIZT	.000	RUDDER	.000				

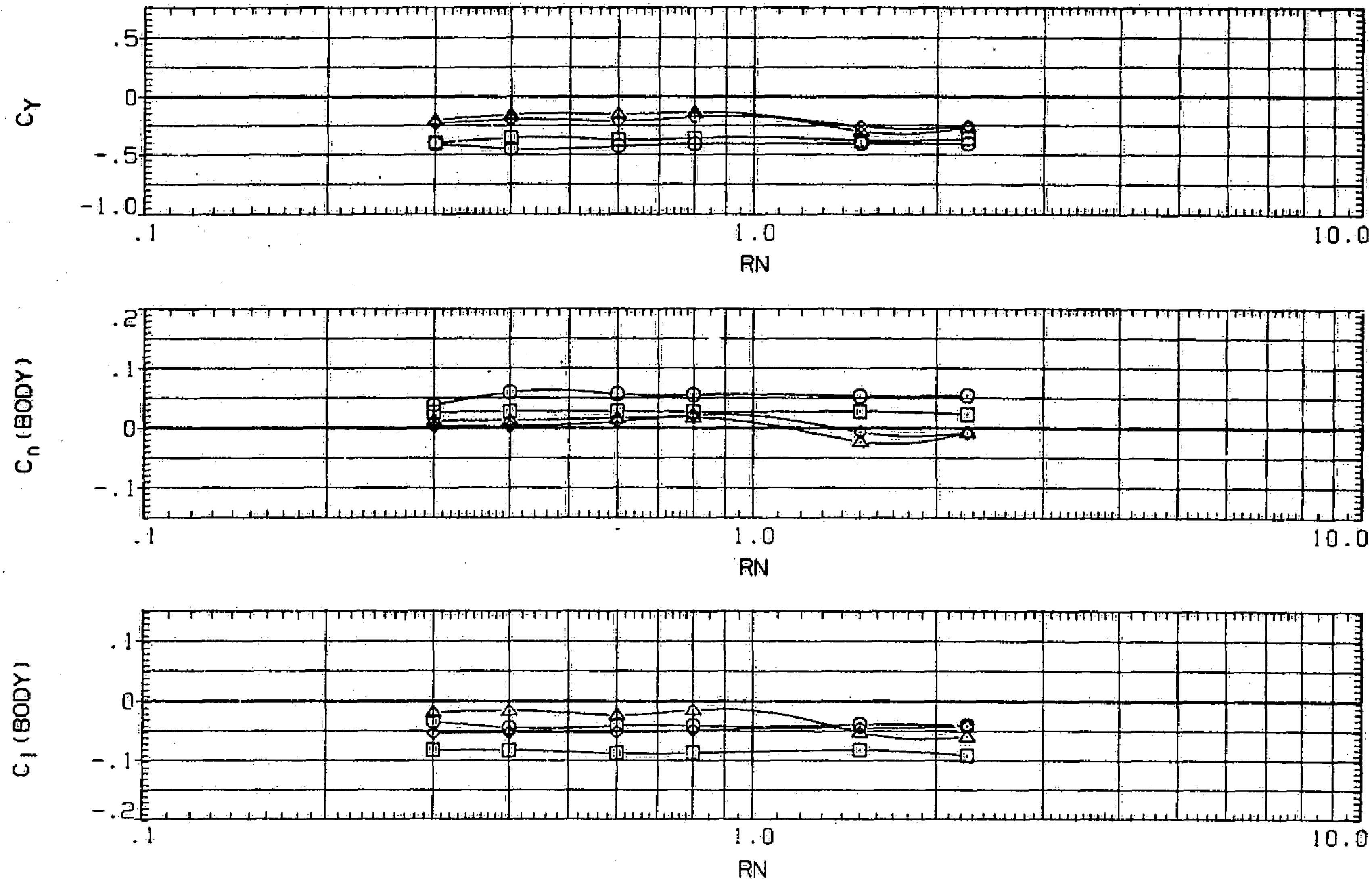

FIG.5 LONGITUD. AND LATERAL-DIRECT. AERO CHARAC. VARIATION WITH REYNOLDS NUMBER

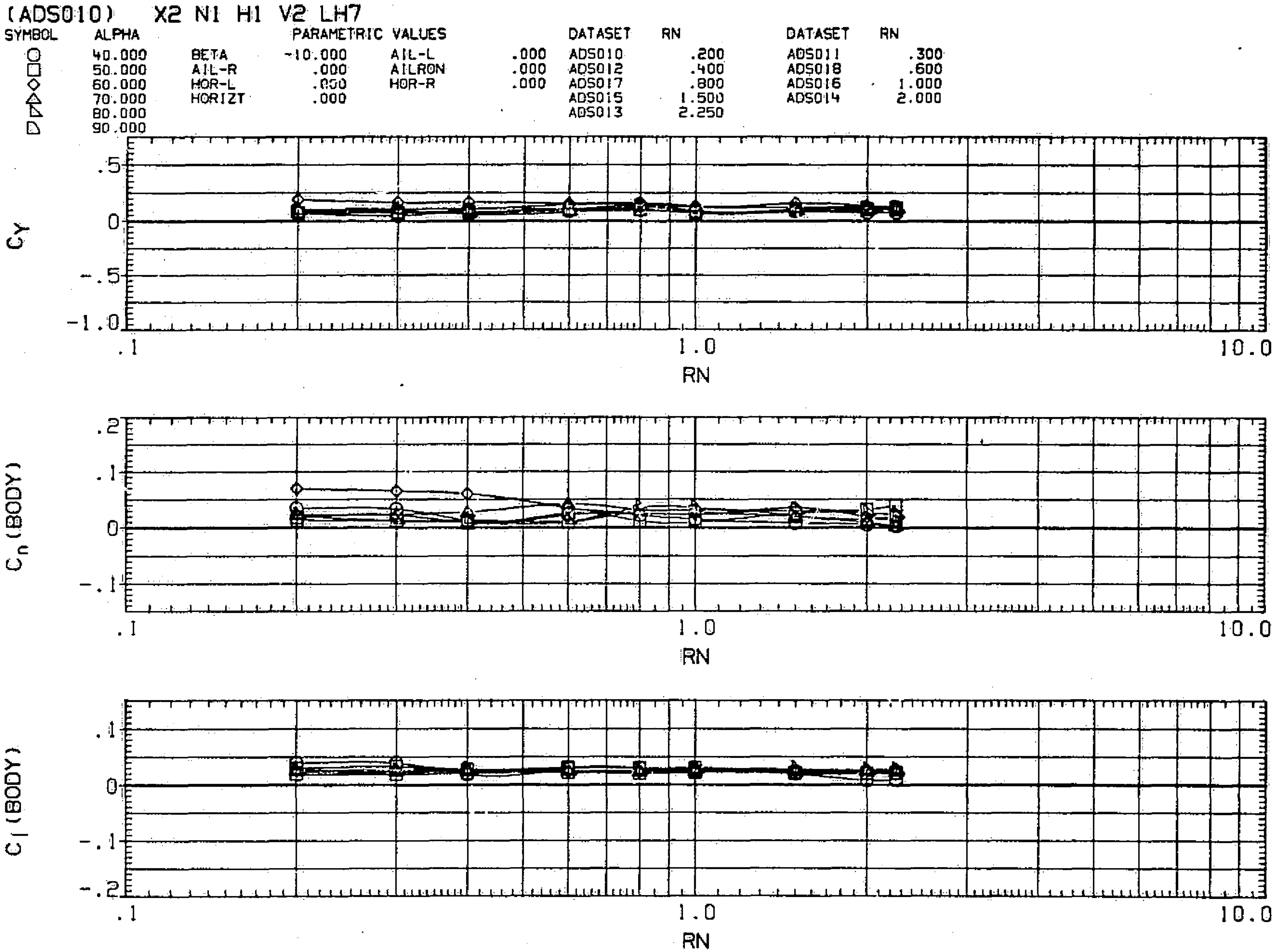

FIG.5 LONGITUD. AND LATERAL-DIRECT. AERO CHARAC. VARIATION WITH REYNOLDS NUMBER

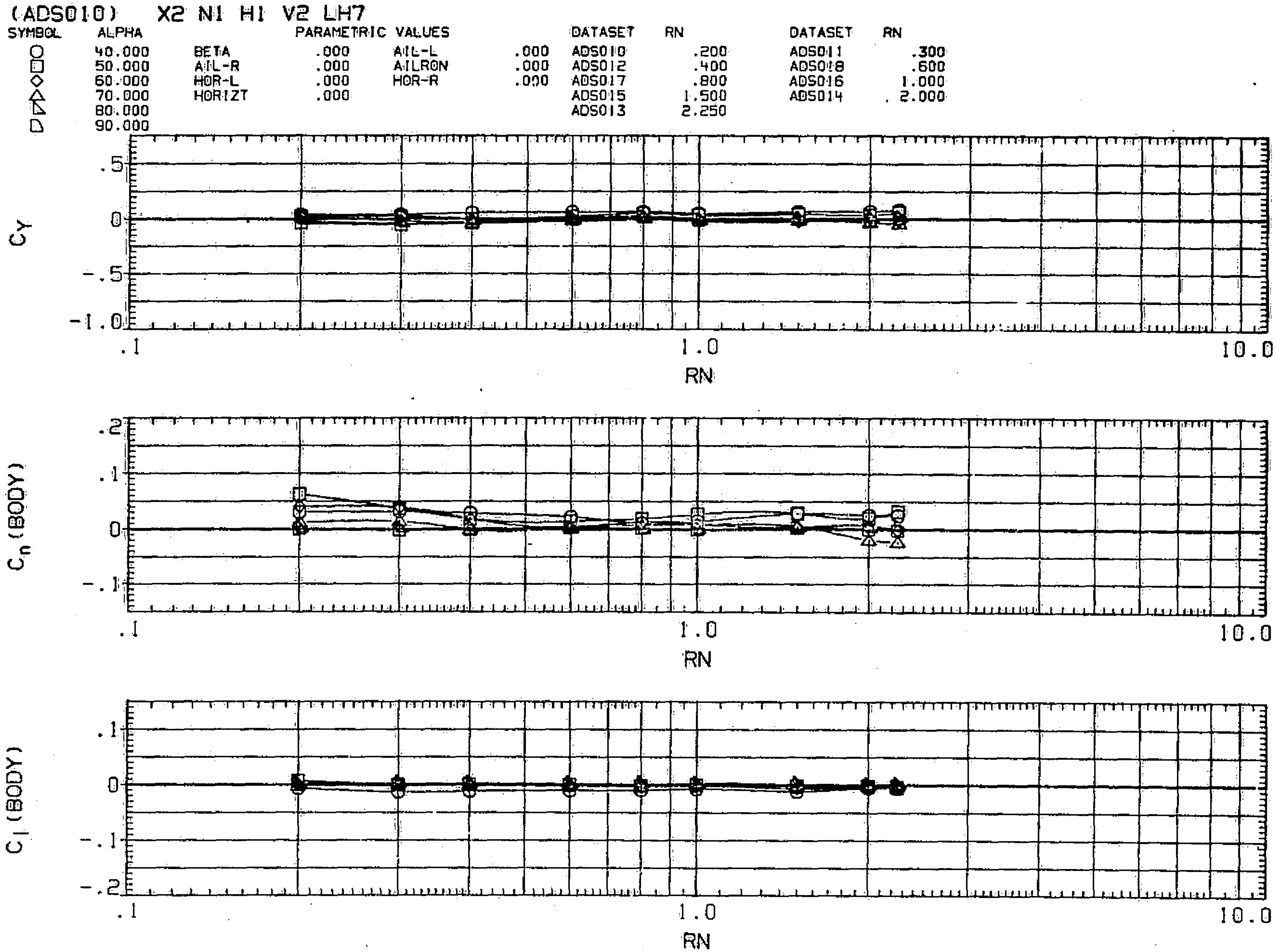

FIG.5 LONGITUD. AND LATERAL-DIRECT. AERO CHARAC. VARIATION WITH REYNOLDS NUMBER

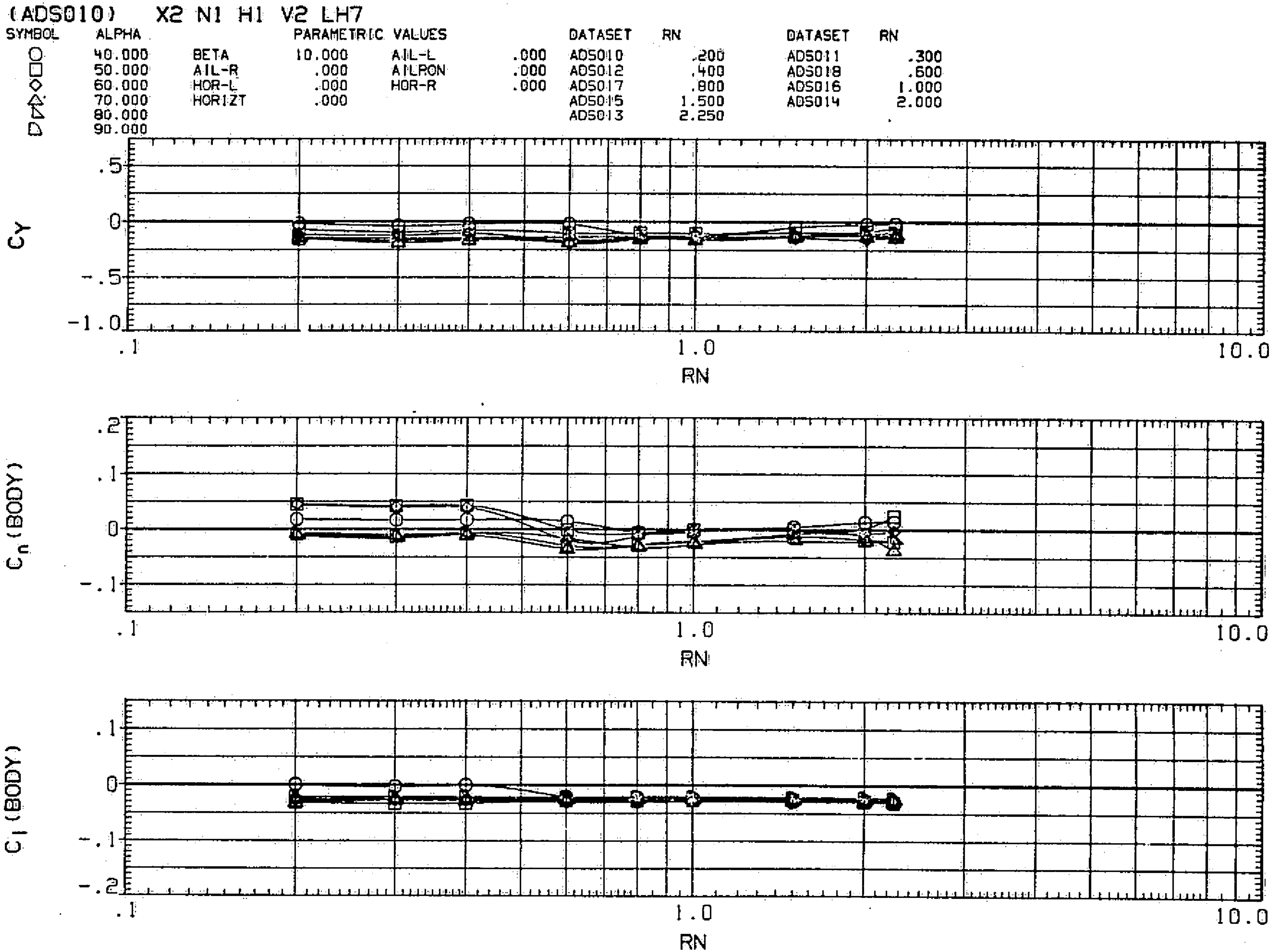

FIG.5 LONGITUD. AND LATERAL-DIRECT. AERO CHARAC. VARIATION WITH REYNOLDS NUMBER

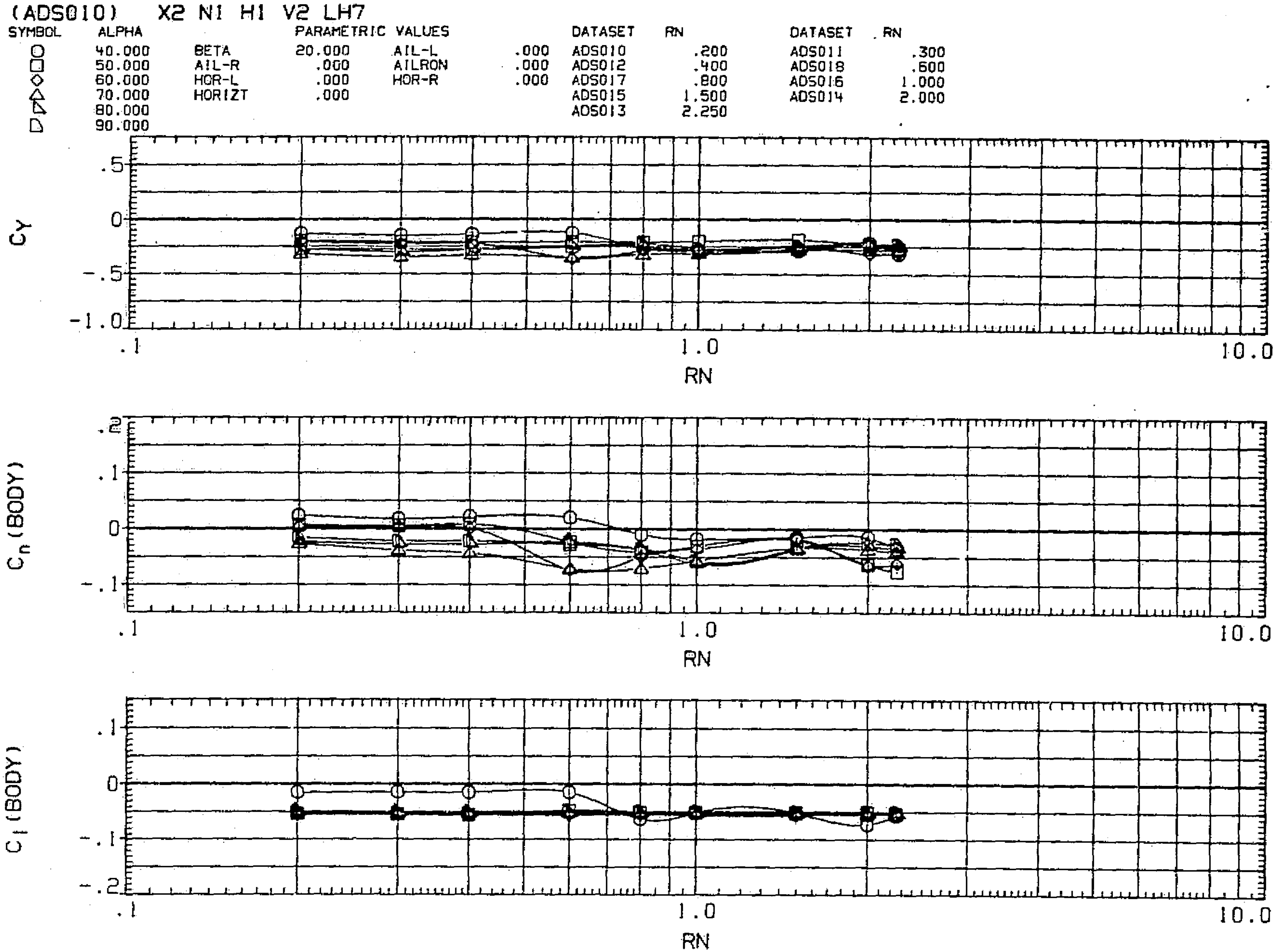

FIG.5 LONGITUD. AND LATERAL-DIRECT. AERO CHARAC. VARIATION WITH REYNOLDS NUMBER

DATA SET	SYMBOL	CONFIGURATION DESCRIPTION	RN
(RDS047)	○	X1 N3 I1 H1 V2 LH7	.300
(RDS048)	□	X1 N3 I1 H1 V2 LH7	2.250
(RDS049)	◇	X1 N3 H1 V2 LH7	.300
(RDS054)	△	X1 N3 H1 V2 LH7	2.250

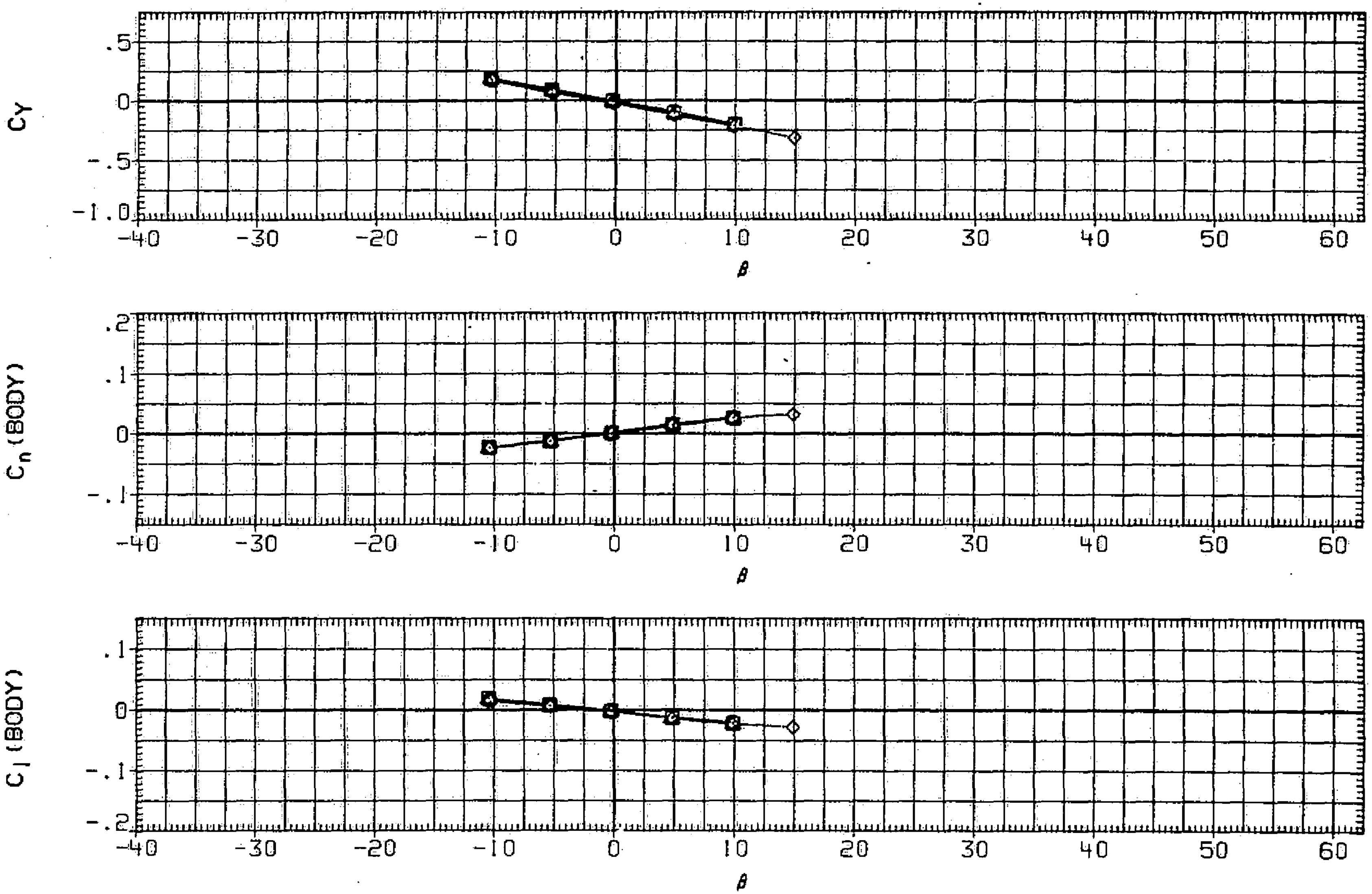

FIG.6 BOOM(I1) AND REY. NO. EFFECTS ON LATERAL-DIRECT. AERO CHARACTERISTICS

(A)ALPHA = 10.10

DATA SET	SYMBOL	CONFIGURATION DESCRIPTION	RN
(RDS047)	○	X1 N3 I1 H1 V2 LH7	.300
(RDS048)	□	X1 N3 I1 H1 V2 LH7	2.250
(RDS049)	◇	X1 N3 H1 V2 LH7	.300
(RDS054)	△	X1 N3 H1 V2 LH7	2.250

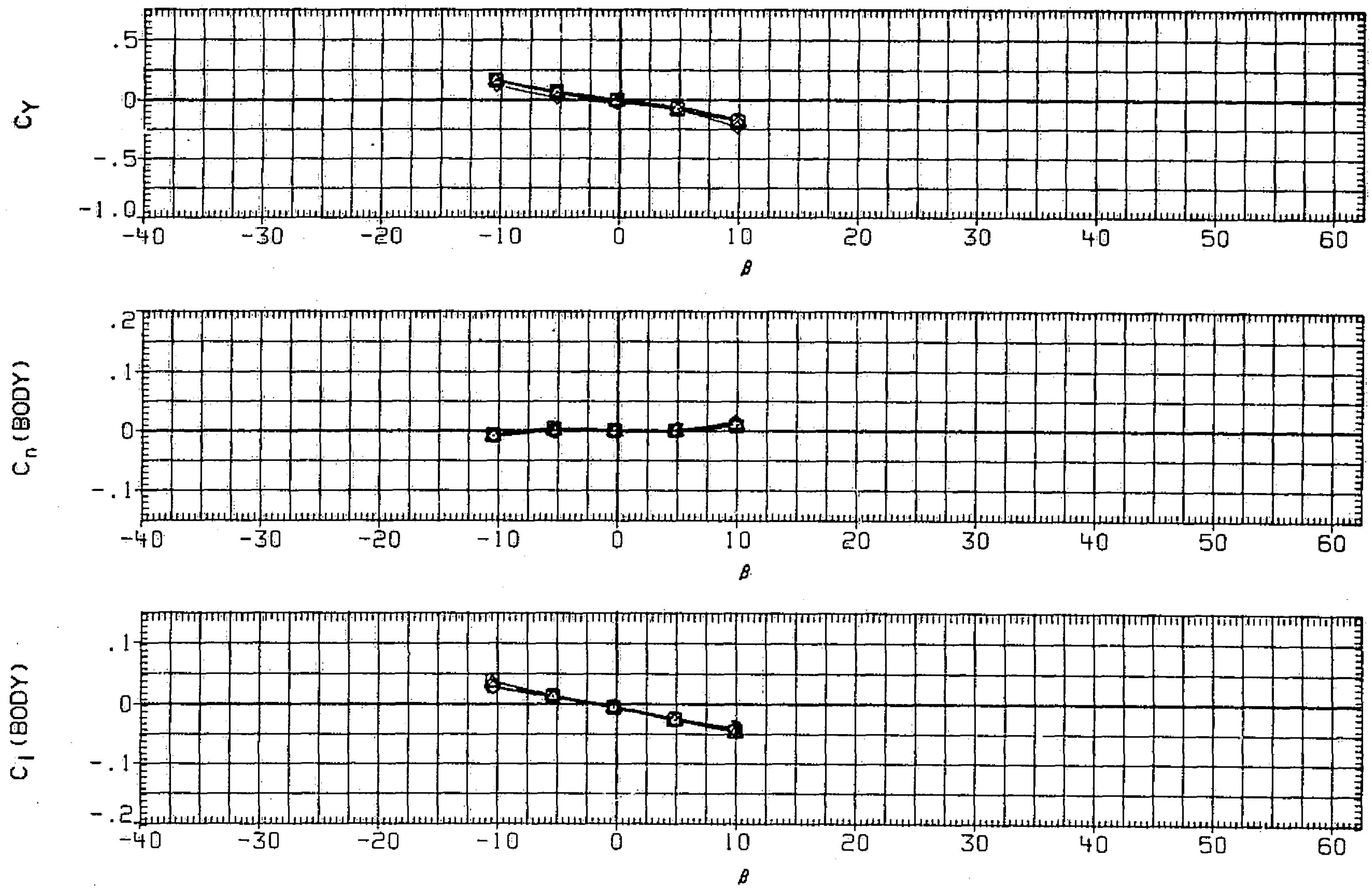

FIG.6 BOOM(I1) AND REY. NO. EFFECTS ON LATERAL-DIRECT. AERO CHARACTERISTICS

(B)ALPHA = 20.27

DATA SET	SYMBOL	CONFIGURATION DESCRIPTION	RN
(RDS047)	○	X1 N3 I1 H1 V2 LH7	.300
(RDS048)	□	X1 N3 I1 H1 V2 LH7	2.250
(RDS049)	◇	X1 N3 H1 V2 LH7	.300
(RDS054)	△	X1 N3 H1 V2 LH7	2.250

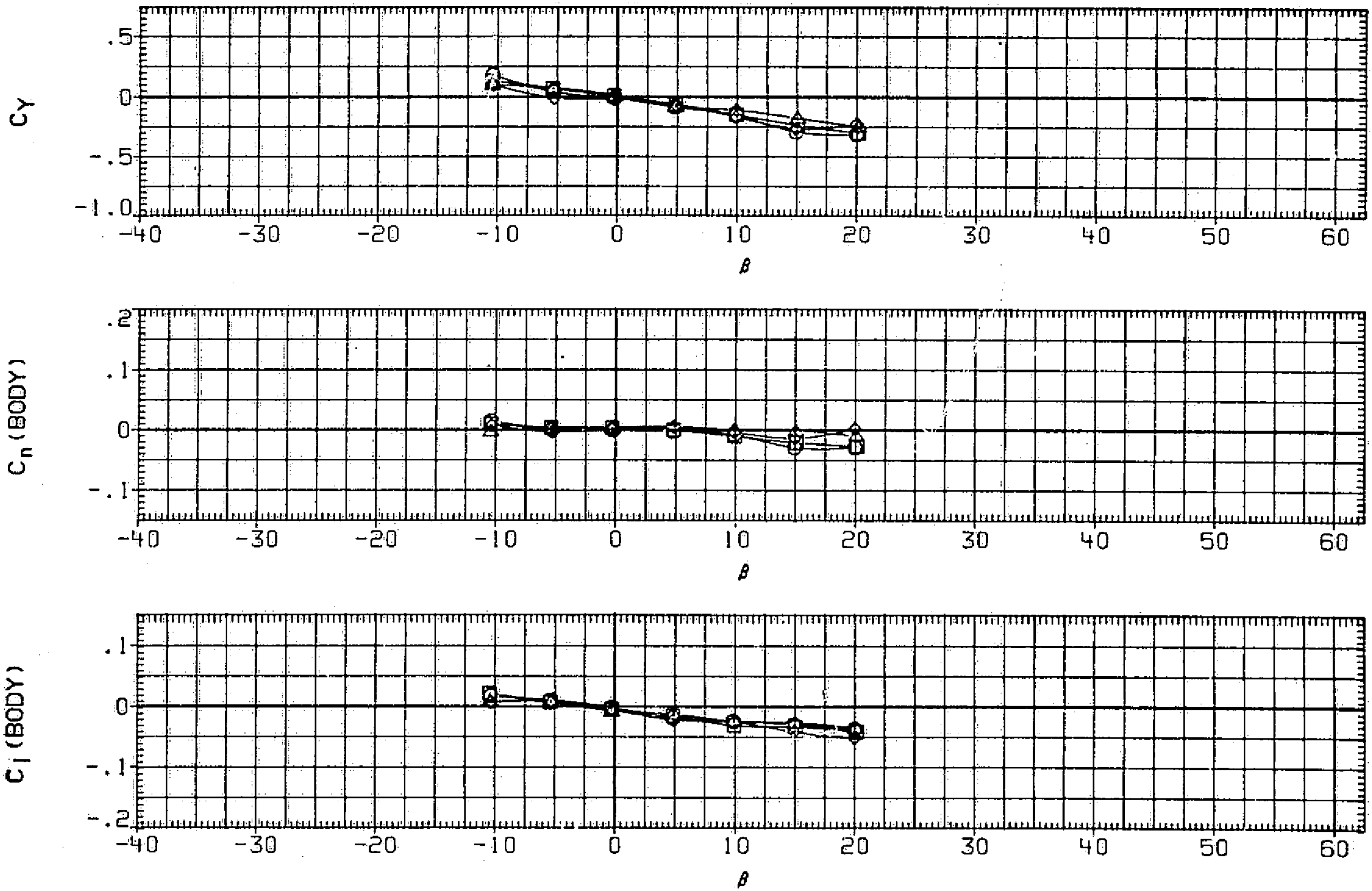

FIG.6 BOOM(II) AND REY. NO. EFFECTS ON LATERAL-DIRECT. AERO CHARACTERISTICS

(C) ALPHA = 30.39

DATA SET	SYMBOL	CONFIGURATION DESCRIPTION	RN
(RDS047)	○	X1 N3 I1 H1 V2 LH7	.300
(RDS048)	□	X1 N3 I1 H1 V2 LH7	2.250
(RDS049)	◇	X1 N3 H1 V2 LH7	.300
(RDS054)	△	X1 N3 H1 V2 LH7	2.250

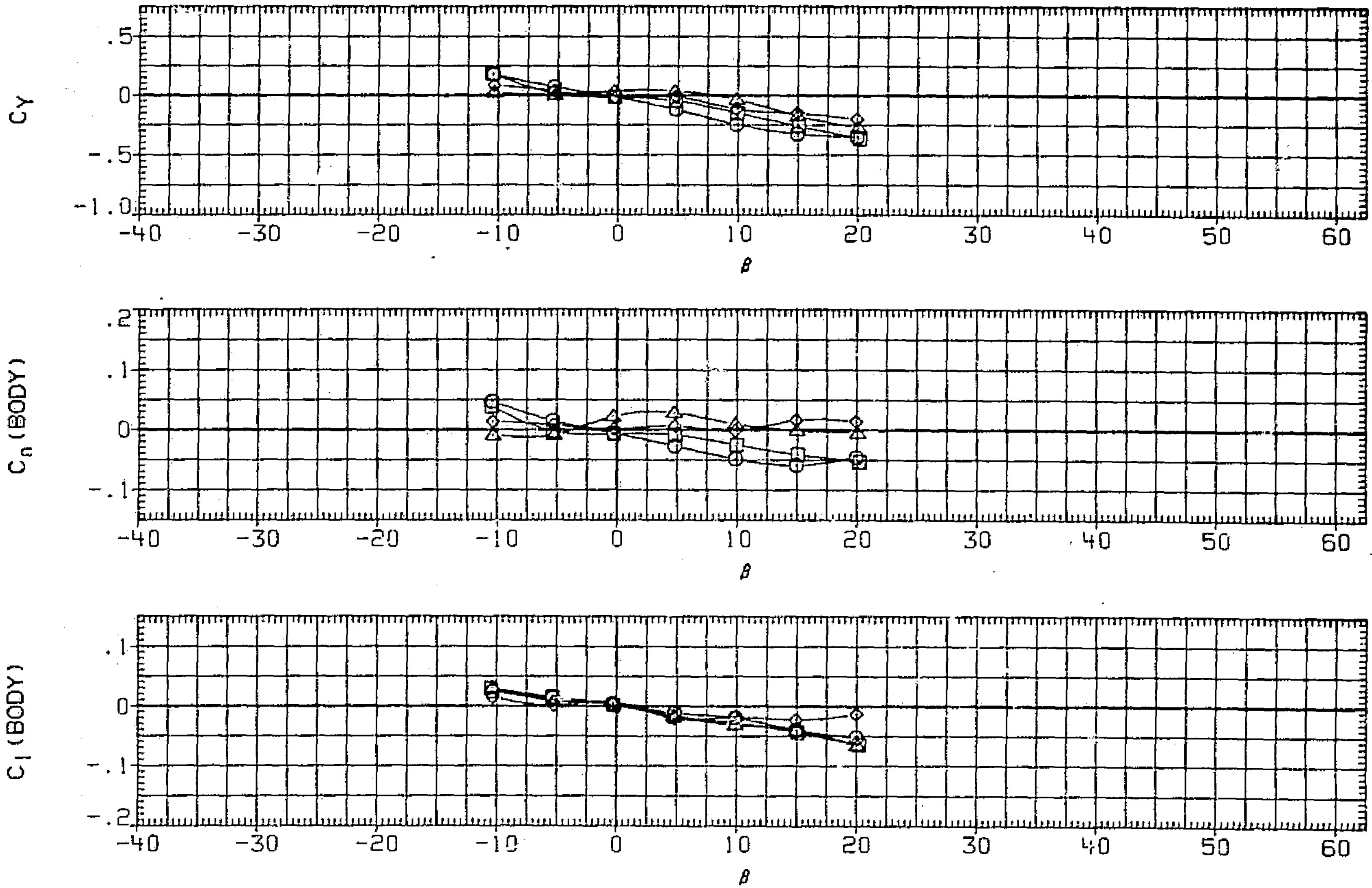

FIG.6 BOOM(I1) AND REY. NO. EFFECTS ON LATERAL-DIRECT. AERO CHARACTERISTICS

(D) ALPHA = 40.42

DATA SET	SYMBOL	CONFIGURATION DESCRIPTION	RN
(RDS008)	○	X2 N1 I1 H1 V2 LH7	.200
(RDS009)	□	X2 N1 I1 H1 V2 LH7	2.250
(RDS010)	◇	X2 N1 H1 V2 LH7	.200
(RDS013)	△	X2 N1 H1 V2 LH7	2.250

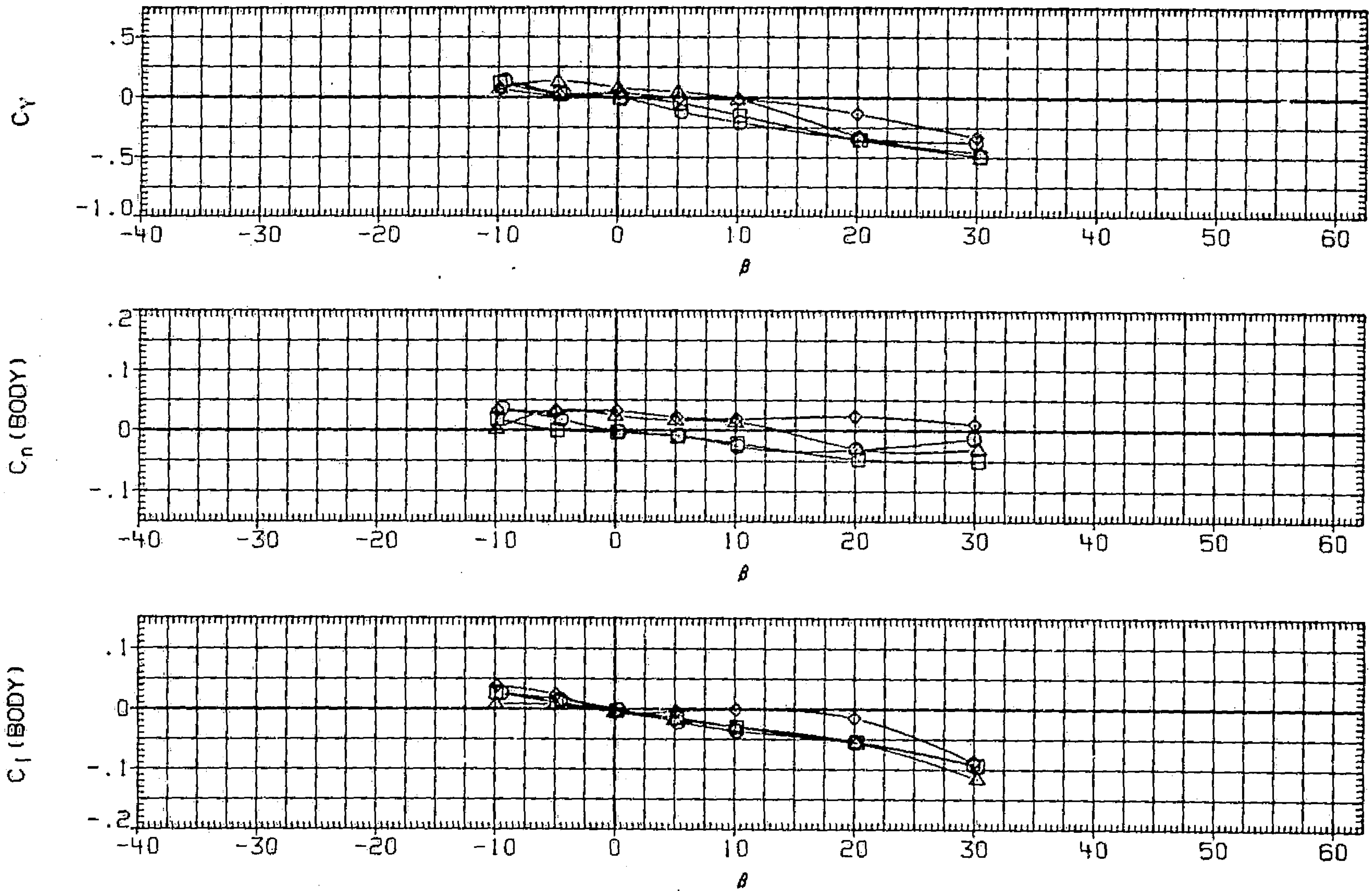

FIG.6 BOOM(II) AND REY. NO. EFFECTS ON LATERAL-DIRECT. AERO CHARACTERISTICS

(A) ALPHA = 40.35

DATA SET	SYMBOL	CONFIGURATION DESCRIPTION	RN
(RDS008)	○	X2 N1 I1 H1 V2 LH7	.200
(RDS009)	□	X2 N1 I1 H1 V2 LH7	2.250
(RDS010)	◇	X2 N1 H1 V2 LH7	.200
(RDS013)	△	X2 N1 H1 V2 LH7	2.250

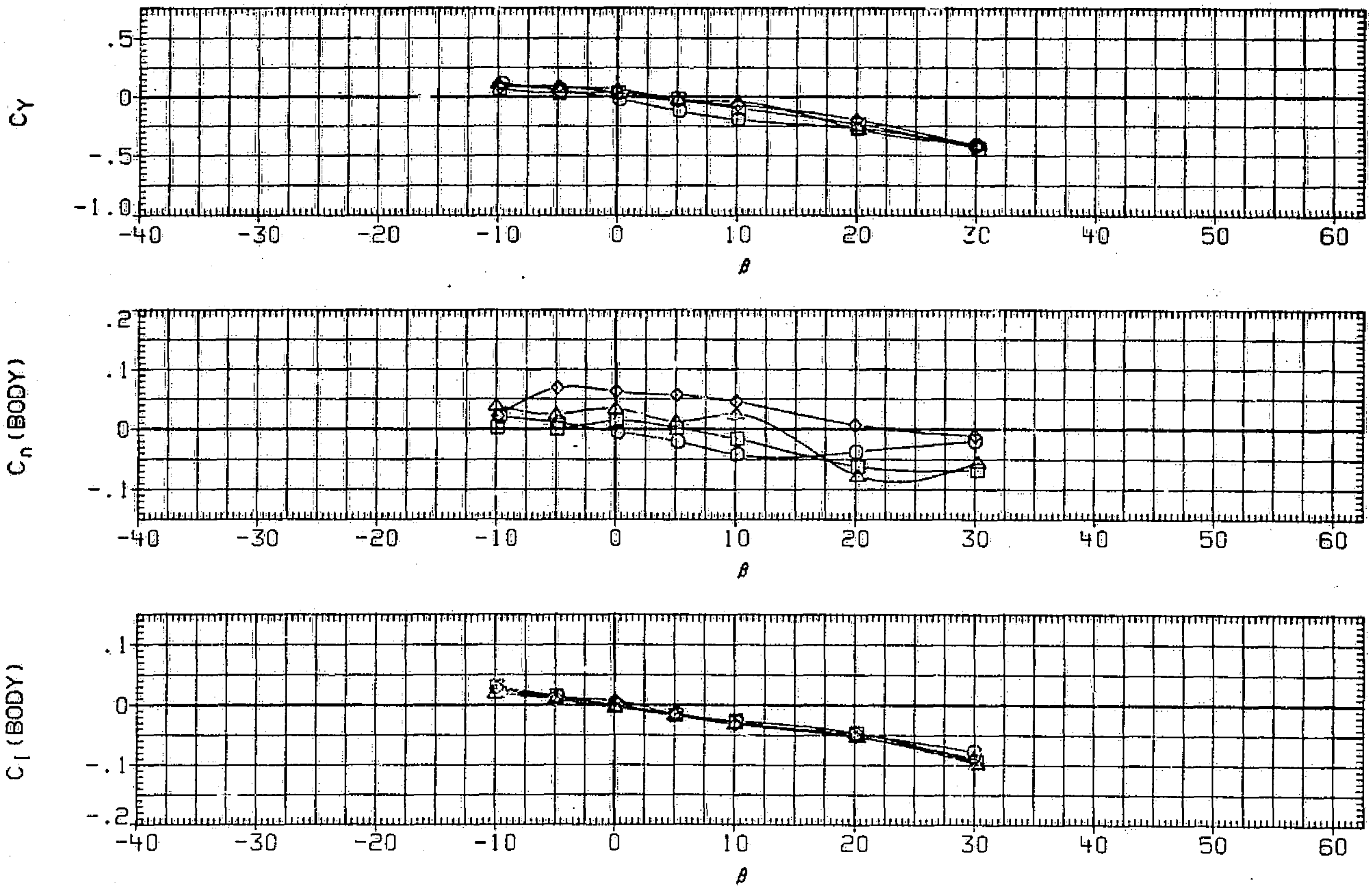

FIG.6 BOOM(I1) AND REY. NO. EFFECTS ON LATERAL-DIRECT. AERO CHARACTERISTICS

(B) ALPHA = 50.33

DATA SET	SYMBOL	CONFIGURATION DESCRIPTION	RN
(RDS008)	○	X2 N1 I1 H1 V2 LH7	.200
(RDS009)	□	X2 N1 I1 H1 V2 LH7	2.250
(RDS010)	◇	X2 N1 H1 V2 LH7	.200
(RDS013)	△	X2 N1 H1 V2 LH7	2.250

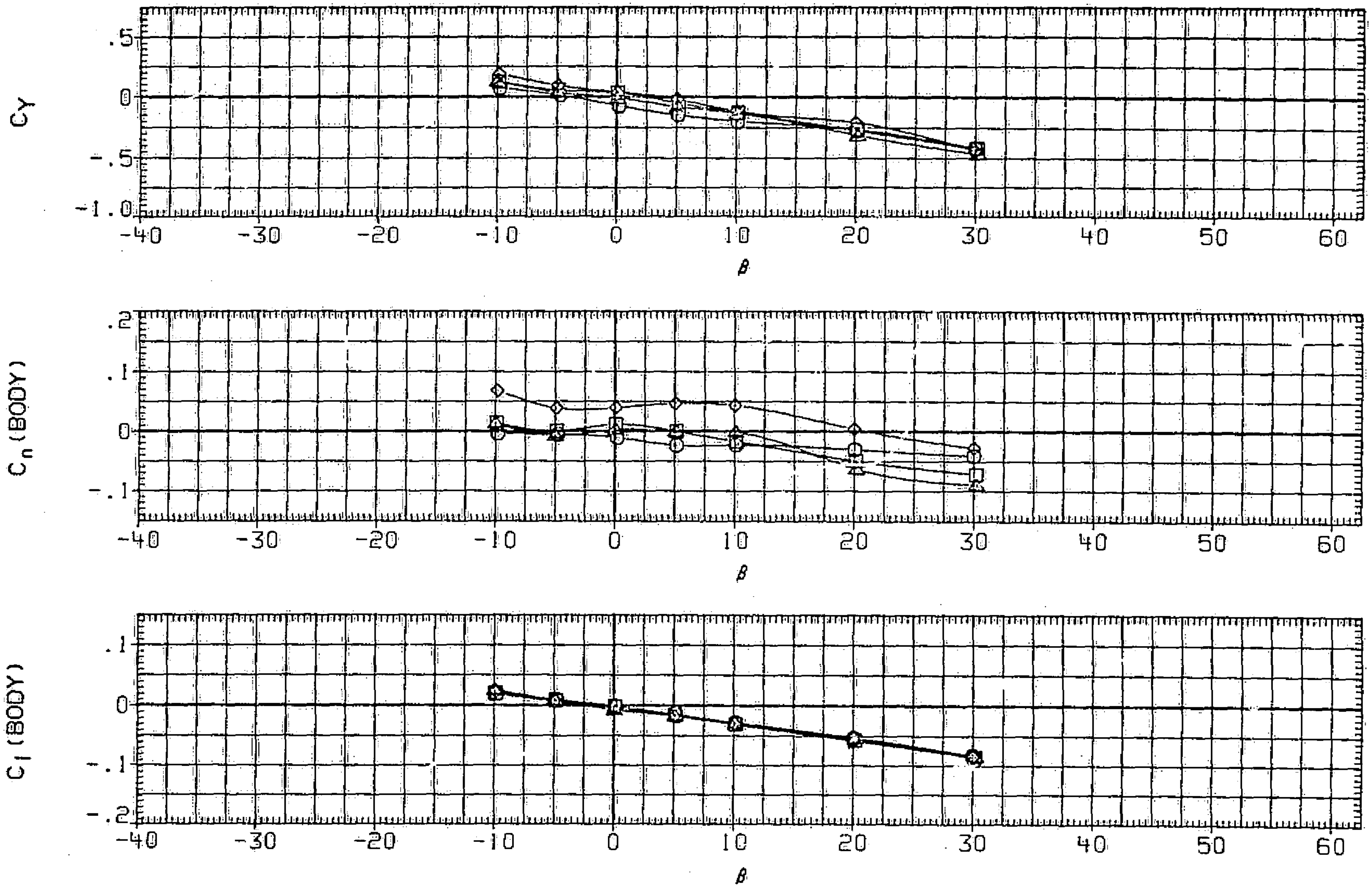

FIG.6 BOOM(II) AND REY. NO. EFFECTS ON LATERAL-DIRECT. AERO CHARACTERISTICS

(C)ALPHA = 60.28

DATA SET	SYMBOL	CONFIGURATION DESCRIPTION	RN
(RDS008)	○	X2 N1 I1 H1 V2 LH7	.200
(RDS009)	□	X2 N1 I1 H1 V2 LH7	2.250
(RDS010)	◇	X2 N1 H1 V2 LH7	.200
(RDS013)	△	X2 N1 H1 V2 LH7	2.250

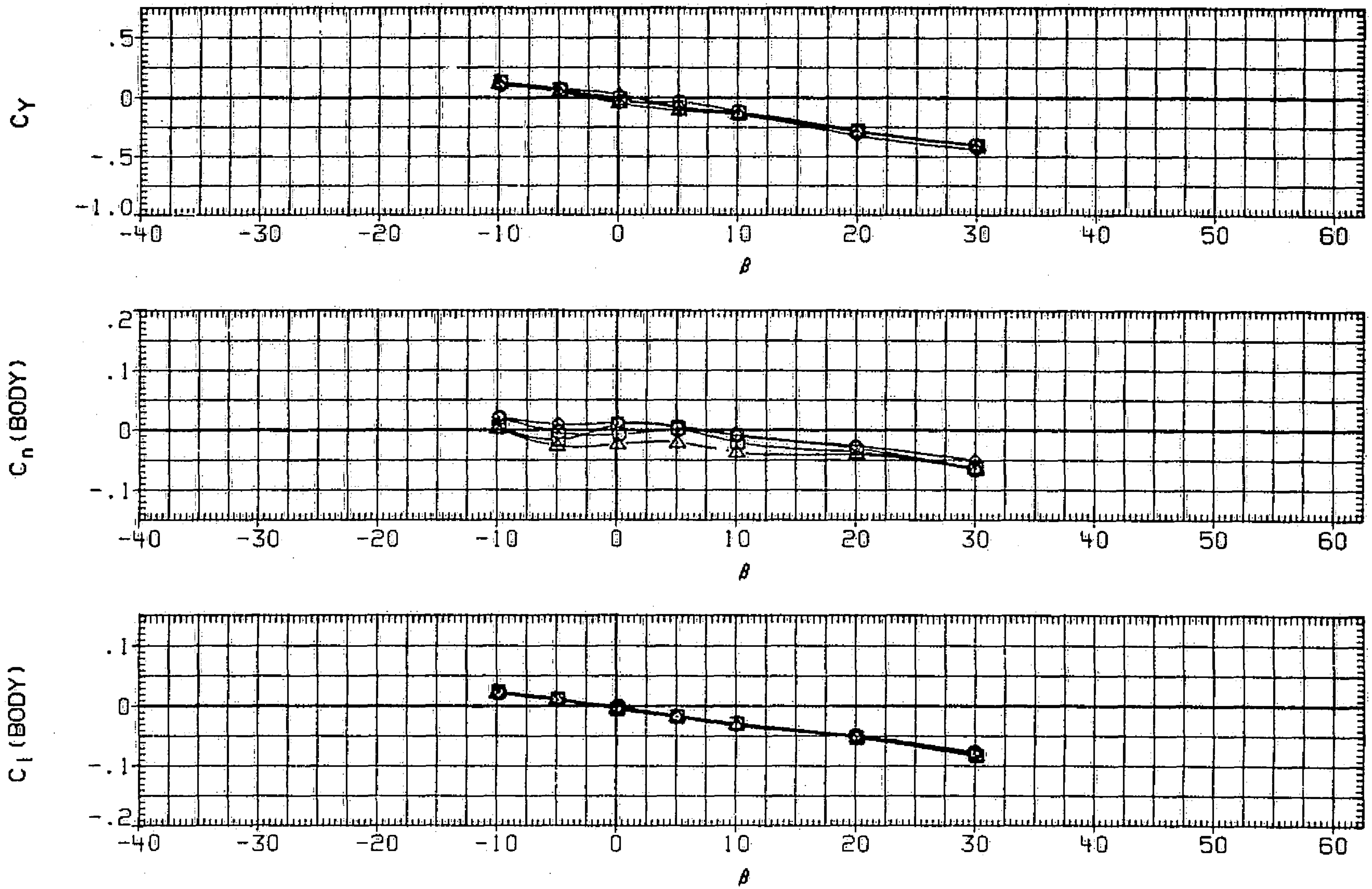

FIG.6 BOOM(I1) AND REY. NO. EFFECTS ON LATERAL-DIRECT. AERO CHARACTERISTICS

(D) ALPHA = 70.30

DATA SET	SYMBOL	CONFIGURATION DESCRIPTION	RN
(RDS008)	○	X2 N1 I1 H1 V2 LH7	.200
(RDS009)	□	X2 N1 I1 H1 V2 LH7	2.250
(RDS010)	◇	X2 N1 H1 V2 LH7	.200
(RDS013)	△	X2 N1 H1 V2 LH7	2.250

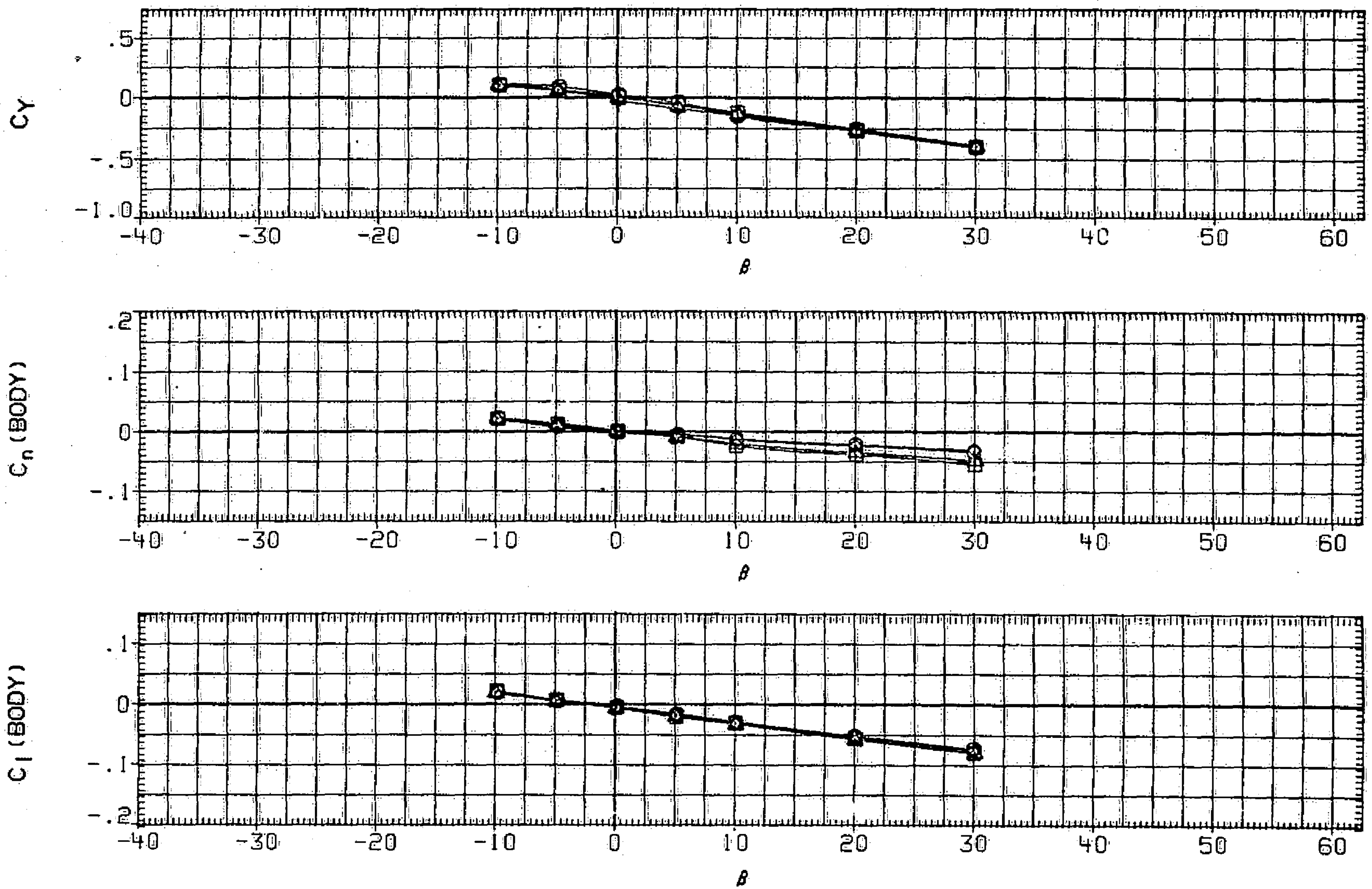

FIG.6 BOOM(II) AND REY. NO. EFFECTS ON LATERAL-DIRECT. AERO CHARACTERISTICS

(E) ALPHA = 80.30

DATA SET	SYMBOL	CONFIGURATION DESCRIPTION	RN
(RDS008)	○	X2 N1 I1 H1 V2 LH7	.200
(RDS009)	□	X2 N1 I1 H1 V2 LH7	2.250
(RDS010)	◇	X2 N1 H1 V2 LH7	.200
(RDS013)	△	X2 N1 H1 V2 LH7	2.250

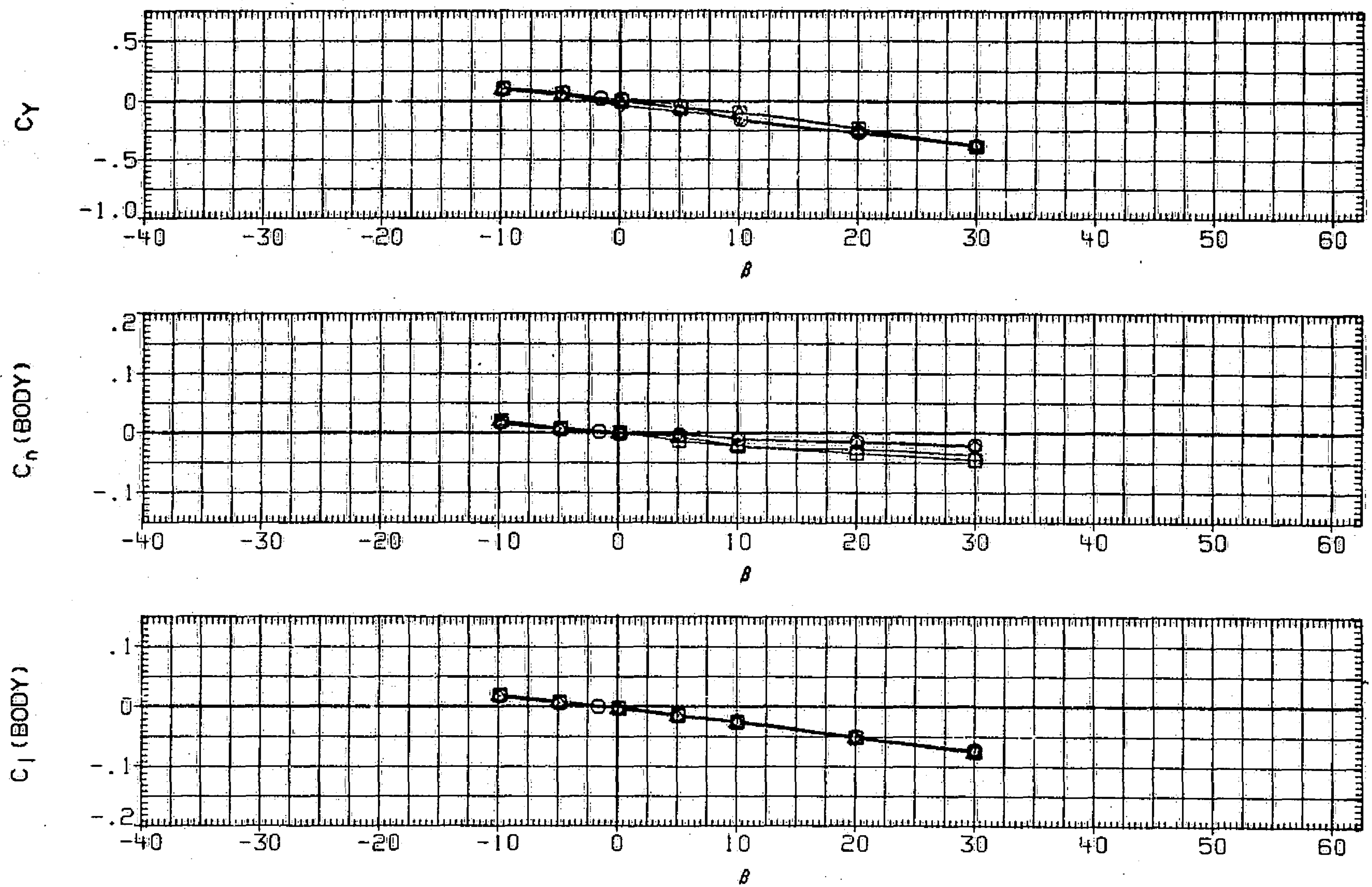

FIG.6 BOOM(I1) AND REY. NO. EFFECTS ON LATERAL-DIRECT. AERO CHARACTERISTICS

(F) ALPHA = 89.22

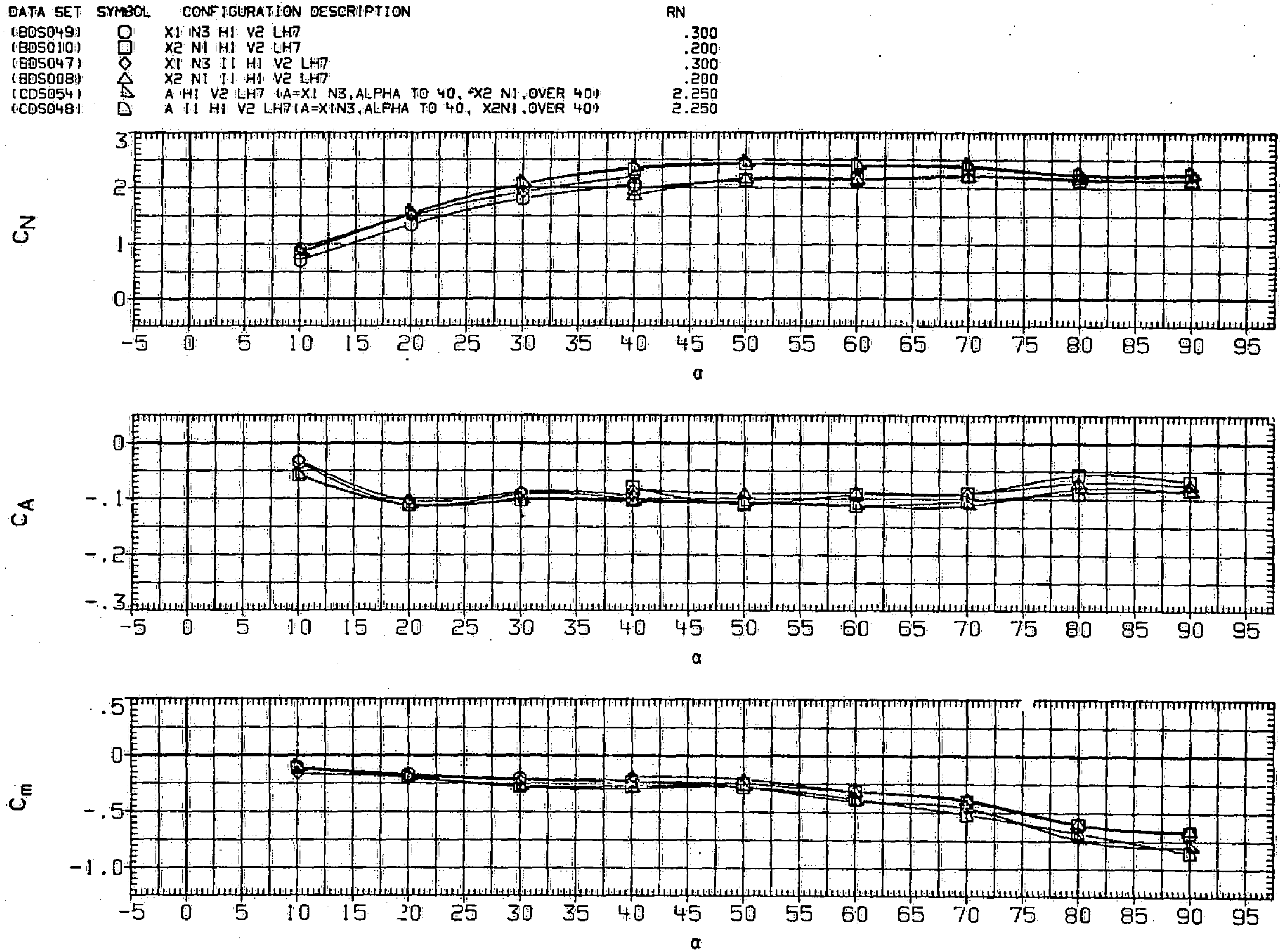

FIG.7 BOOM(I1) AND REY. NO. EFFECTS ON LONGITUD. AERO CHARACTERISTICS

(A)BETA = .00

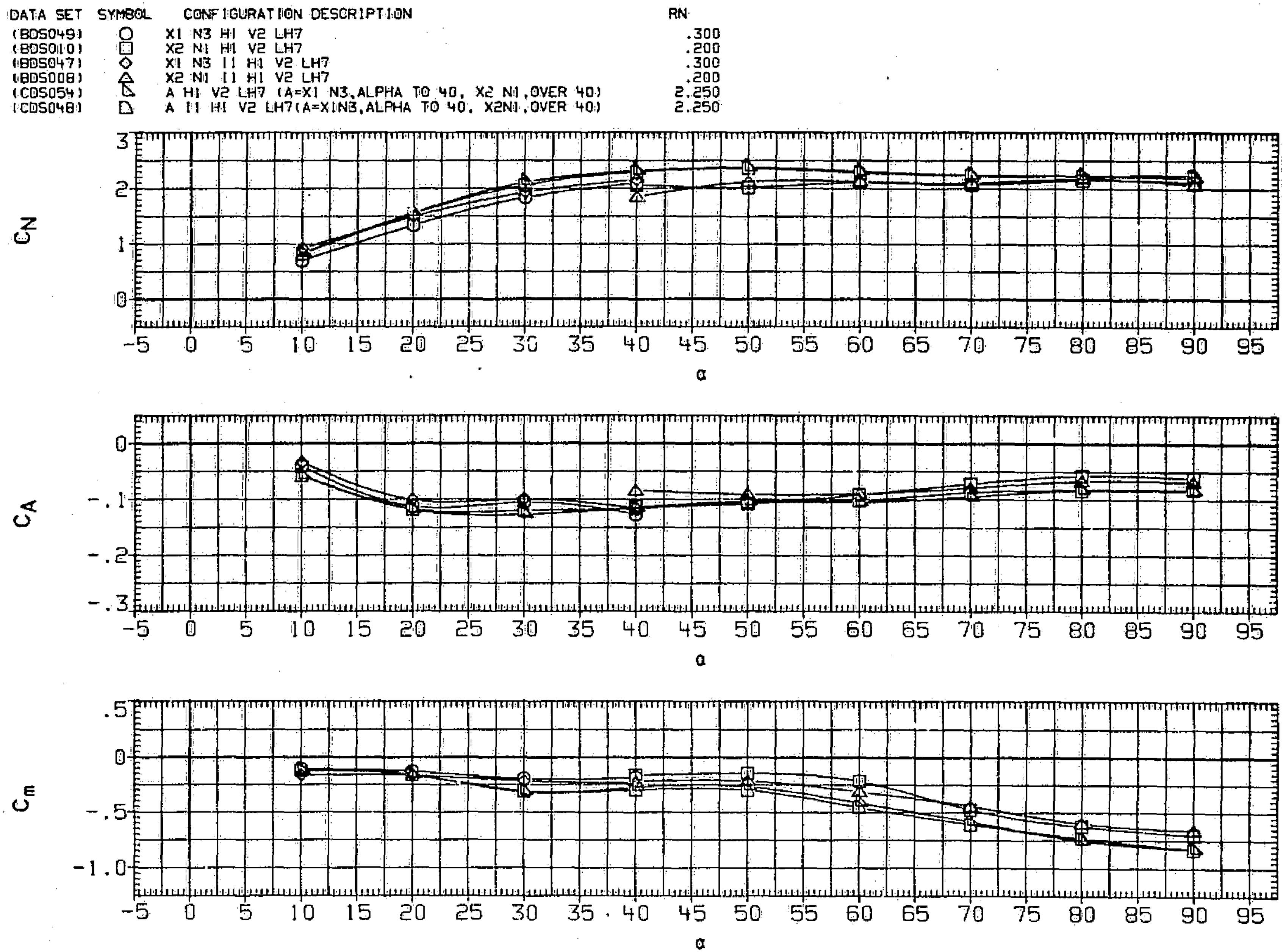

FIG.7 BOOM(I1) AND REY. NO. EFFECTS ON LONGITUD. AERO CHARACTERISTICS

(B)BETA = 10.00

DATA SET	SYMBOL	CONFIGURATION DESCRIPTION	RN
(BDS049)	○	X1 N3 H1 V2 LH7	.300
(BDS010)	□	X2 N1 H1 V2 LH7	.200
(BDS047)	◇	X1 N3 I1 H1 V2 LH7	.300
(BDS008)	△	X2 N1 I1 H1 V2 LH7	.200
(CDS054)	⊿	A H1 V2 LH7 (A=X1 N3,ALPHA TO 40, X2 N1,OVER 40)	2.250
(CDS048)	◺	A I1 H1 V2 LH7(A=X1N3,ALPHA TO 40, X2N1,OVER 40)	2.250

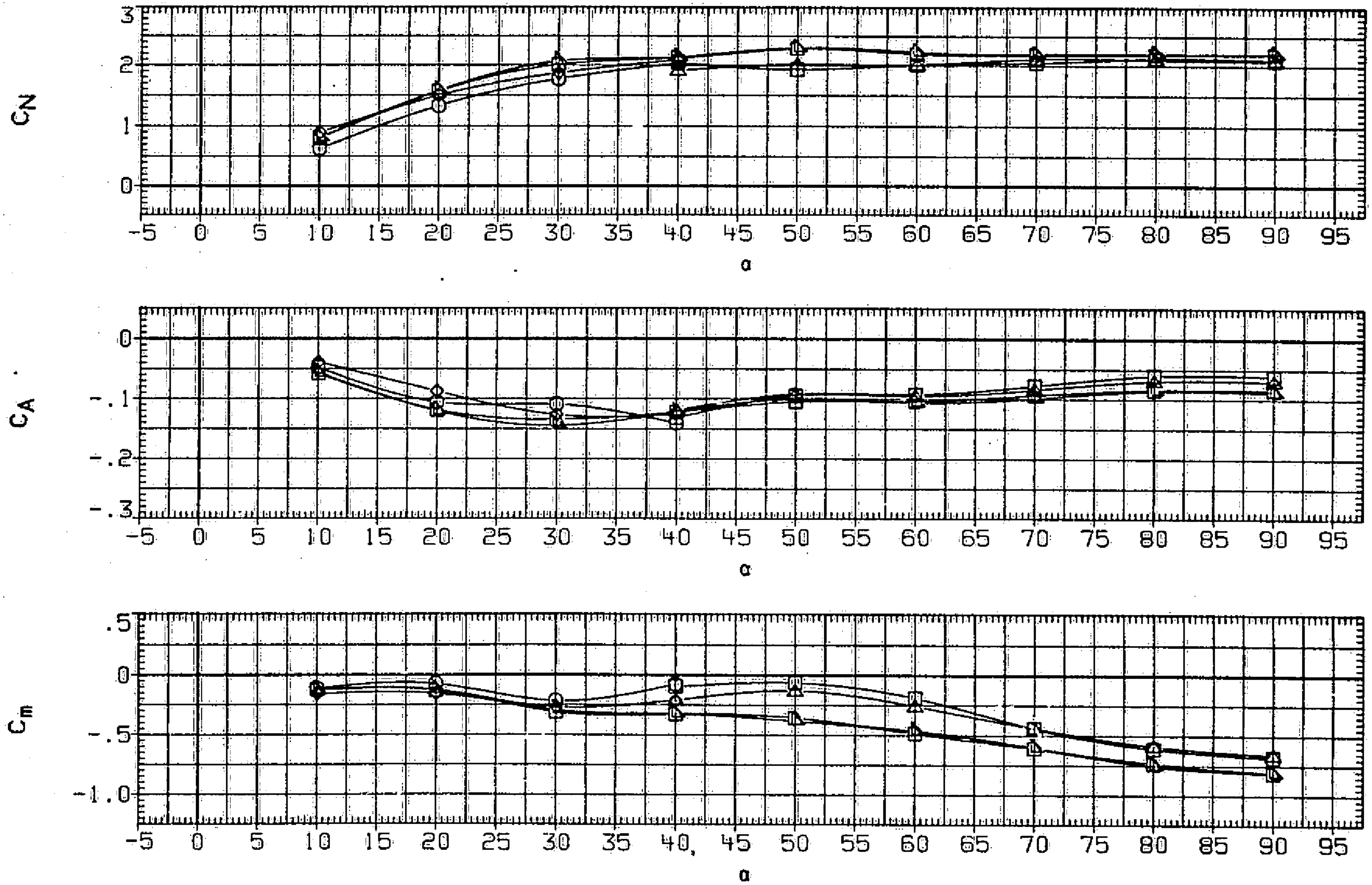

FIG.7 BOOM(II) AND REY. NO. EFFECTS ON LONGITUD. AERO CHARACTERISTICS

(C)BETA = 20.00

DATA SET	SYMBOL	CONFIGURATION DESCRIPTION	RN
(RDS049)	○	X1 N3 H1 V2 LH7	.300
(RDS045)	□	X1 N3 S2 H1 V2 LH7	.300
(RDS054)	◇	X1 N3 H1 V2 LH7	2.250
(RDS046)	△	X1 N3 S2 H1 V2 LH7	2.250

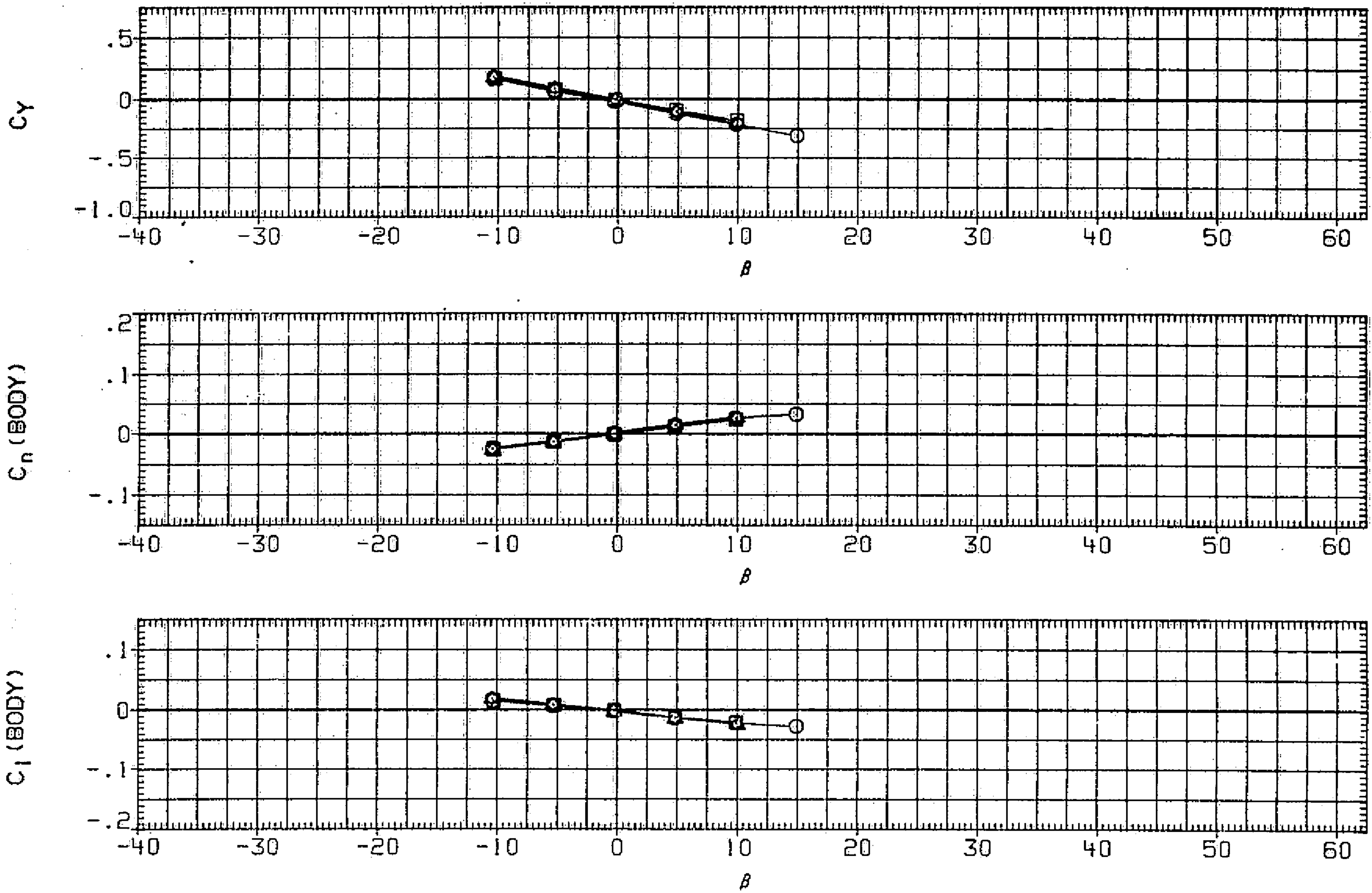

FIG.8 STRAKES(S2) AND REY. NO. EFFECTS ON LATERAL-DIRECT. AERO CHARACTERISTICS

(A) ALPHA = 10.09

DATA SET	SYMBOL	CONFIGURATION DESCRIPTION	RN
(RDS049)	○	X1 N3 H1 V2 LH7	.300
(RDS045)	□	X1 N3 S2 H1 V2 LH7	.300
(RDS054)	◇	X1 N3 H1 V2 LH7	2.250
(RDS046)	△	X1 N3 S2 H1 V2 LH7	2.250

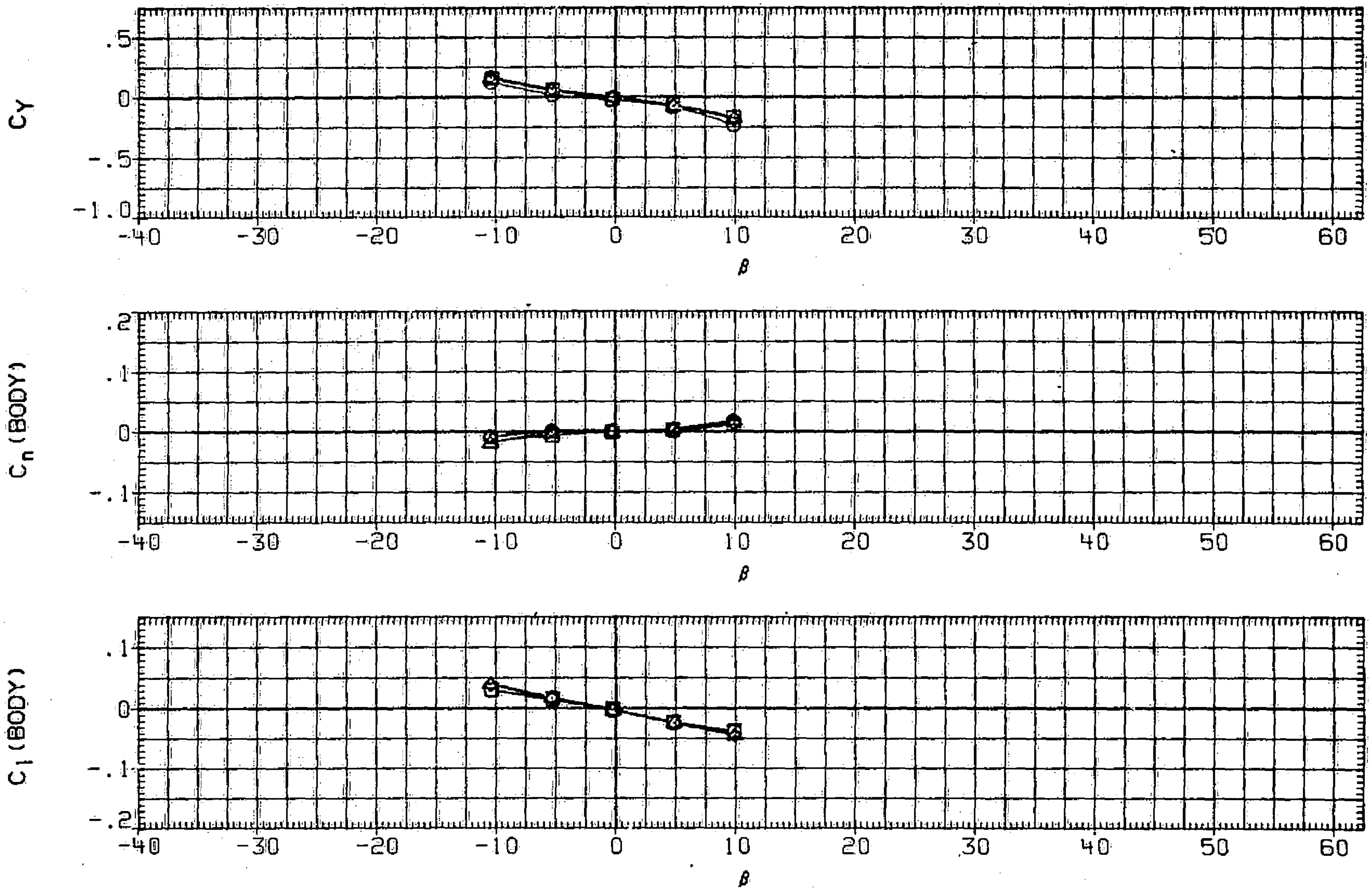

FIG.8 STRAKES(S2) AND REY. NO. EFFECTS ON LATERAL-DIRECT. AERO CHARACTERISTICS

(B) ALPHA = 20.27

DATA SET	SYMBOL	CONFIGURATION DESCRIPTION	RN
(RDS049)	○	X1 N3 H1 V2 LH7	.300
(RDS045)	□	X1 N3 S2 H1 V2 LH7	.300
(RDS054)	◇	X1 N3 H1 V2 LH7	2.250
(RDS046)	△	X1 N3 S2 H1 V2 LH7	2.250

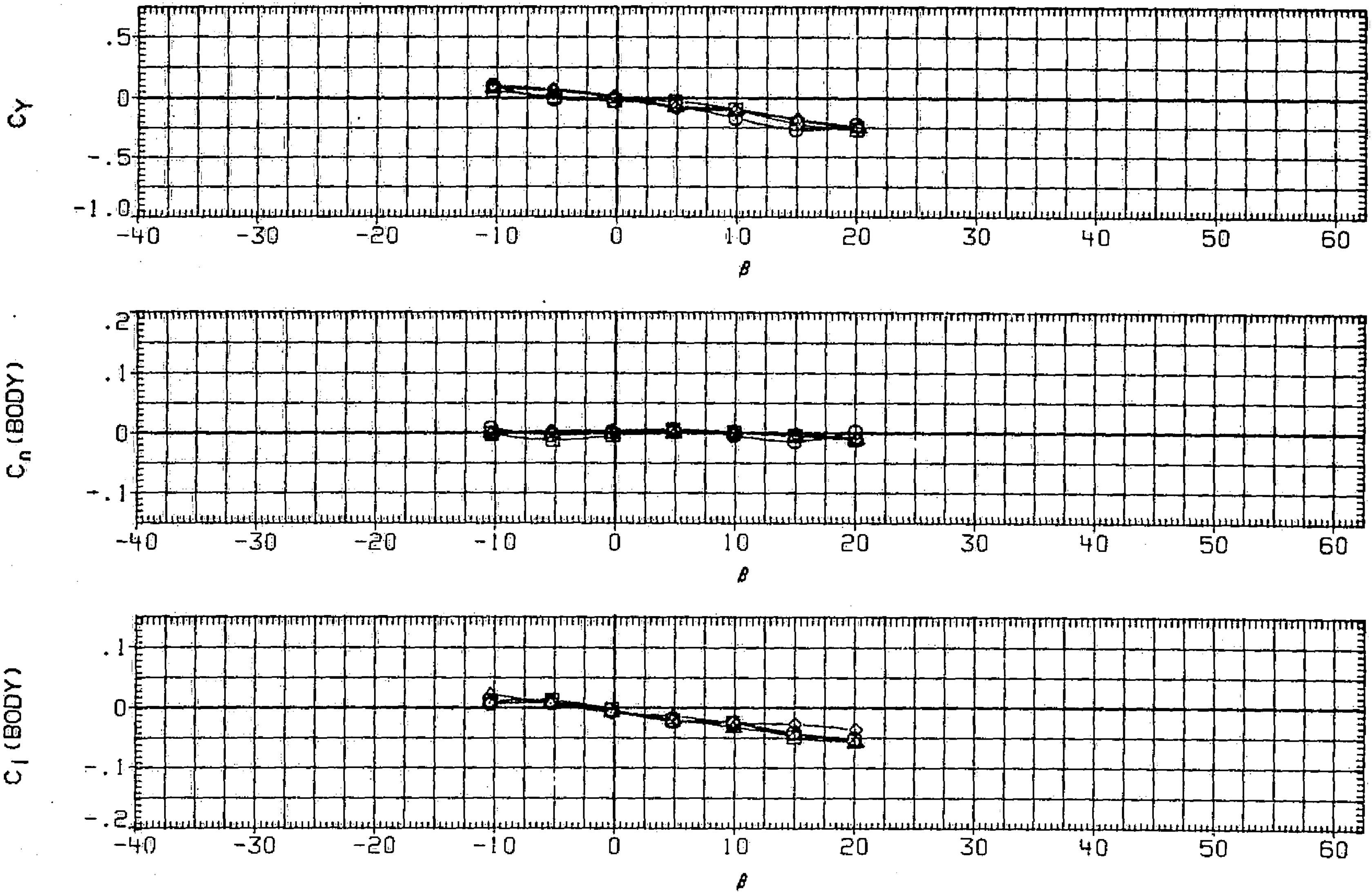

FIG.8 STRAKES(S2) AND REY. NO. EFFECTS ON LATERAL-DIRECT. AERO CHARACTERISTICS

(C) ALPHA = 30.44

DATA SET	SYMBOL	CONFIGURATION DESCRIPTION	RN
(RDS049)	○	X1 N3 H1 V2 LH7	.300
(RDS045)	□	X1 N3 S2 H1 V2 LH7	.300
(RDS054)	◇	X1 N3 H1 V2 LH7	2.250
(RDS046)	△	X1 N3 S2 H1 V2 LH7	2.250

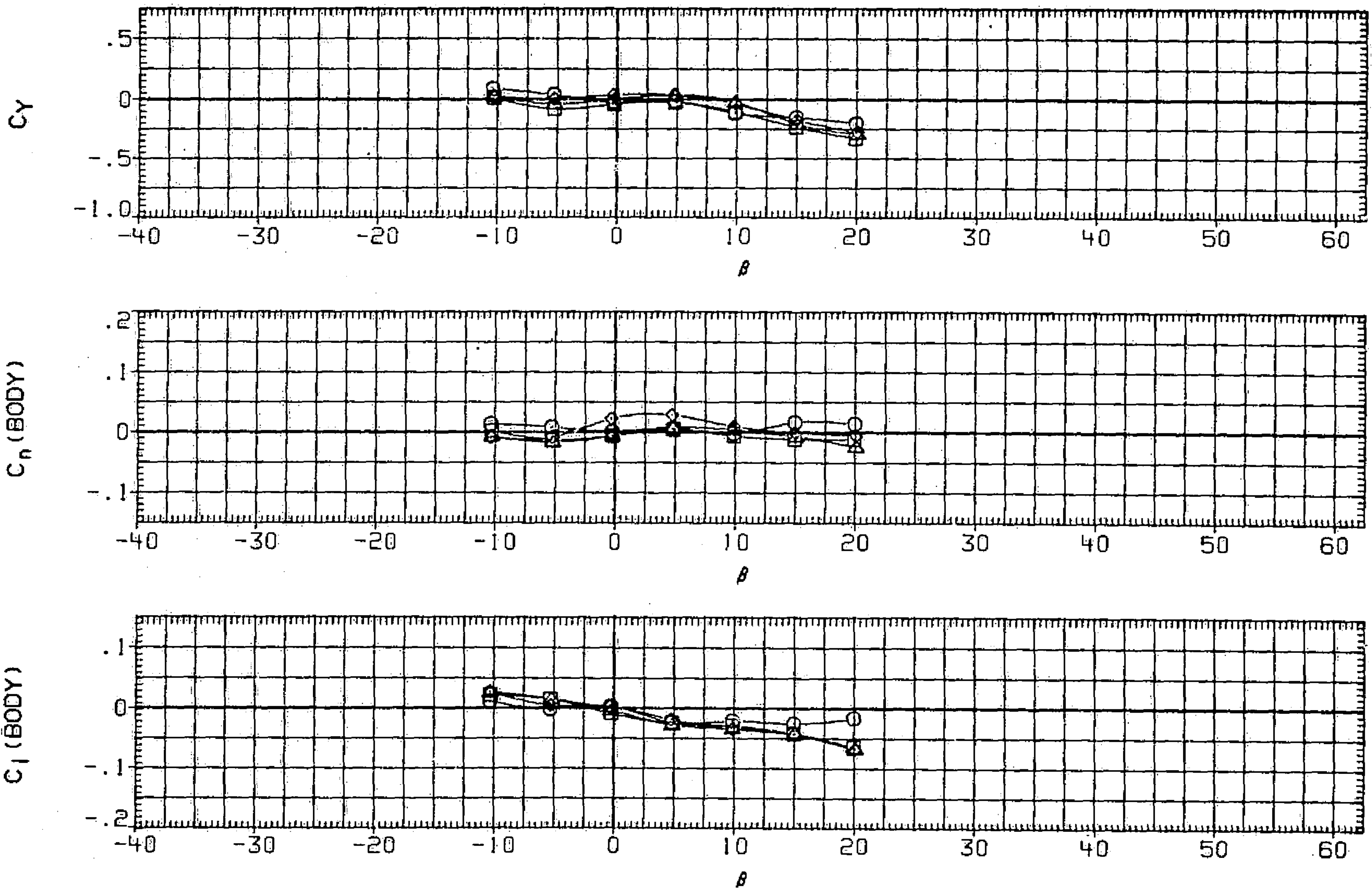

FIG.8 STRAKES(S2) AND REY. NO. EFFECTS ON LATERAL-DIRECT. AERO CHARACTERISTICS

(D) ALPHA = 40.44

DATA SET	SYMBOL	CONFIGURATION DESCRIPTION	RN
(RDS010)	○	X2 N1 H1 V2 LH7	.200
(RDS001)	□	X2 N1 S2 H1 V2 LH7	.200
(RDS013)	◇	X2 N1 H1 V2 LH7	2.250
(RDS003)	△	X2 N1 S2 H1 V2 LH7	2.250

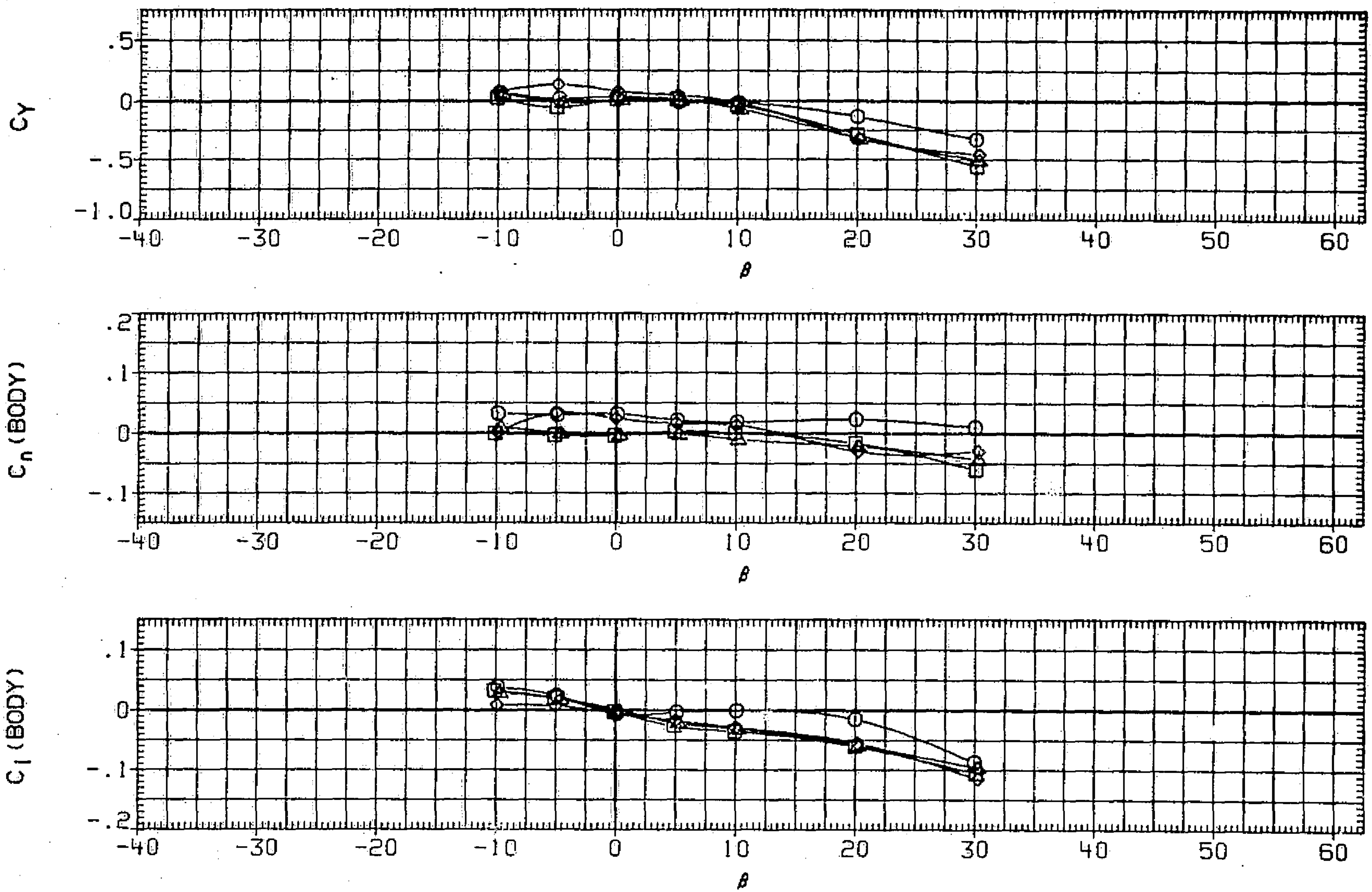

FIG.8 STRAKES(S2) AND REY. NO. EFFECTS ON LATERAL-DIRECT. AERO CHARACTERISTICS

(A) ALPHA = 40.33

DATA SET	SYMBOL	CONFIGURATION DESCRIPTION	RN
(RDS010)	○	X2 N1 H1 V2 LH7	.200
(RDS001)	□	X2 N1 S2 H1 V2 LH7	.200
(RDS013)	◇	X2 N1 H1 V2 LH7	2.250
(RDS003)	△	X2 N1 S2 H1 V2 LH7	2.250

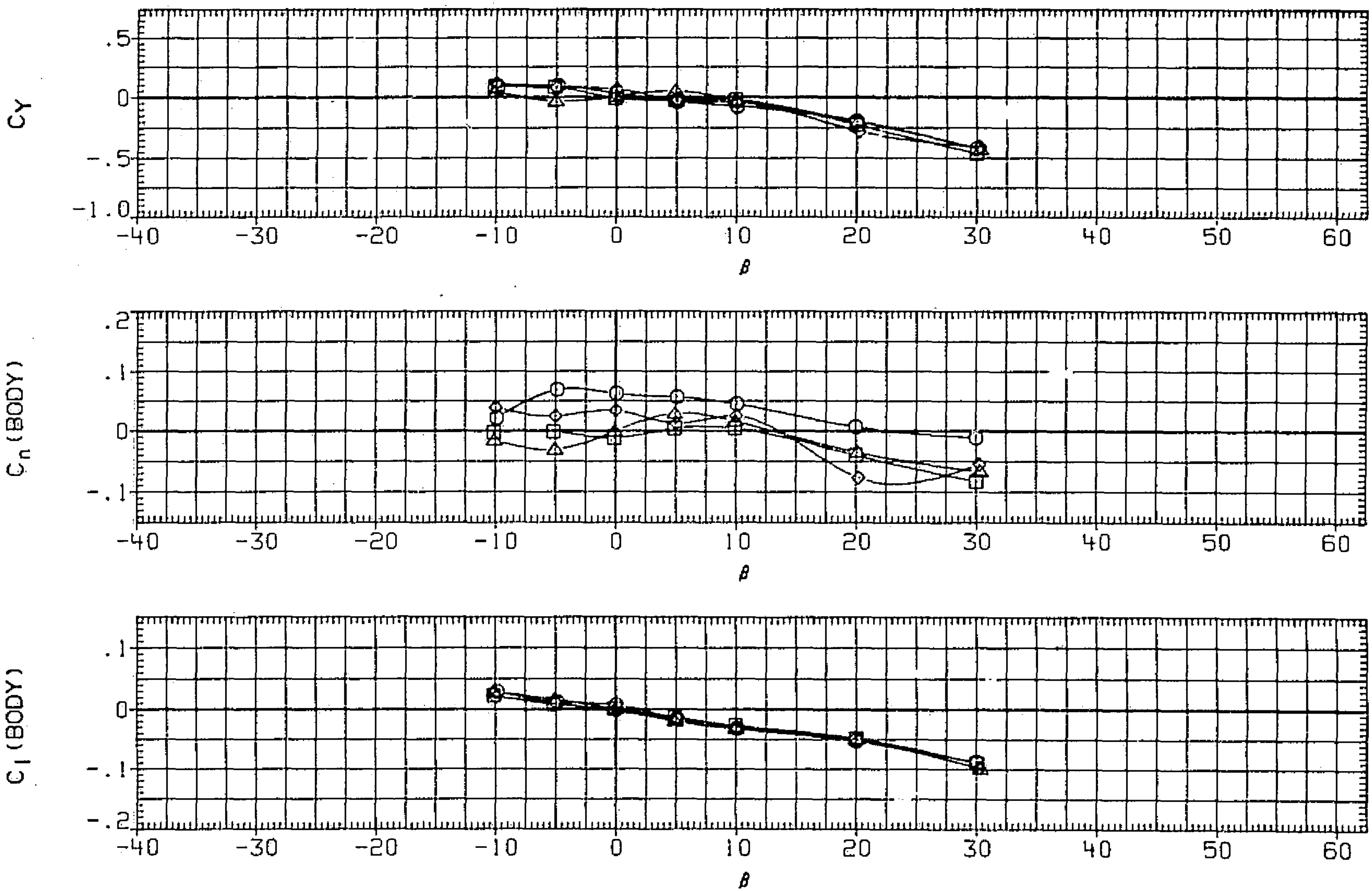

FIG.8 STRAKES(S2) AND REY. NO. EFFECTS ON LATERAL-DIRECT. AERO CHARACTERISTICS

(B) ALPHA = 50.36

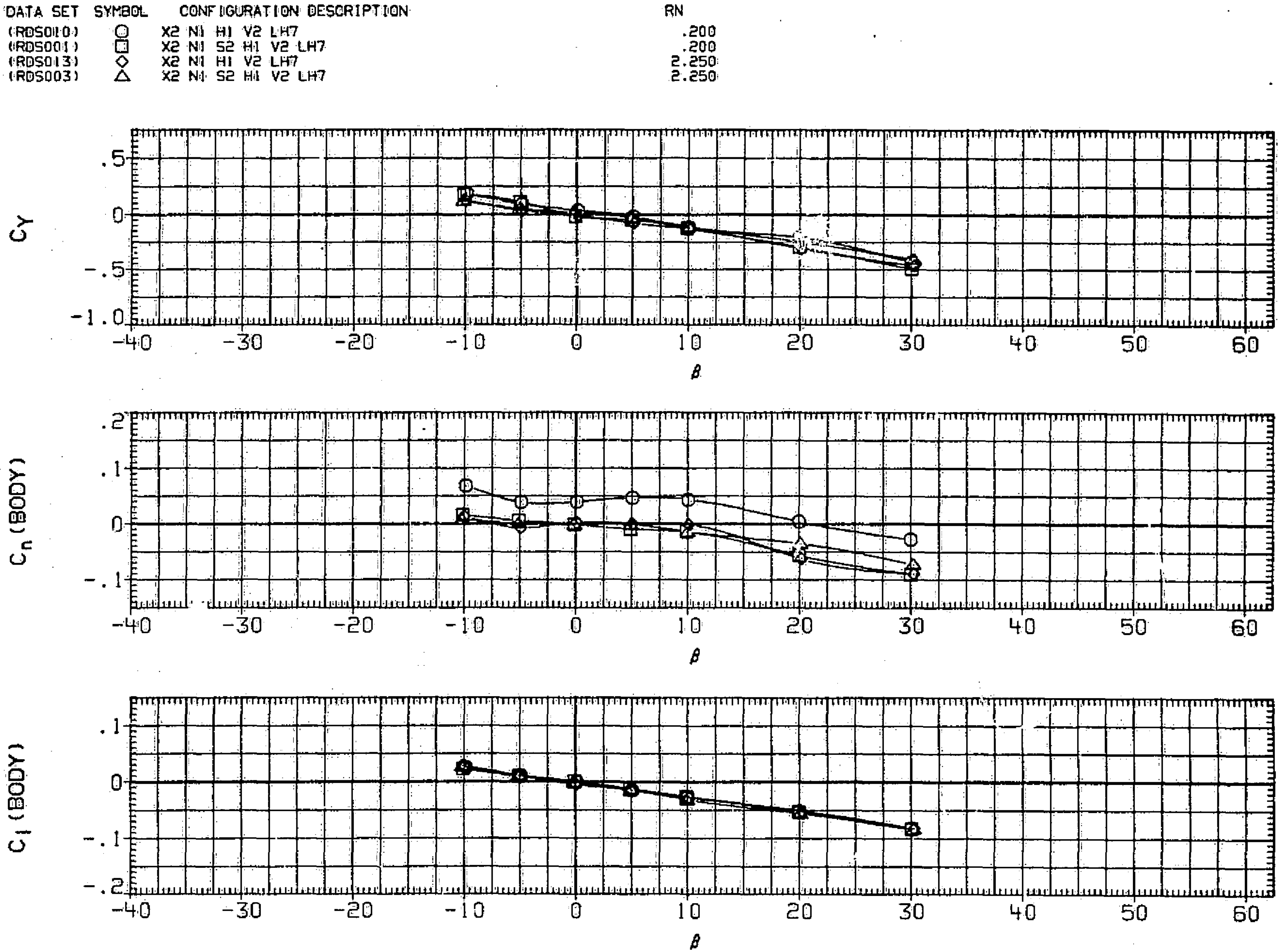

FIG.8 STRAKES(S2) AND REY. NO. EFFECTS ON LATERAL-DIRECT. AERO CHARACTERISTICS

(C) ALPHA = 60.27

DATA SET	SYMBOL	CONFIGURATION DESCRIPTION	RN
(RDS010)	○	X2 N1 H1 V2 LH7	.200
(RDS001)	□	X2 N1 S2 H1 V2 LH7	.200
(RDS013)	◇	X2 N1 H1 V2 LH7	2.250
(RDS003)	△	X2 N1 S2 H1 V2 LH7	2.25U

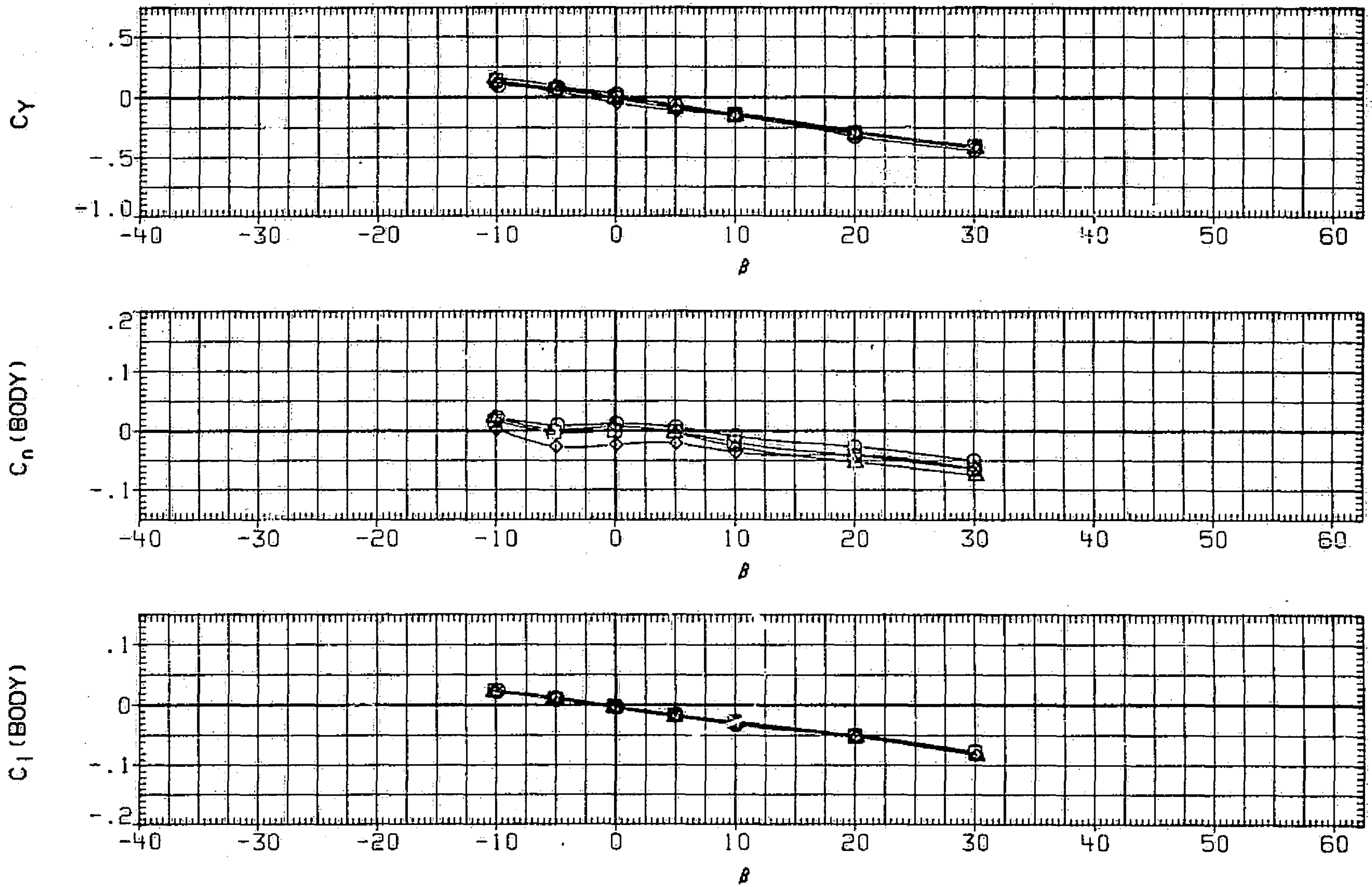

FIG.8 STRAKES(S2) AND REY. NO. EFFECTS ON LATERAL-DIRECT. AERO CHARACTERISTICS

(D) ALPHA = 70.27

DATA SET	SYMBOL	CONFIGURATION DESCRIPTION	RN
(RDS010)	○	X2 N1 H1 V2 LH7	.200
(RDS001)	□	X2 N1 S2 H1 V2 LH7	.200
(RDS013)	◇	X2 N1 H1 V2 LH7	2.250
(RDS003)	△	X2 N1 S2 H1 V2 LH7	2.250

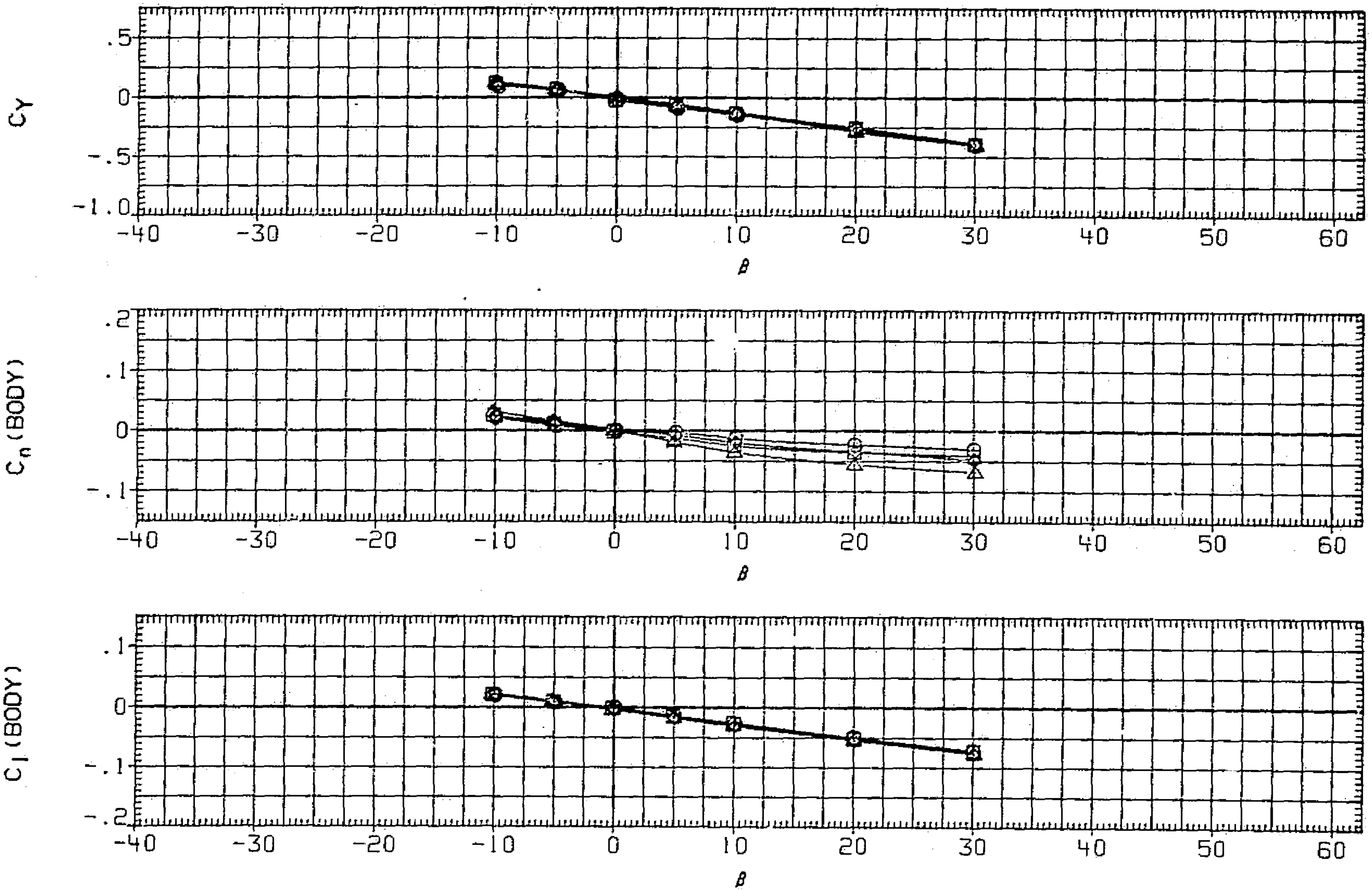

FIG.8 STRAKES(S2) AND REY. NO. EFFECTS ON LATERAL-DIRECT. AERO CHARACTERISTICS
(E) ALPHA = 80.21

DATA SET	SYMBOL	CONFIGURATION DESCRIPTION	RN
(RDS010)	○	X2 N1 H1 V2 LH7	.200
(RDS001)	□	X2 N1 S2 H1 V2 LH7	.200
(RDS013)	◇	X2 N1 H1 V2 LH7	2.250
(RDS003)	△	X2 N1 S2 H1 V2 LH7	2.250

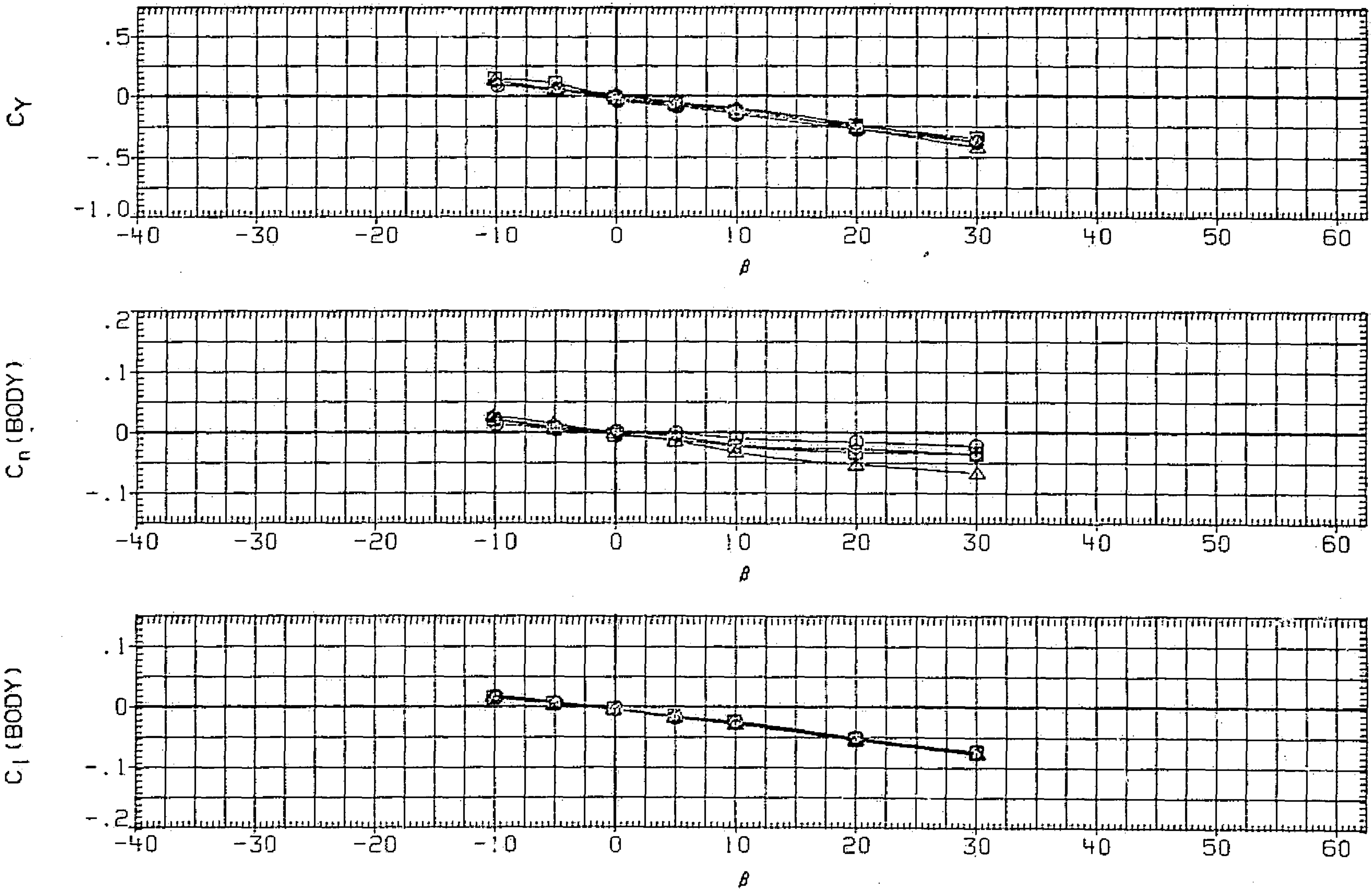

FIG.8 STRAKES(S2) AND REY. NO. EFFECTS ON LATERAL-DIRECT. AERO CHARACTERISTICS

(F) ALPHA = 89.21

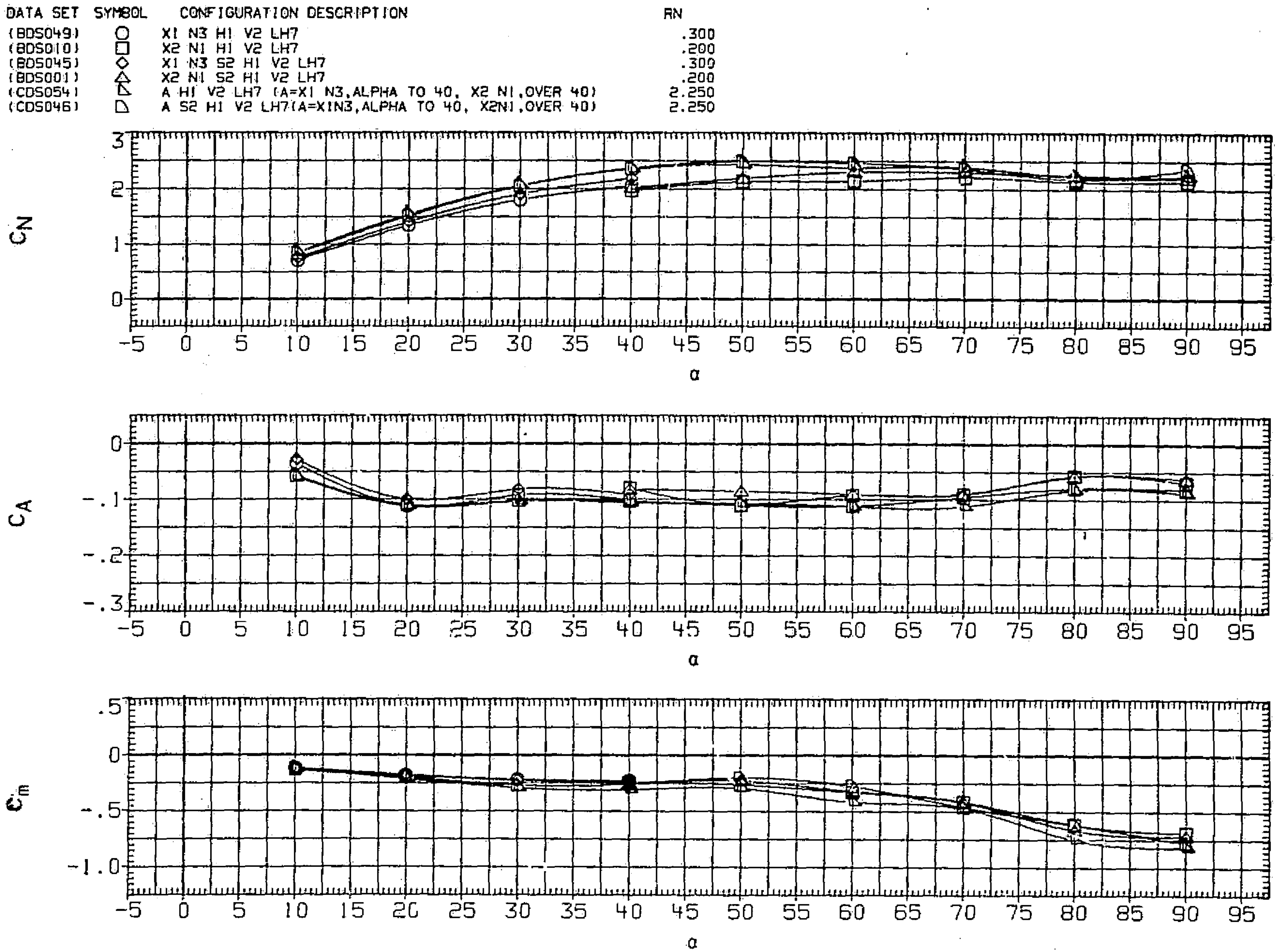

FIG.9 STRAKES(S2) AND REY. NO. EFFECTS ON LONGITUD. AERO CHARACTERISTICS

(A)BETA = .00

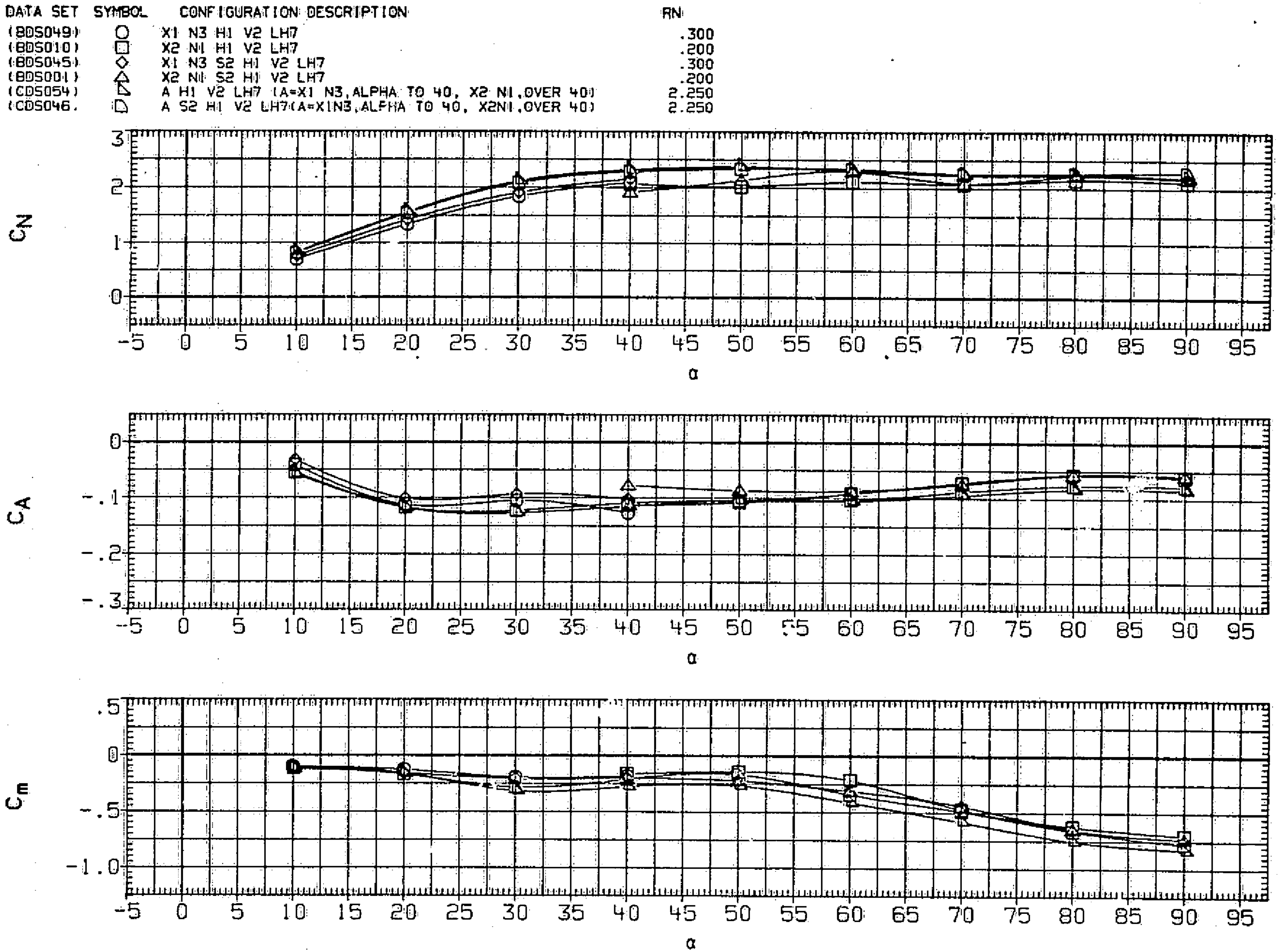

FIG.9 STRAKES(S2) AND REY. NO. EFFECTS ON LONGITUD. AERO CHARACTERISTICS

(B) BETA = 10.00

DATA SET	SYMBOL	CONFIGURATION DESCRIPTION	RN
(BDS049)	○	X1 N3 H1 V2 LH7	.300
(BDS010)	□	X2 N1 H1 V2 LH7	.200
(BDS045)	◇	X1 N3 S2 H1 V2 LH7	.300
(BDS001)	△	X2 N1 S2 H1 V2 LH7	.200
(CDS054)	⊿	A H1 V2 LH7 (A=X1 N3,ALPHA TO 40, X2 N1,OVER 40)	2.250
(CDS046)	D	A S2 H1 V2 LH7(A=X1N3,ALPHA TO 40, X2N1,OVER 40)	2.250

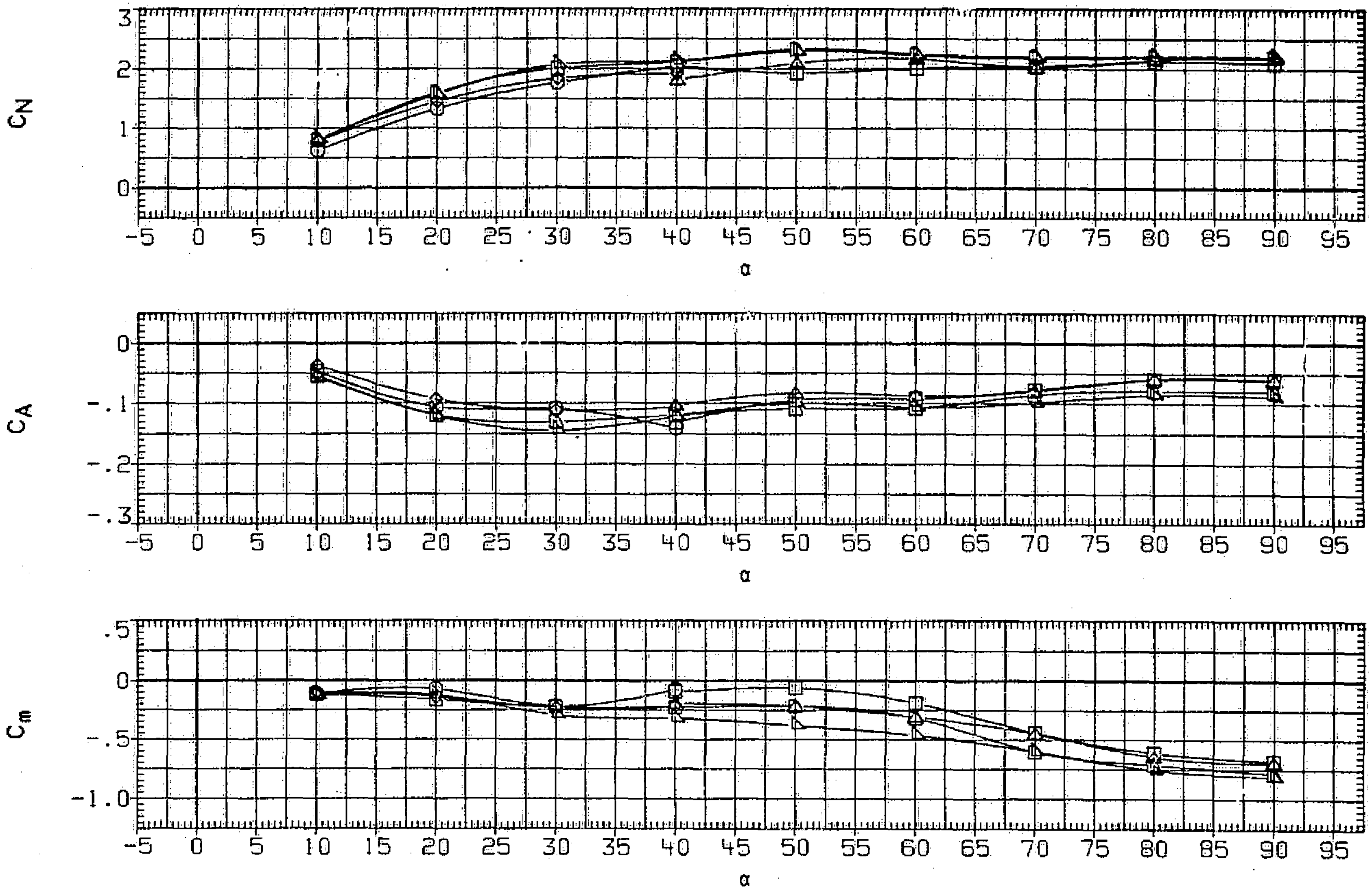

FIG.9 STRAKES(S2) AND REY. NO. EFFECTS ON LONGITUD. AERO CHARACTERISTICS

(C)BETA = 20.00

DATA SET	SYMBOL	CONFIGURATION DESCRIPTION	RN
(RDS049)	○	X1 N3 H1 V2 LH7	.300
(RDS042)	□	X1 N3 I1 S1 H1 V2 LH7	.300
(RDS054)	◇	X1 N3 H1 V2 LH7	2.250
(RDS044)	△	X1 N3 I1 S1 H1 V2 LH7	2.250

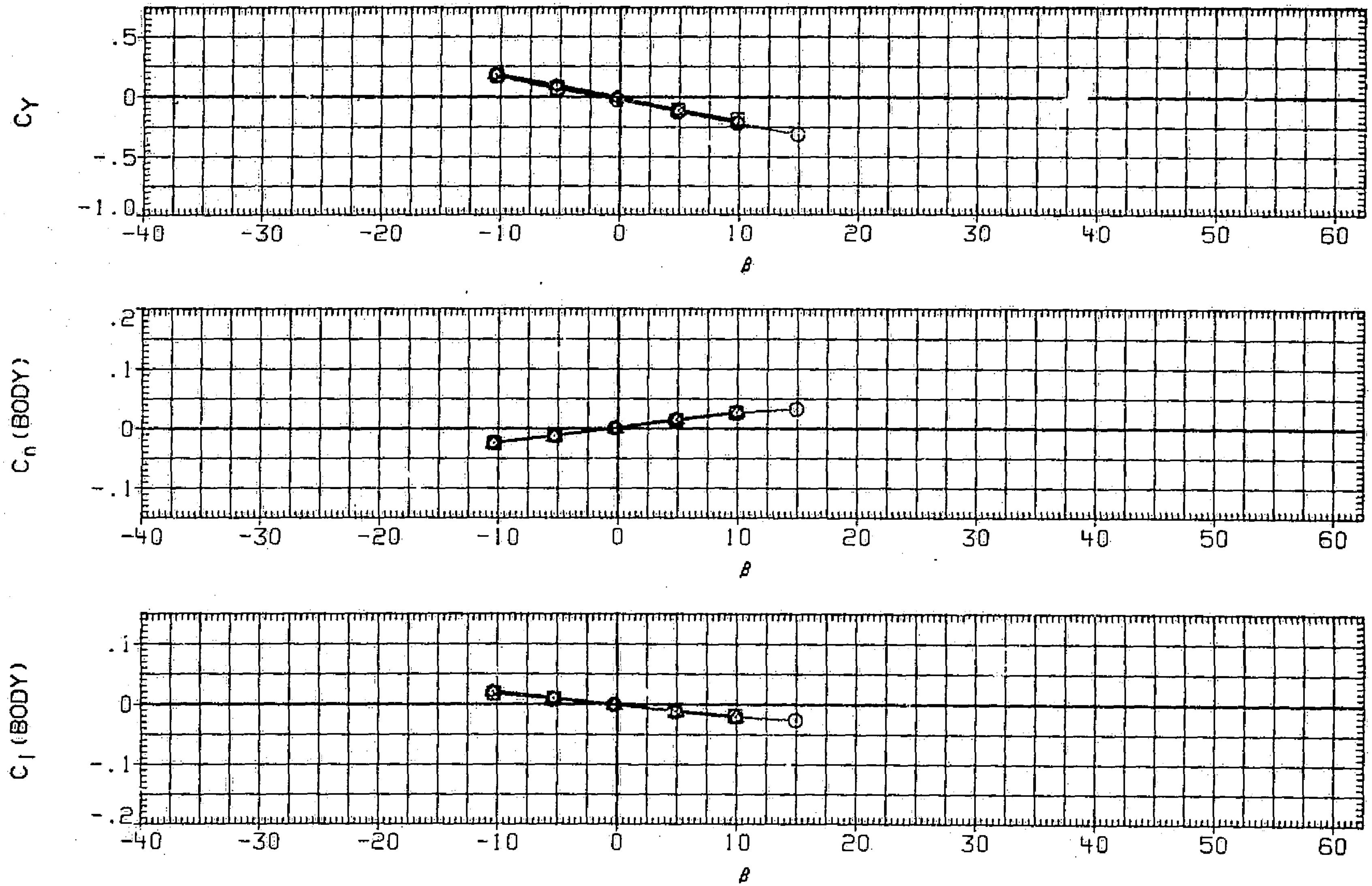

FIG.10 BOOM(I1)+STRAKES(S1) AND REY. NO. EFFECTS ON LATERAL-DIRECT. AERO CHARAC.

(A) ALPHA = 10.09

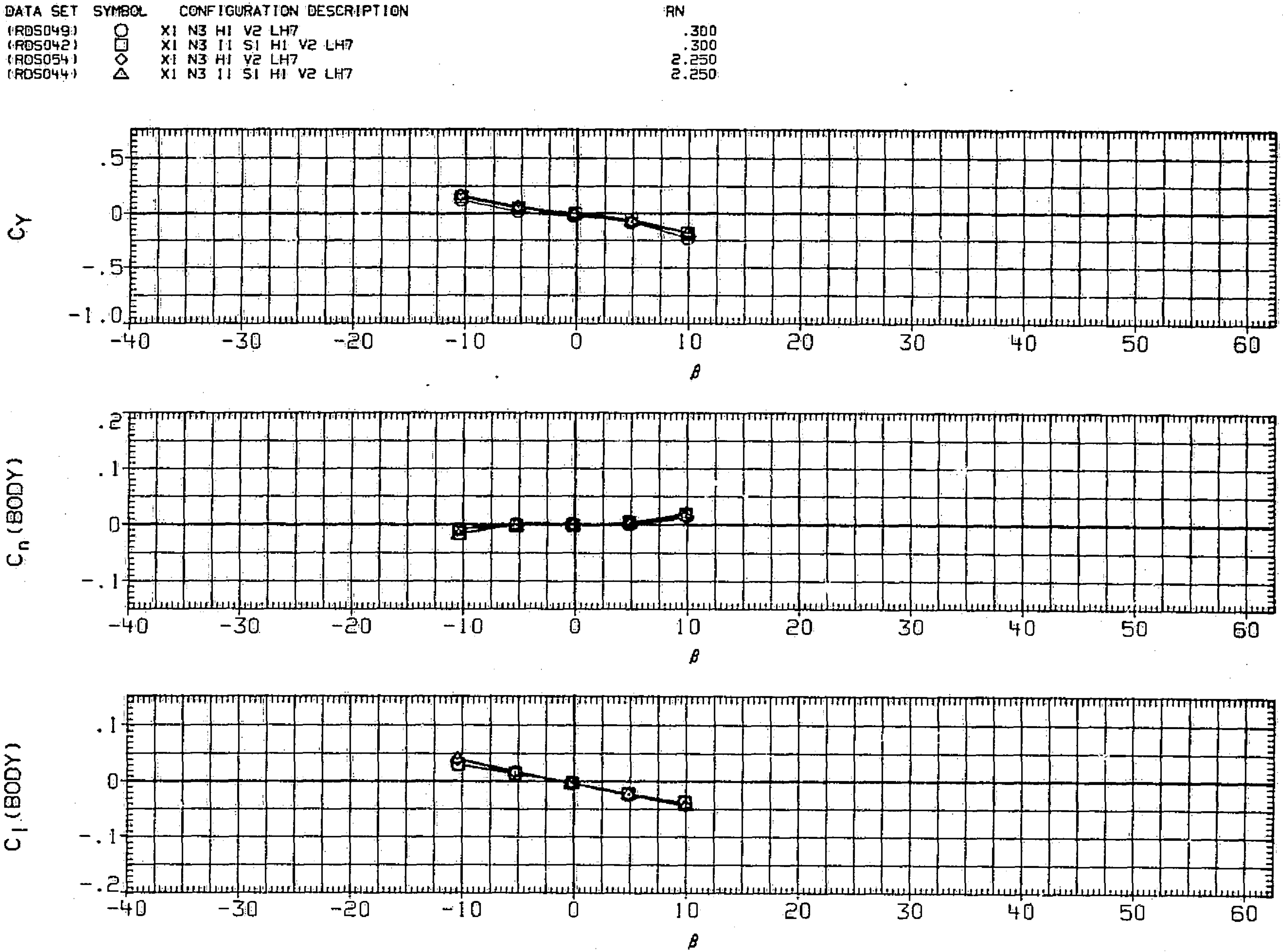

FIG.10 BOOM(I1)+STRAKES(S1) AND REY. NO. EFFECTS ON LATERAL-DIRECT. AERO CHARAC.

(B) ALPHA = 20.27

DATA SET	SYMBOL	CONFIGURATION DESCRIPTION	RN
(RDS049)	○	X1 N3 H1 V2 LH7	.300
(RDS042)	□	X1 N3 I1 S1 H1 V2 LH7	.300
(RDS054)	◇	X1 N3 H1 V2 LH7	2.250
(RDS044)	△	X1 N3 I1 S1 H1 V2 LH7	2.250

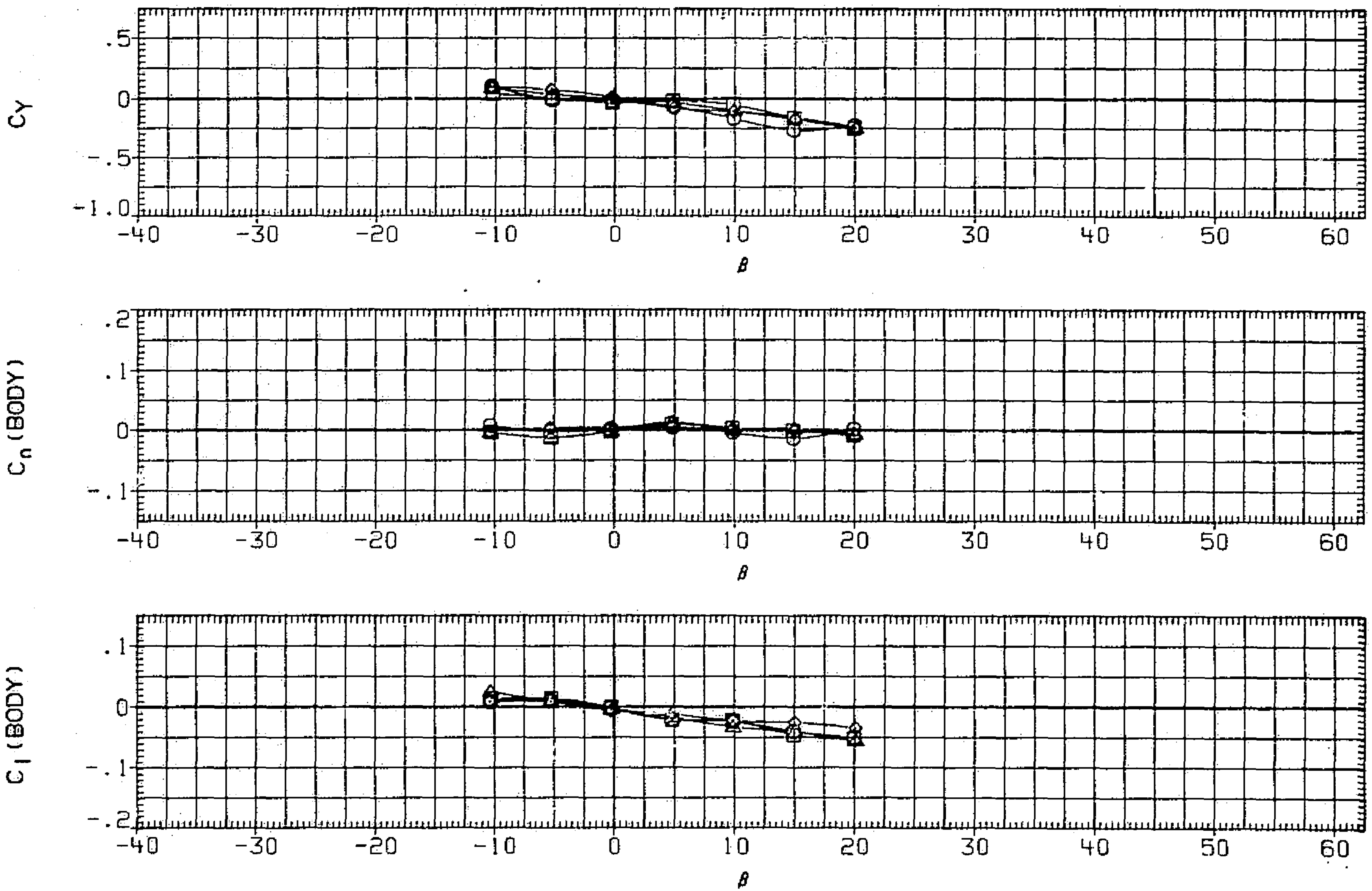

FIG.10 BOOM(I1)+STRAKES(S1) AND REY. NO. EFFECTS ON LATERAL-DIRECT. AERO CHARAC.

(C)ALPHA = 30.44

DATA SET	SYMBOL	CONFIGURATION DESCRIPTION	RN
(RDS049)	○	X1 N3 H1 V2 LH7	.300
(RDS042)	□	X1 N3 I1 S1 H1 V2 LH7	.300
(RDS054)	◇	X1 N3 H1 V2 LH7	2.250
(RDS044)	△	X1 N3 I1 S1 H1 V2 LH7	2.250

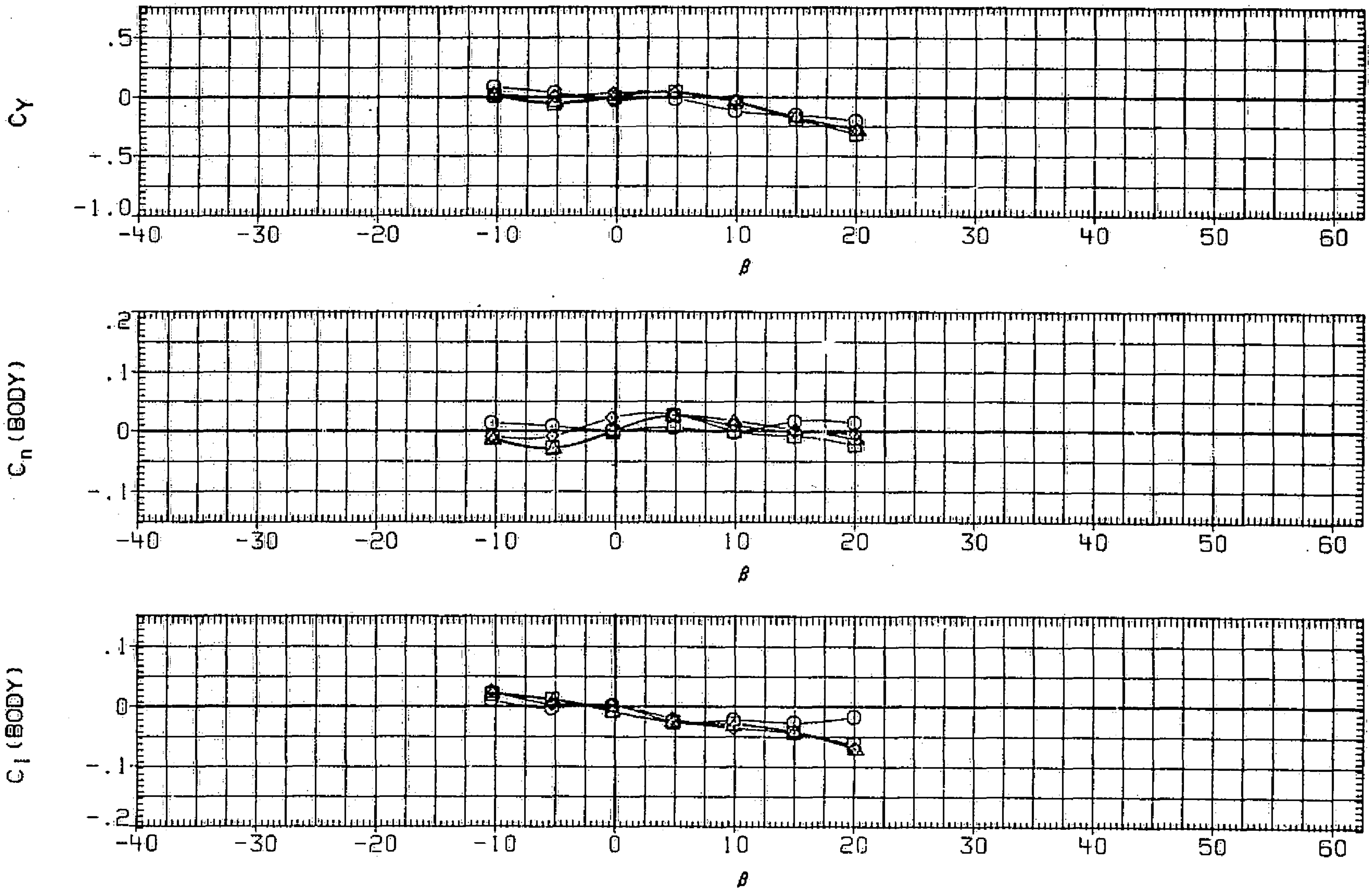

FIG.10 BOOM(I1)+STRAKES(S1) AND REY. NO. EFFECTS ON LATERAL-DIRECT. AERO CHARAC.

(D) ALPHA = 40.44

DATA SET	SYMBOL	CONFIGURATION DESCRIPTION	RN
(RDS010)	○	X2 N1 H1 V2 LH7	.200
(RDS004)	□	X2 N1 I1 S1 H1 V2 LH7	.200
(RDS013)	◇	X2 N1 H1 V2 LH7	2.250
(RDS007)	△	X2 N1 I1 S1 H1 V2 LH7	2.250

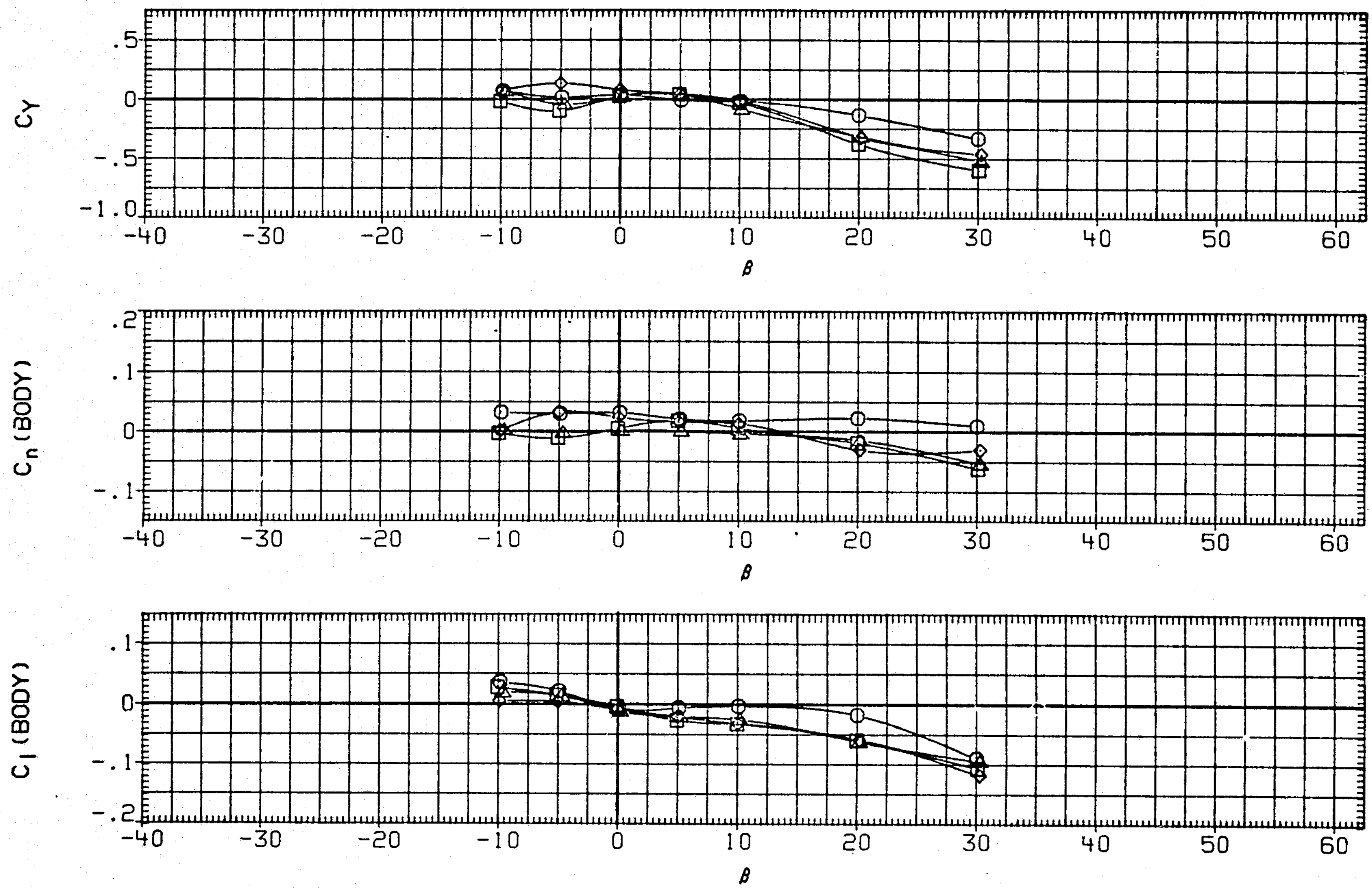

FIG.10 BOOM(I1)+STRAKES(S1) AND REY. NO. EFFECTS ON LATERAL-DIRECT. AERO CHARAC.

(A)ALPHA = 40.33

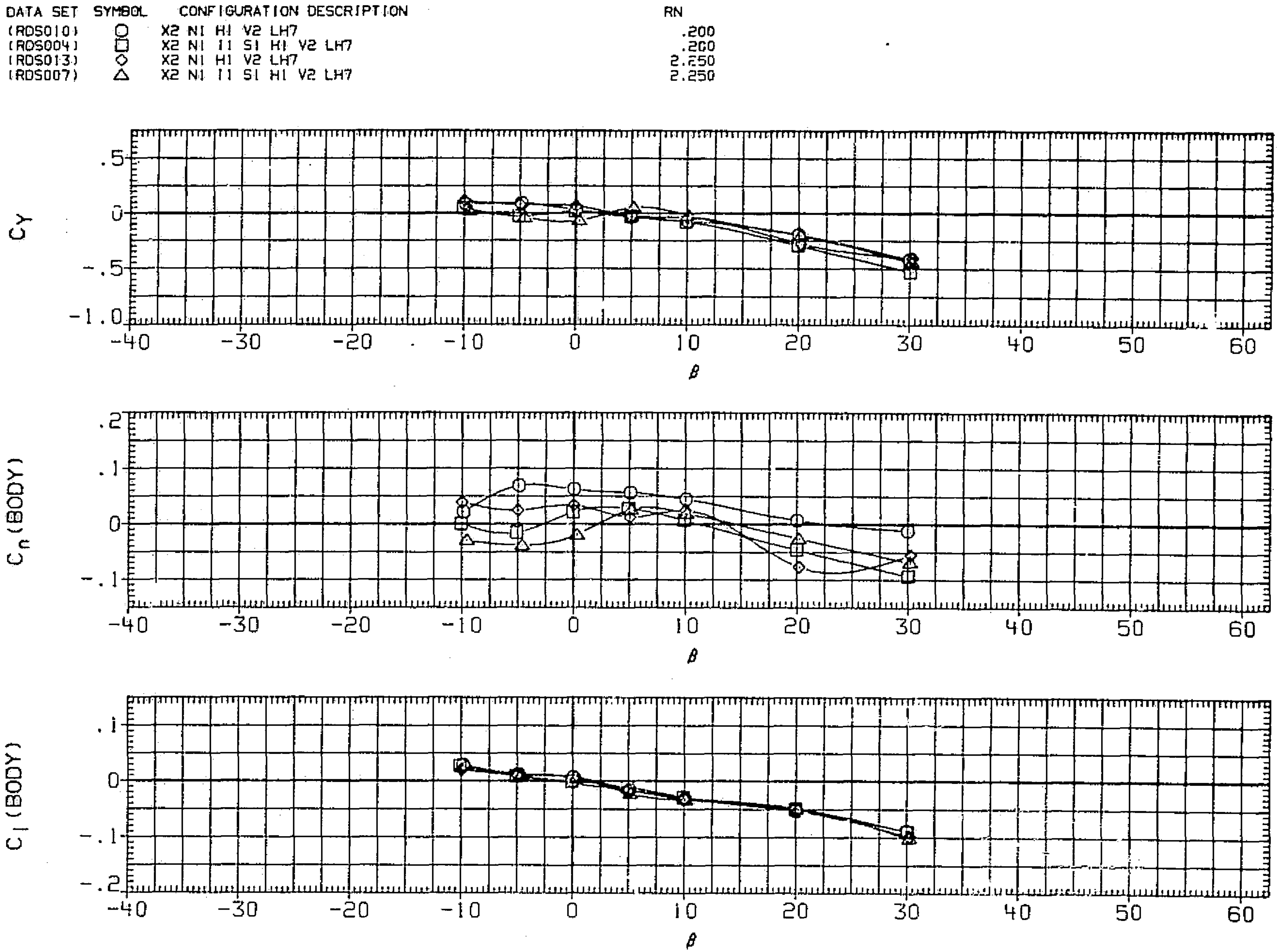

FIG.10 BOOM(I1)+STRAKES(S1) AND REY. NO. EFFECTS ON LATERAL-DIRECT. AERO CHARAC.

(B)ALPHA = 50.36

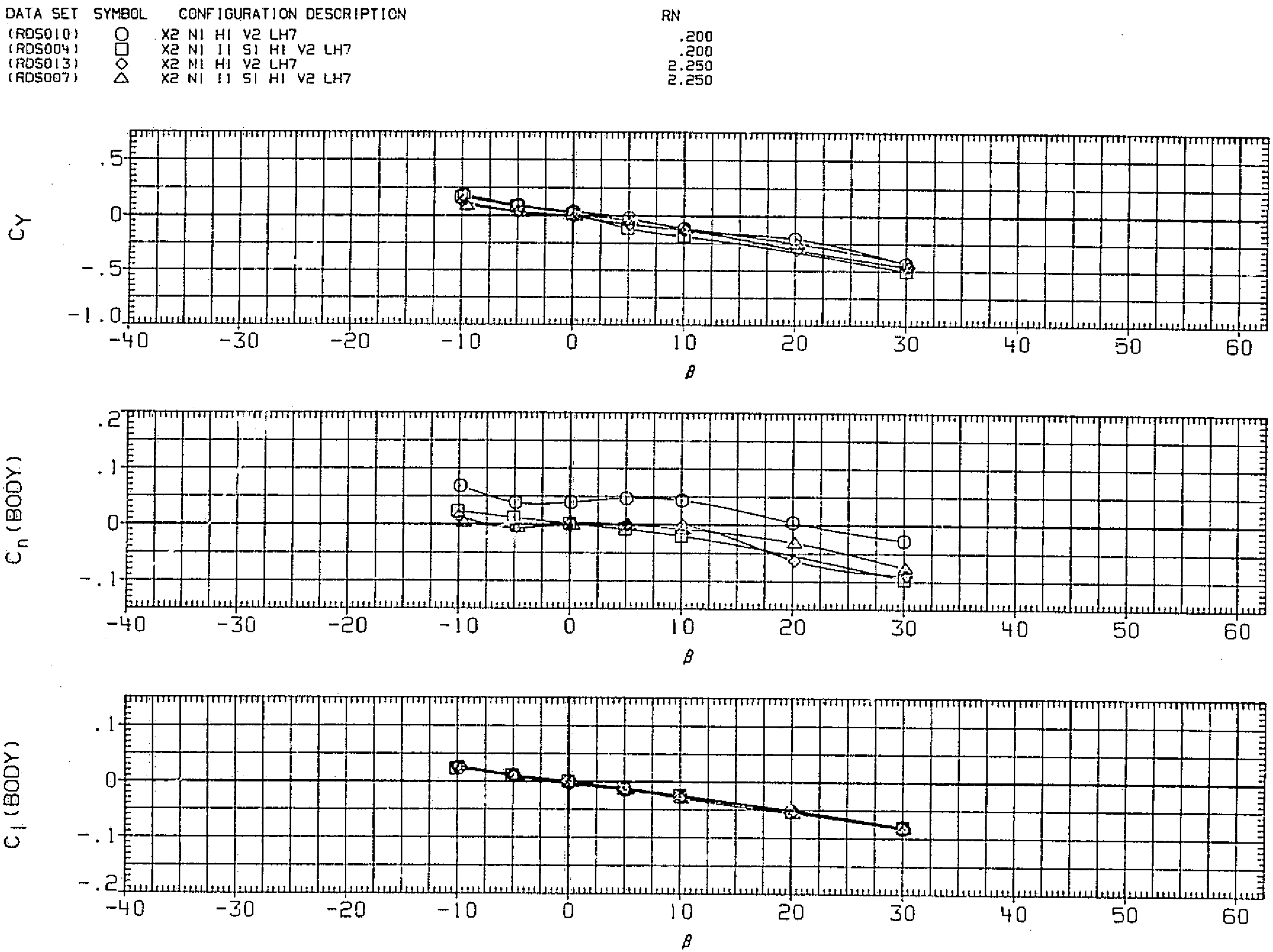

FIG.10 BOOM(I1)+STRAKES(S1) AND REY. NO. EFFECTS ON LATERAL-DIRECT. AERO CHARAC.

(C)ALPHA = 60.27

DATA SET	SYMBOL	CONFIGURATION DESCRIPTION	RN
(RDS010)	○	X2 N1 H1 V2 LH7	.200
(RDS004)	□	X2 N1 I1 S1 H1 V2 LH7	.200
(RDS013)	◇	X2 N1 H1 V2 LH7	2.250
(RDS007)	△	X2 N1 I1 S1 H1 V2 LH7	2.250

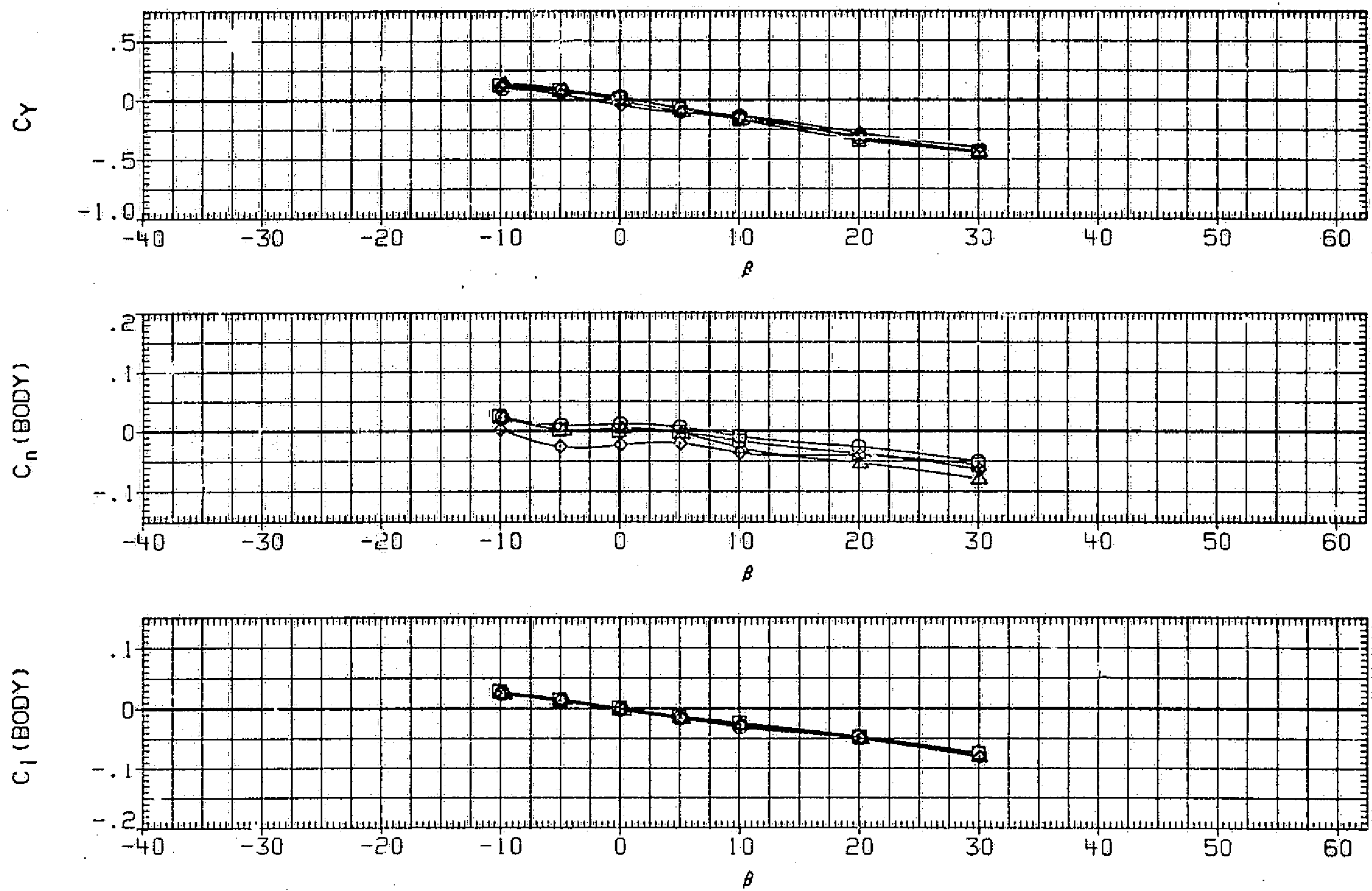

FIG.10 BOOM(I1)+STRAKES(S1) AND REY. NO. EFFECTS ON LATERAL-DIRECT. AERO CHARAC.

(D) ALPHA = 70.27

DATA SET	SYMBOL	CONFIGURATION DESCRIPTION	RN
(RDS010)	○	X2 N1 H1 V2 LH7	.200
(RDS004)	□	X2 N1 I1 S1 H1 V2 LH7	.200
(RDS013)	◇	X2 N1 H1 V2 LH7	2.250
(RDS007)	△	X2 N1 I1 S1 H1 V2 LH7	2.250

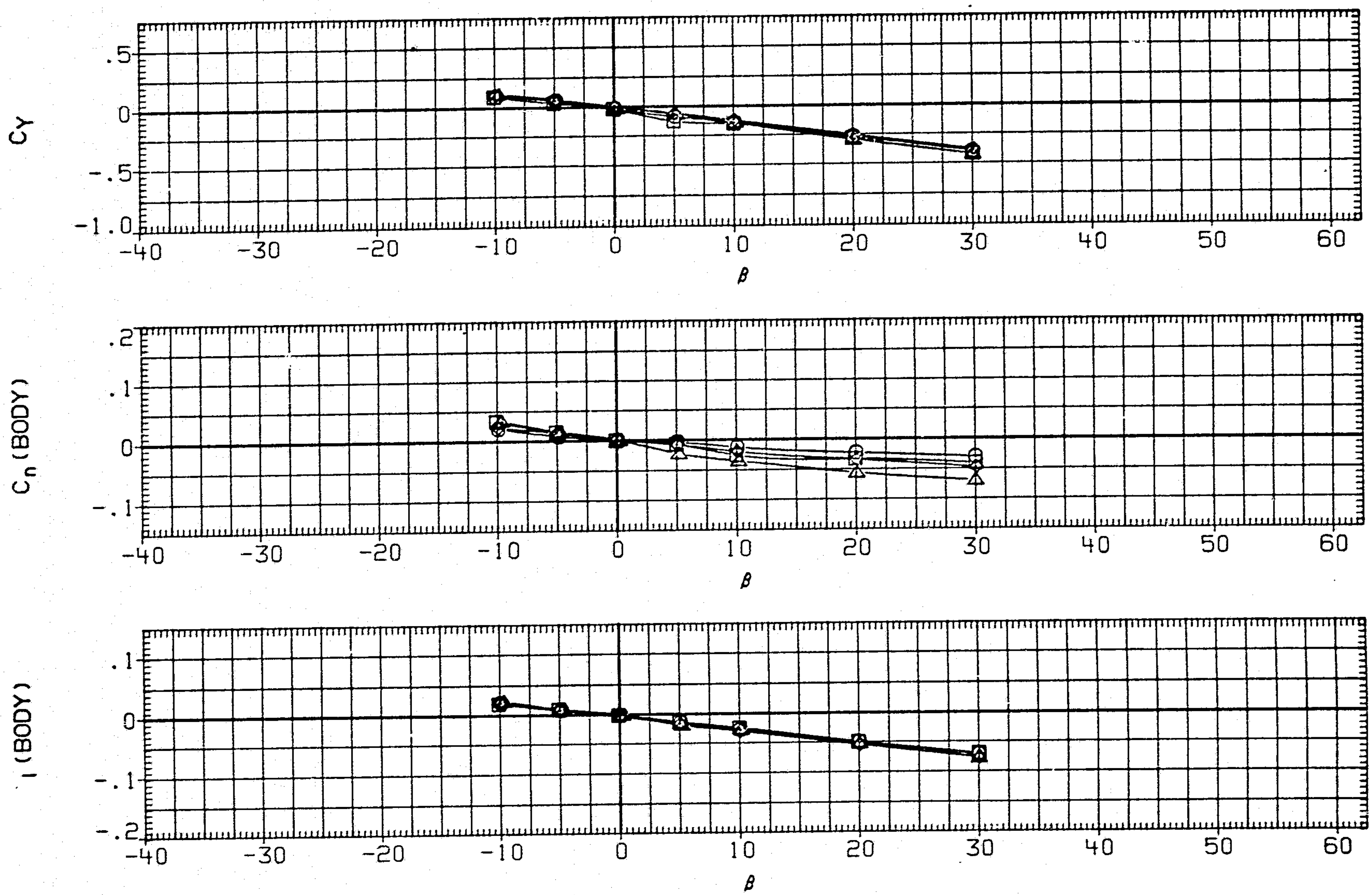

FIG.10 BOOM(I1)+STRAKES(S1) AND REY. NO. EFFECTS ON LATERAL-DIRECT. AERO CHARAC.

(E) ALPHA = 80.21

DATA SET	SYMBOL	CONFIGURATION DESCRIPTION	RN
(RDS010)	○	X2 N1 H1 V2 LH7	.200
(RDS004)	□	X2 N1 I1 S1 H1 V2 LH7	.200
(RDS013)	◇	X2 N1 H1 V2 LH7	2.250
(RDS007)	△	X2 N1 I1 S1 H1 V2 LH7	2.250

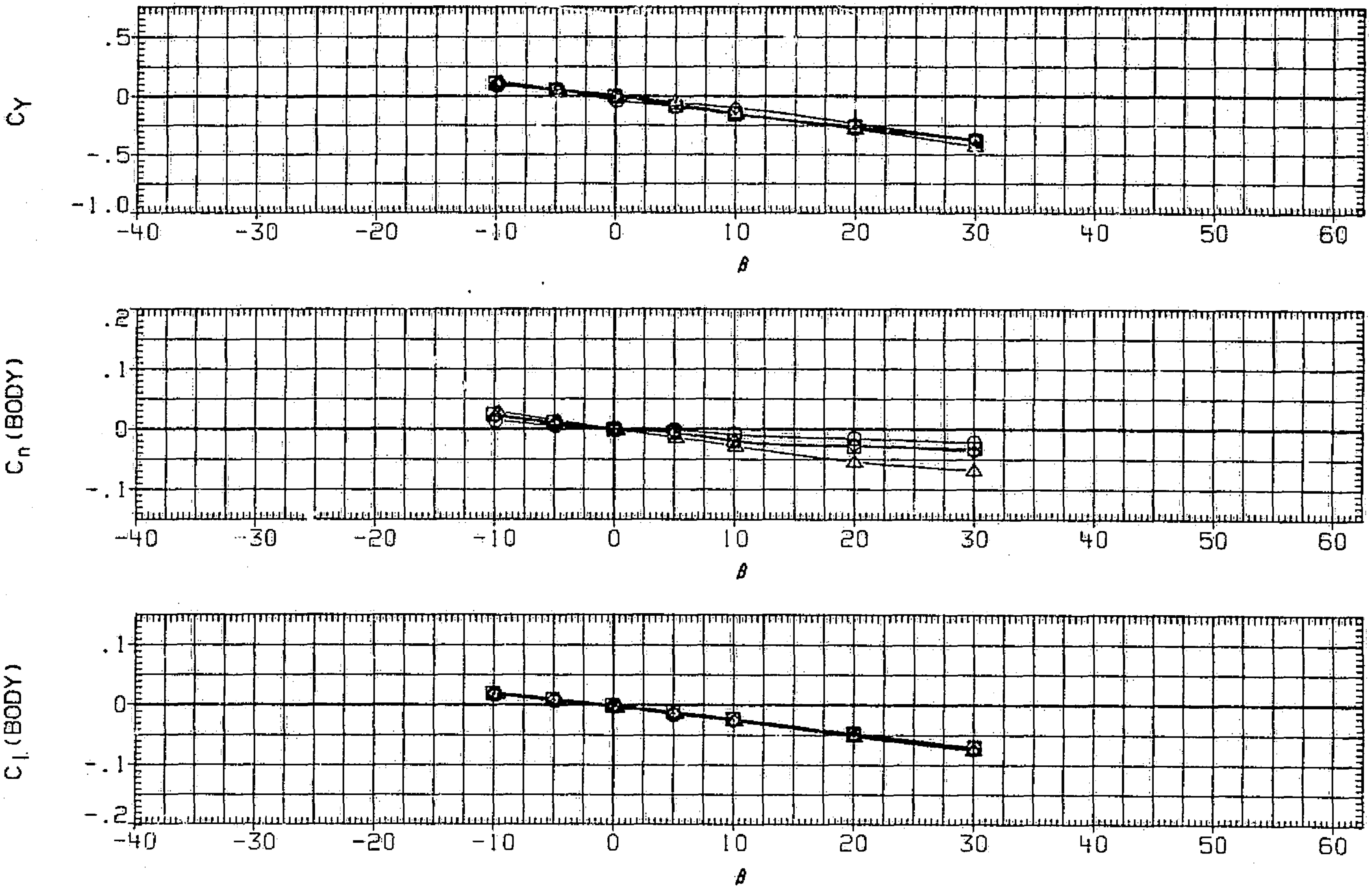

FIG.10 BOOM(I1)+STRAKES(S1) AND REY. NO. EFFECTS ON LATERAL-DIRECT. AERO CHARAC.

(F)ALPHA = 89.21

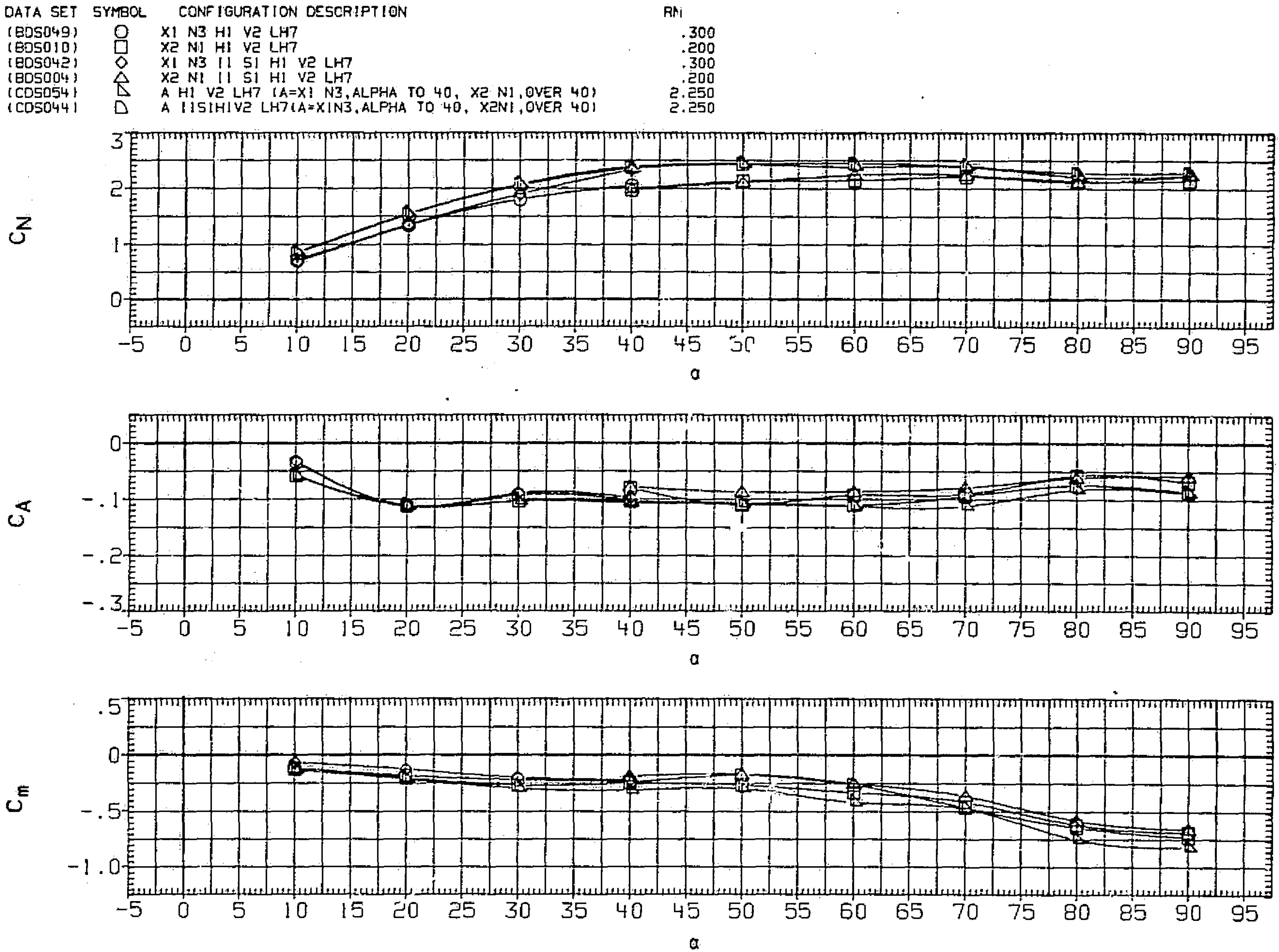

FIG.11 BOOM(I1)+STRAKES(S1) AND REY. NO. EFFECTS ON LONGITUD. AERO CHARAC.

(A)BETA = .00

DATA SET	SYMBOL	CONFIGURATION DESCRIPTION	RN
(BDS049)	○	X1 N3 H1 V2 LH7	.300
(BDS010)	□	X2 N1 H1 V2 LH7	.200
(BDS042)	◇	X1 N3 I1 S1 H1 V2 LH7	.300
(BDS004)	△	X2 N1 I1 S1 H1 V2 LH7	.200
(CDS054)	⊾	A H1 V2 LH7 (A=X1 N3,ALPHA TO 40, X2 N1,OVER 40)	2.250
(CDS044)	◺	A I1S1H1V2 LH7(A=X1N3,ALPHA TO 40, X2N1,OVER 40)	2.250

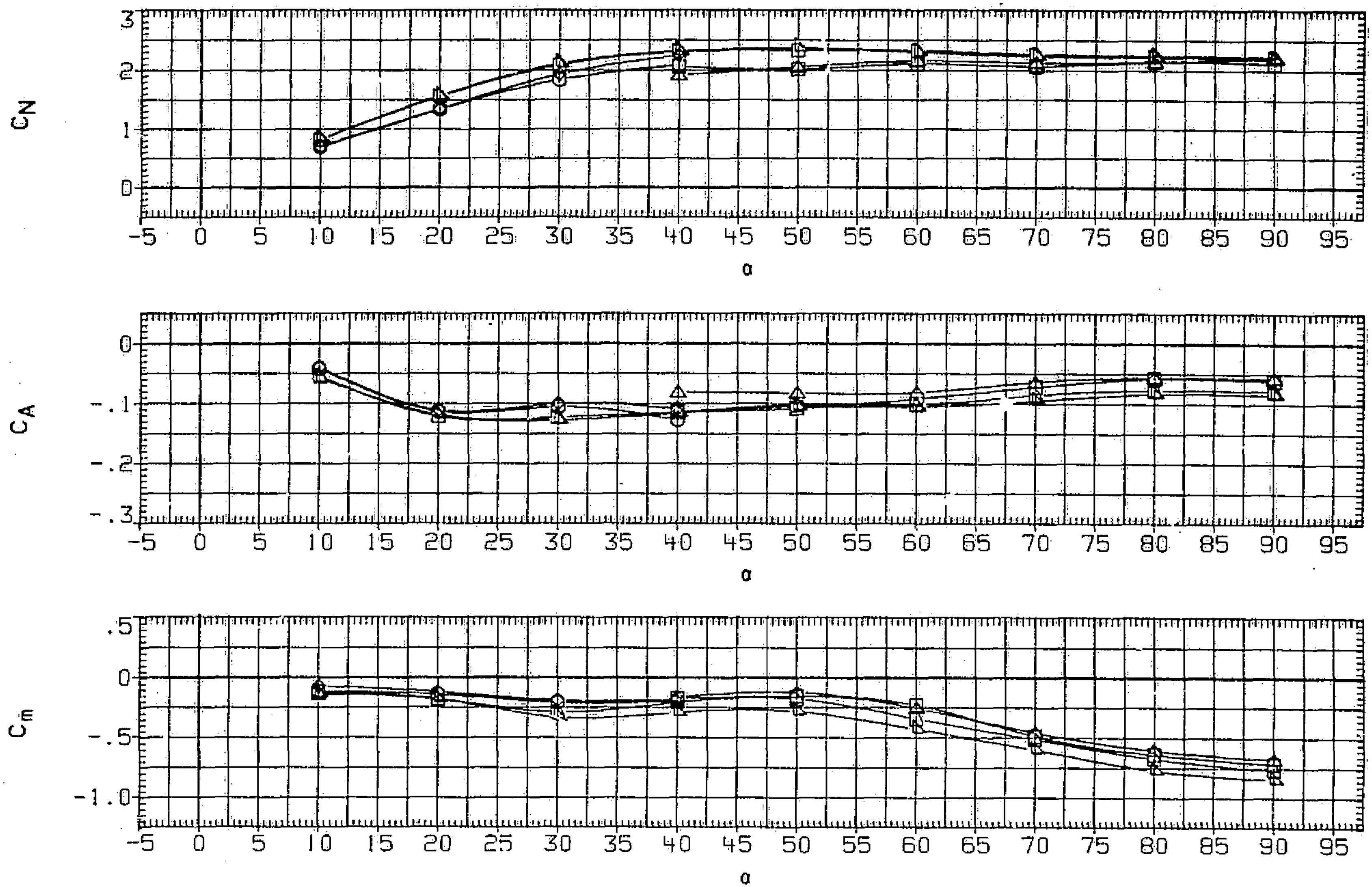

FIG.11 BOOM(I1)+STRAKES(S1) AND REY. NO. EFFECTS ON LONGITUD. AERO CHARAC.

(B)BETA = 10.00

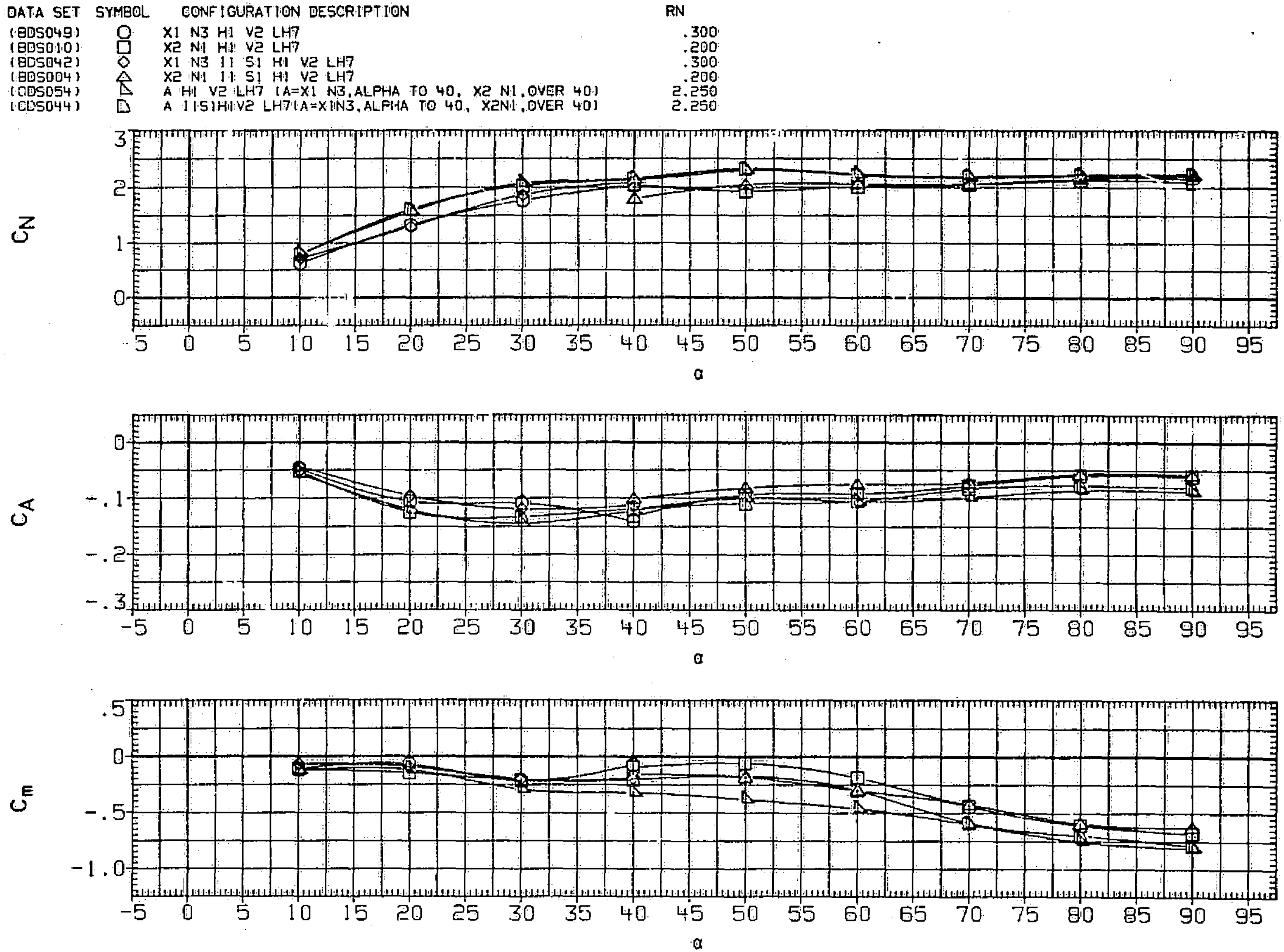

FIG.11 BOOM(I1)+STRAKES(S1) AND REY. NO. EFFECTS ON LONGITUD. AERO CHARAC.

(C)BETA = 20.00

DATA SET	SYMBOL	CONFIGURATION DESCRIPTION	RN
(RDS010)	○	X2 N1 H1 V2 LH7	.200
(RDS013)	□	X2 N1 H1 V2 LH7	2.250
(RDS028)	◇	X2 N1 S11 H1 V2 LH7	.200
(RDS029)	△	X2 N1 S21 H1 V2 LH7	.200
(RDS030)	◺	X2 N1 S31 H1 V2 LH7	.200
(RDS031)	◿	X2 N1 S41 H1 V2 LH7	.200

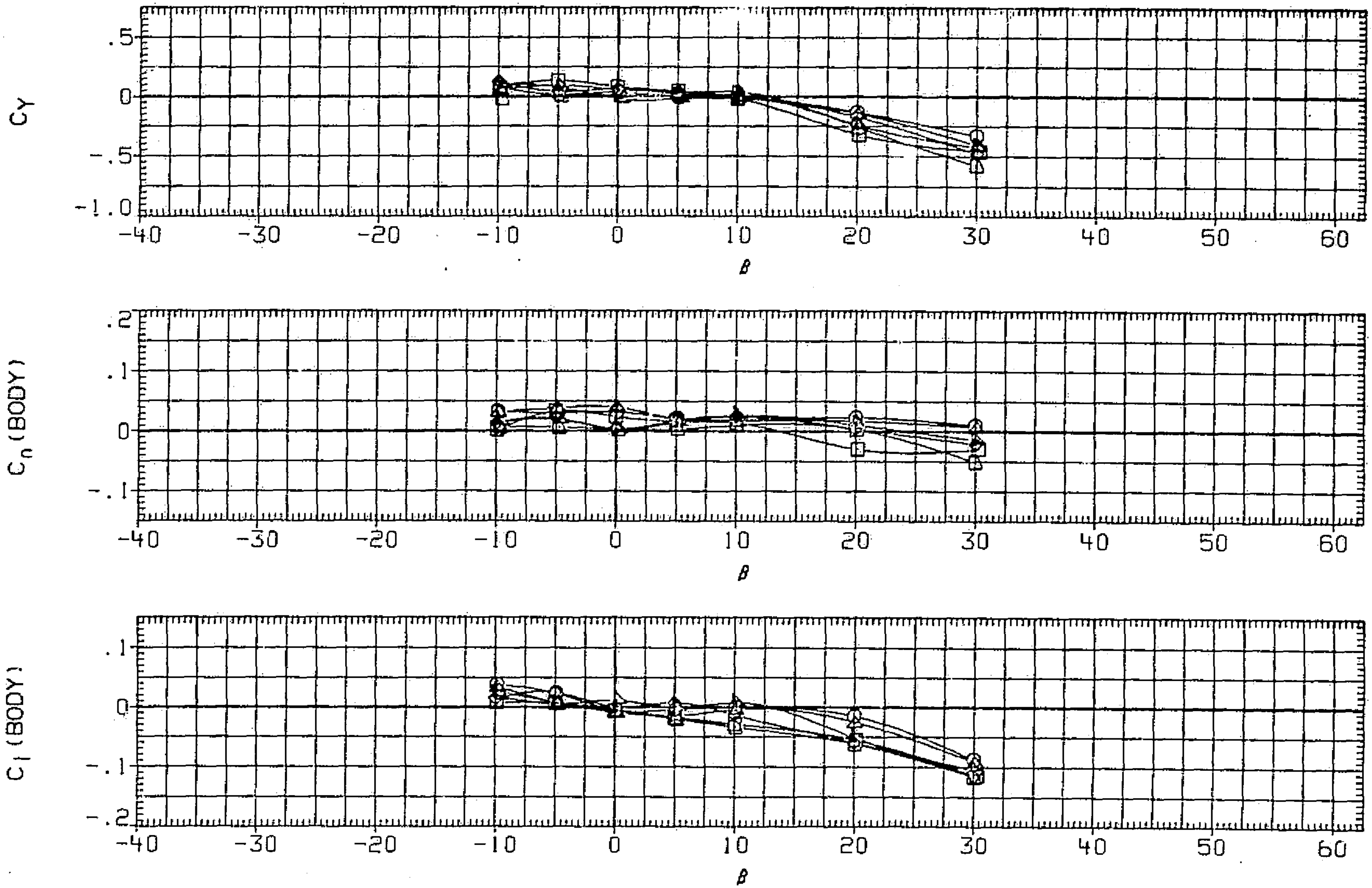

FIG.12 EFFECTS OF VARIOUS STRAKE CONFIGS. ON LONG. AND LAT.-DIRECT. AERO CHARAC.

(A) ALPHA = 40.33

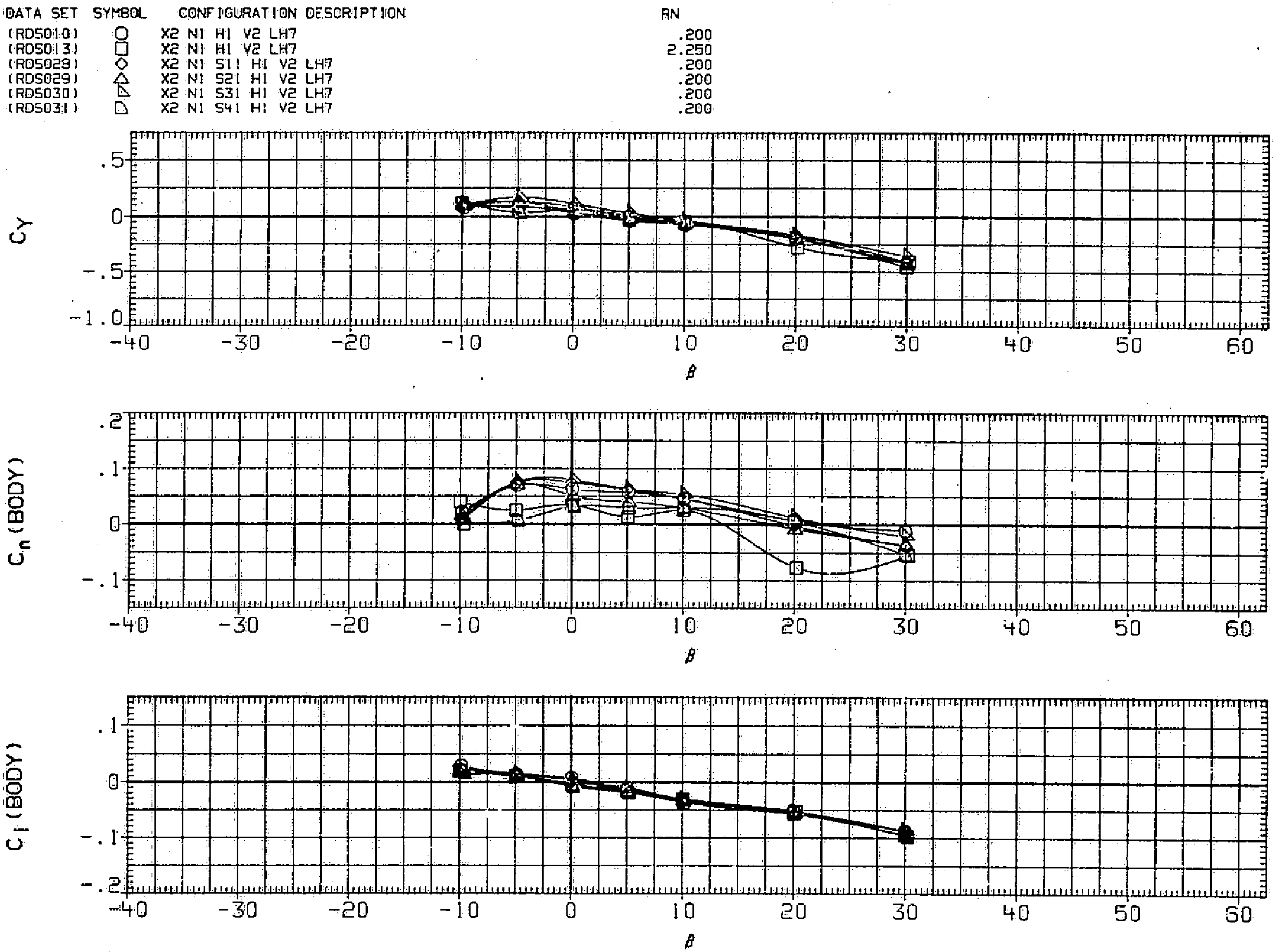

FIG.12 EFFECTS OF VARIOUS STRAKE CONFIGS. ON LONG. AND LAT.-DIRECT. AERO CHARAC.

(B) ALPHA = 50.36

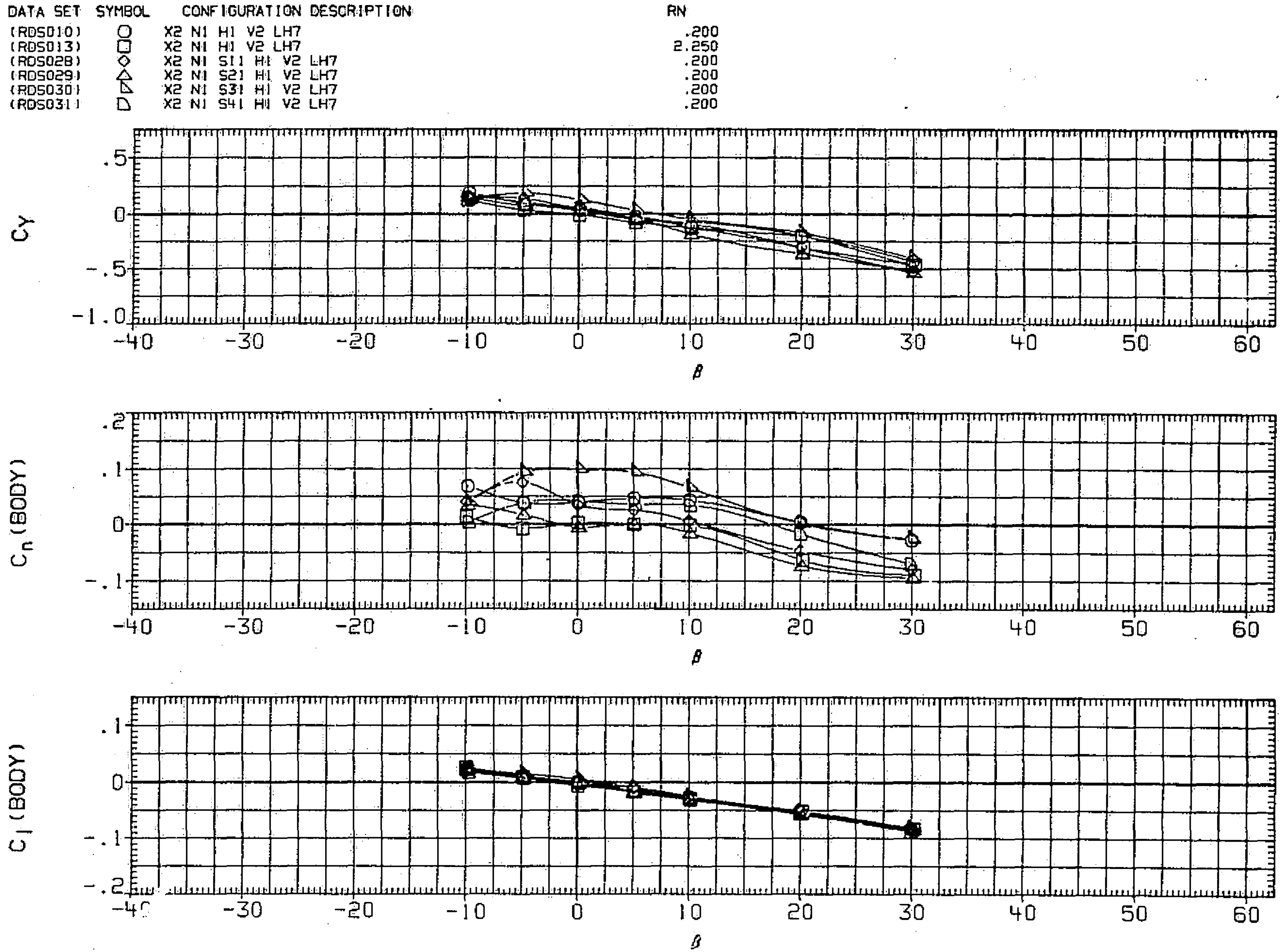

FIG.12 EFFECTS OF VARIOUS STRAKE CONFIGS. ON LONG. AND LAT.-DIRECT. AERO CHARAC.

(C) ALPHA = 60.27

DATA SET	SYMBOL	CONFIGURATION DESCRIPTION	RN
(RDS010)	○	X2 N1 H1 V2 LH7	.200
(RDS013)	□	X2 N1 H1 V2 LH7	2.250
(RDS028)	◇	X2 N1 S11 H1 V2 LH7	.200
(RDS029)	△	X2 N1 S21 H1 V2 LH7	.200
(RDS030)	◺	X2 N1 S31 H1 V2 LH7	.200
(RDS031)	▱	X2 N1 S41 H1 V2 LH7	.200

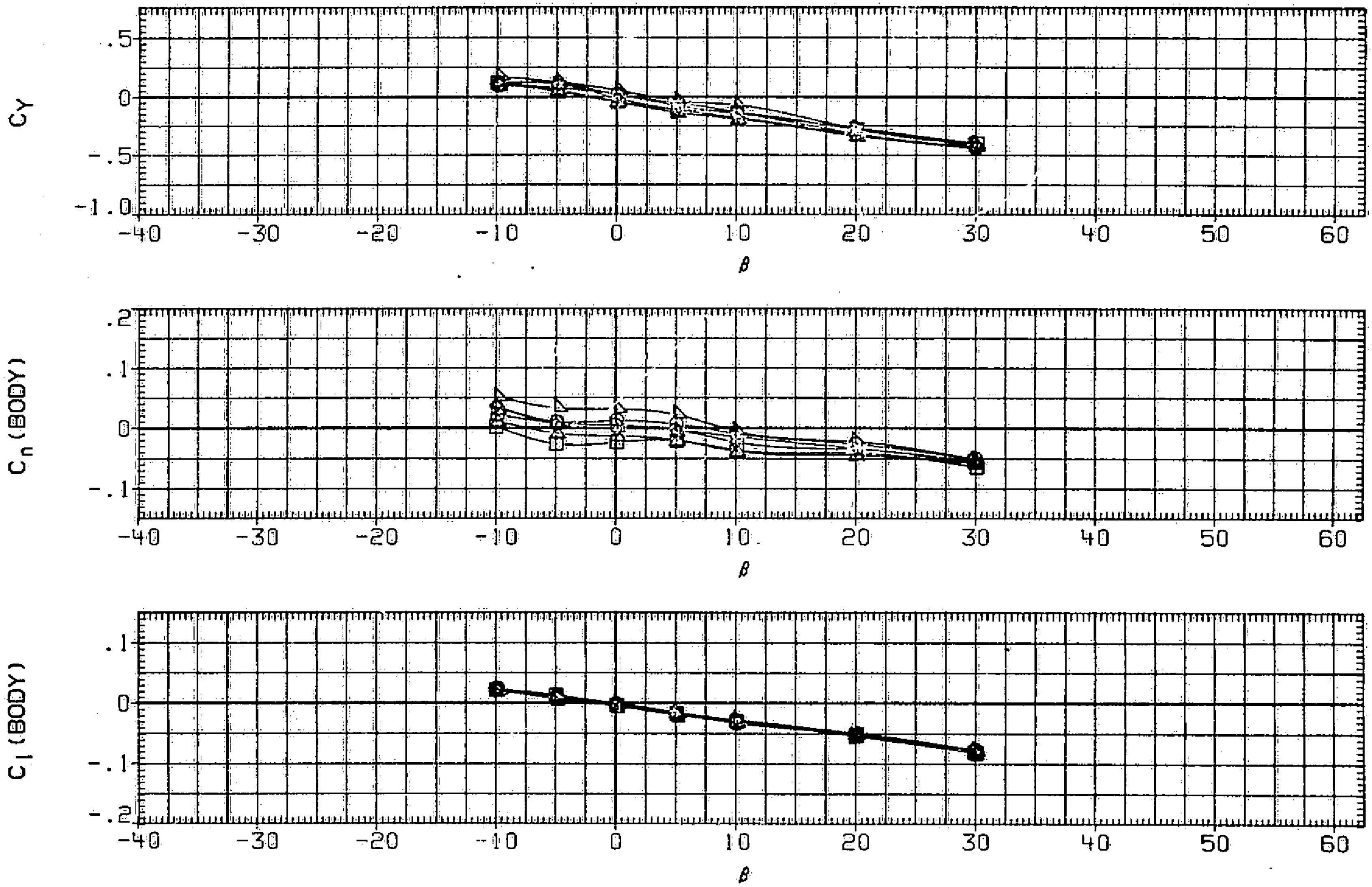

FIG.12 EFFECTS OF VARIOUS STRAKE CONFIGS. ON LONG. AND LAT.-DIRECT. AERO CHARAC.

(D) ALPHA = 70.27

DATA SET	SYMBOL	CONFIGURATION DESCRIPTION	RN
(RDS010)	○	X2 N1 H1 V2 LH7	.200
(RDS013)	□	X2 N1 H1 V2 LH7	2.250
(RDS028)	◇	X2 N1 S11 H1 V2 LH7	.200
(RDS029)	△	X2 N1 S21 H1 V2 LH7	.200
(RDS030)	◺	X2 N1 S31 H1 V2 LH7	.200
(RDS031)	D	X2 N1 S41 H1 V2 LH7	.200

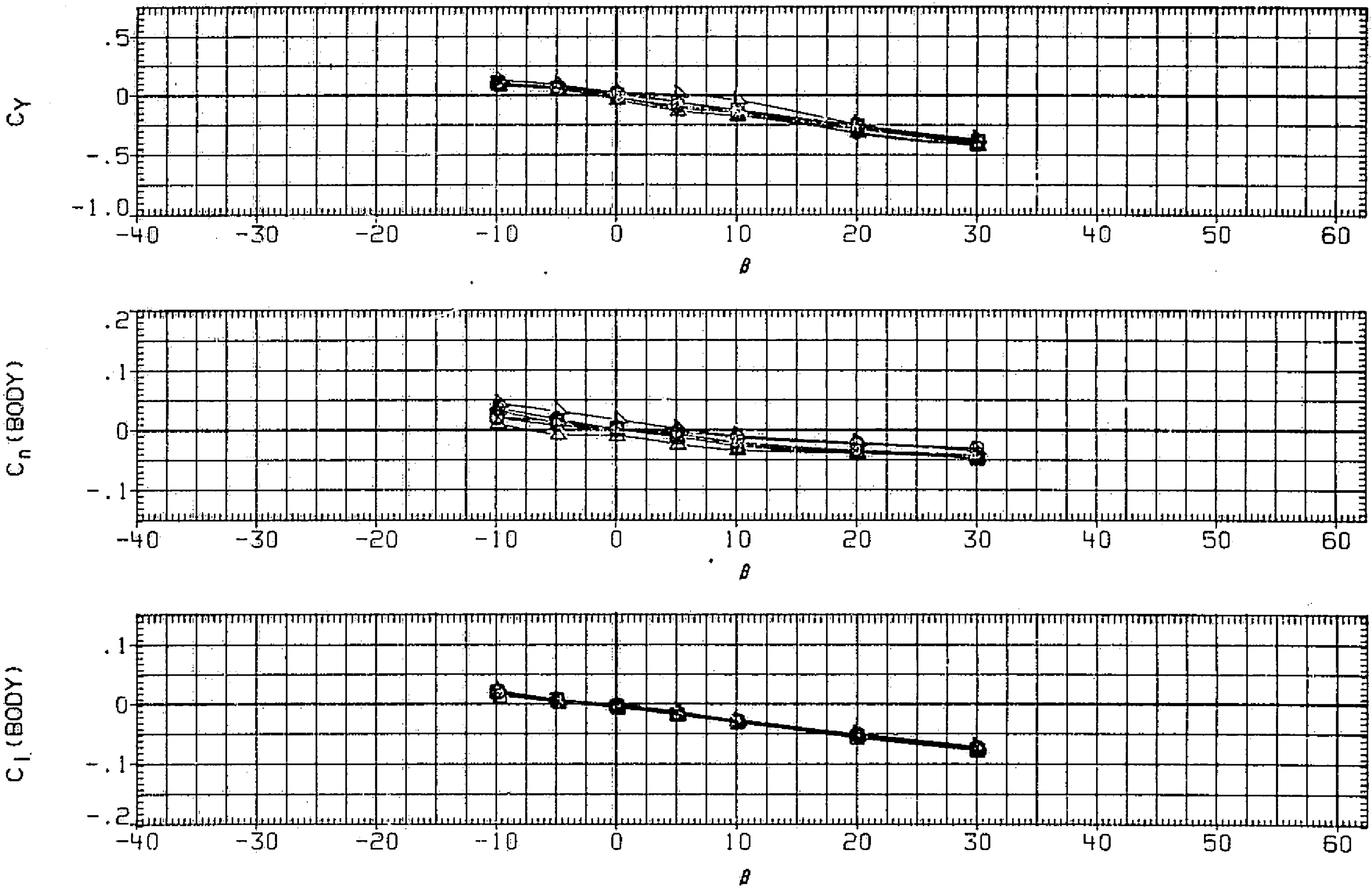

FIG. 12 EFFECTS OF VARIOUS STRAKE CONFIGS. ON LONG. AND LAT.-DIRECT. AERO CHARAC.

(E) ALPHA = 80.21

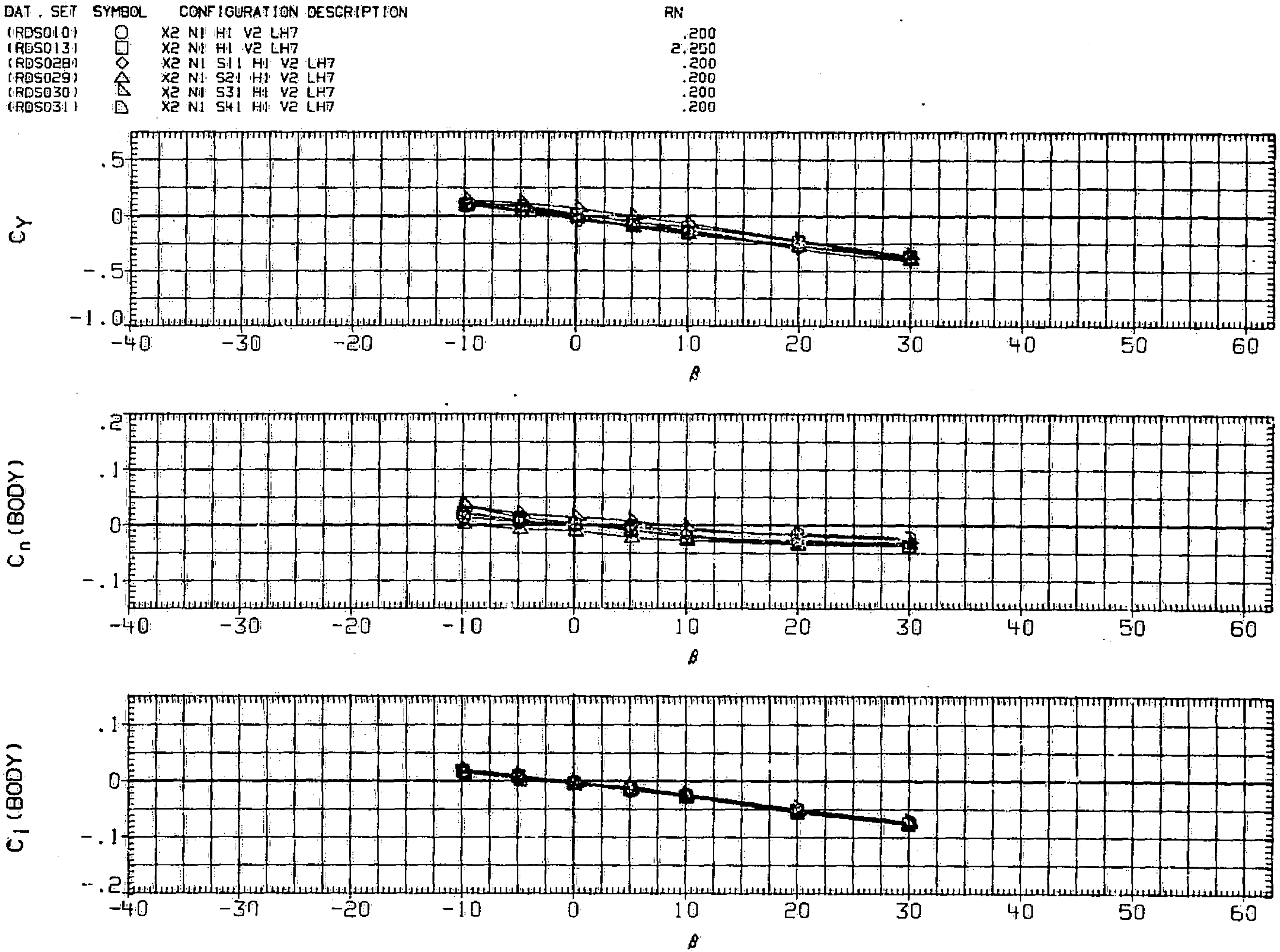

FIG.12 EFFECTS OF VARIOUS STRAKE CONFIGS. ON LONG. AND LAT.-DIRECT. AERO CHARAC.

(F) ALPHA = 89.21

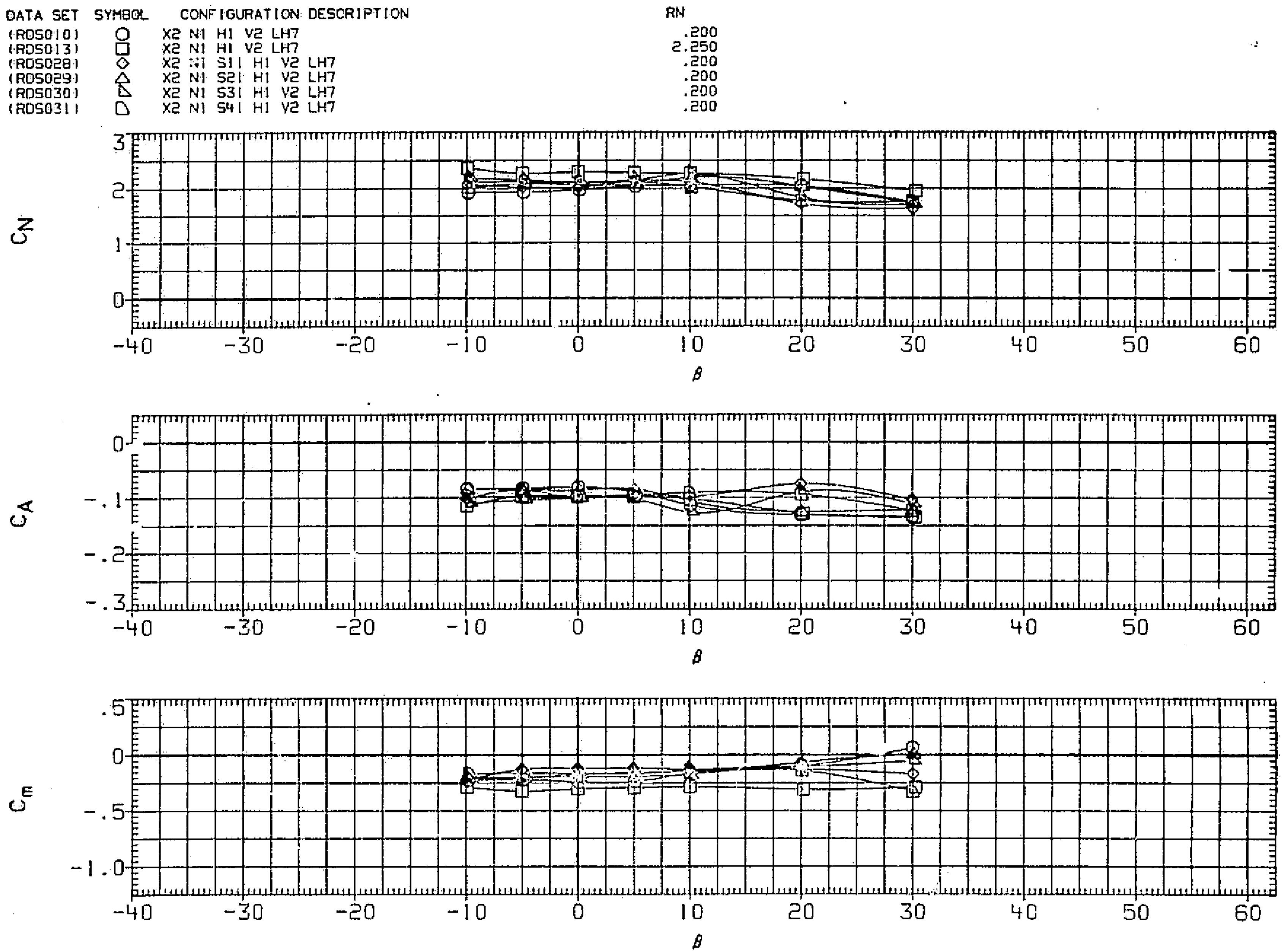

FIG.12 EFFECTS OF VARIOUS STRAKE CONFIGS. ON LONG. AND LAT.-DIRECT. AERO CHARAC.

(A)ALPHA = 40.33

DATA SET	SYMBOL	CONFIGURATION DESCRIPTION	RN
(RDS010)	○	X2 N1 H1 V2 LH7	.200
(RDS013)	□	X2 N1 H1 V2 LH7	2.250
(RDS028)	◇	X2 N1 S11 H1 V2 LH7	.200
(RDS029)	△	X2 N1 S21 H1 V2 LH7	.200
(RDS030)	◺	X2 N1 S31 H1 V2 LH7	.200
(RDS031)	◗	X2 N1 S41 H1 V2 LH7	.200

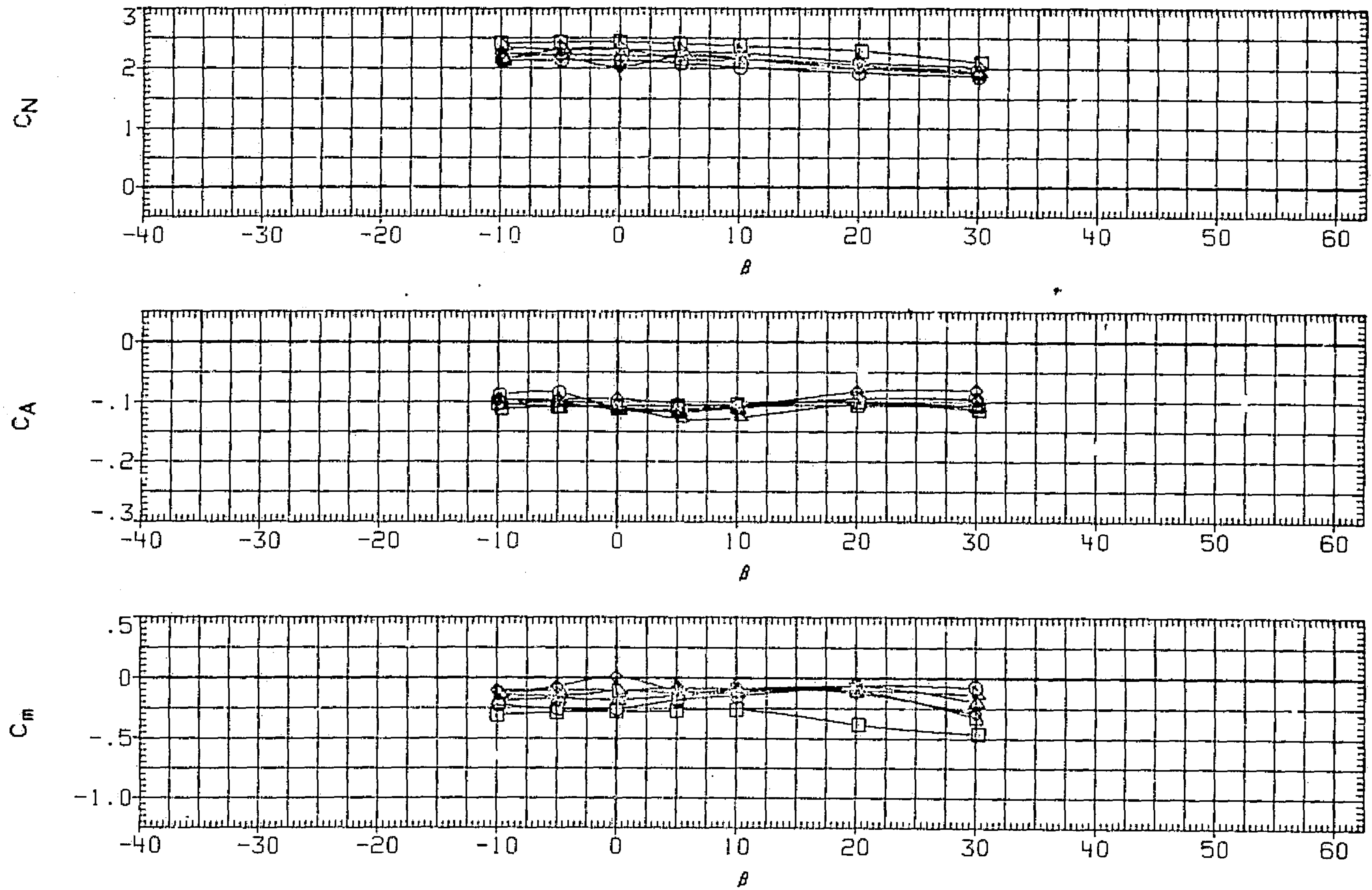

FIG.12 EFFECTS OF VARIOUS STRAKE CONFIGS. ON LONG. AND LAT.-DIRECT. AERO CHARAC.

(B) ALPHA = 50.36

DATA SET	SYMBOL	CONFIGURATION DESCRIPTION	RN
(RDS010)	○	X2 N1 H1 V2 LH7	.200
(RDS013)	□	X2 N1 H1 V2 LH7	2.250
(RDS028)	◇	X2 N1 S11 H1 V2 LH7	.200
(RDS029)	△	X2 N1 S21 H1 V2 LH7	.200
(RDS030)	◺	X2 N1 S31 H1 V2 LH7	.200
(RDS031)	D	X2 N1 S41 H1 V2 LH7	.200

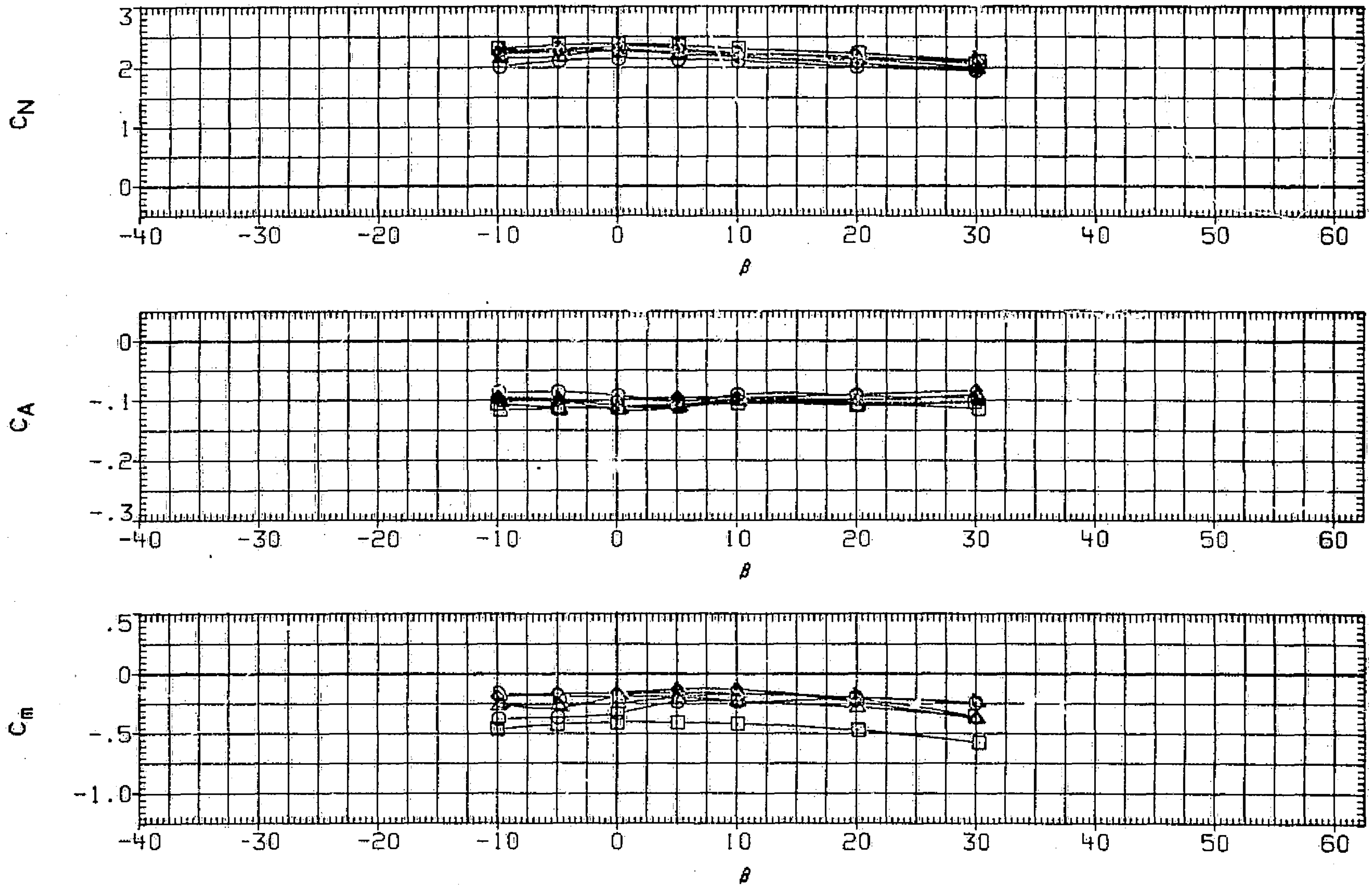

FIG.12 EFFECTS OF VARIOUS STRAKE CONFIGS. ON LONG. AND LAT.-DIRECT. AERO CHARAC.

(C) ALPHA = 60.27

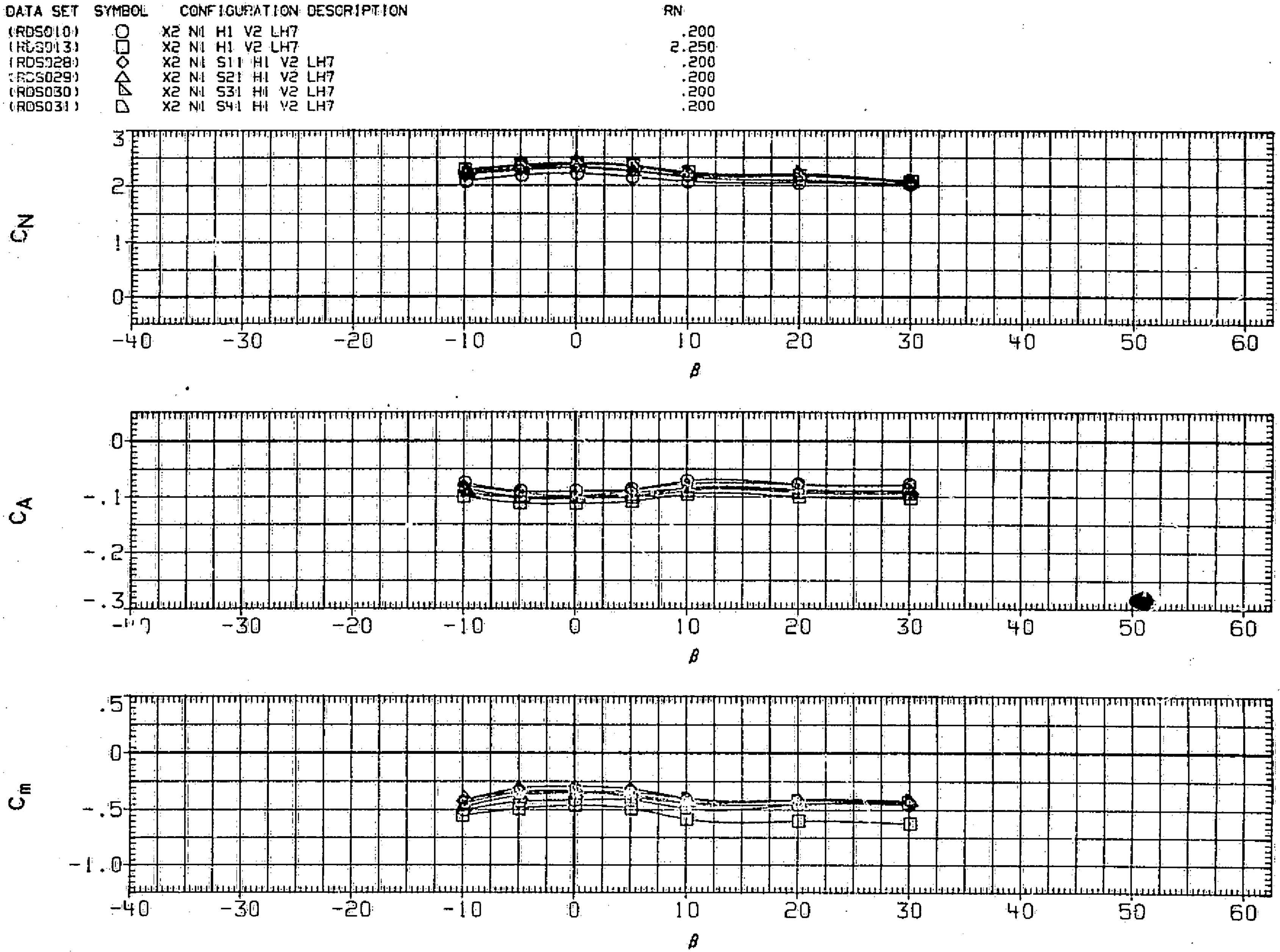

FIG.12 EFFECTS OF VARIOUS STRAKE CONFIGS. ON LONG. AND LAT.-DIRECT. AERO CHARAC.

(D) ALPHA = 70.27

DATA SET	SYMBOL	CONFIGURATION DESCRIPTION	RN
(RDS010)	○	X2 N1 H1 V2 LH7	.200
(RDS013)	□	X2 N1 H1 V2 LH7	2.250
(RDS028)	◇	X2 N1 S11 H1 V2 LH7	.200
(RDS029)	△	X2 N1 S21 H1 V2 LH7	.200
(RDS030)	◺	X2 N1 S31 H1 V2 LH7	.200
(RDS031)	◻	X2 N1 S41 H1 V2 LH7	.200

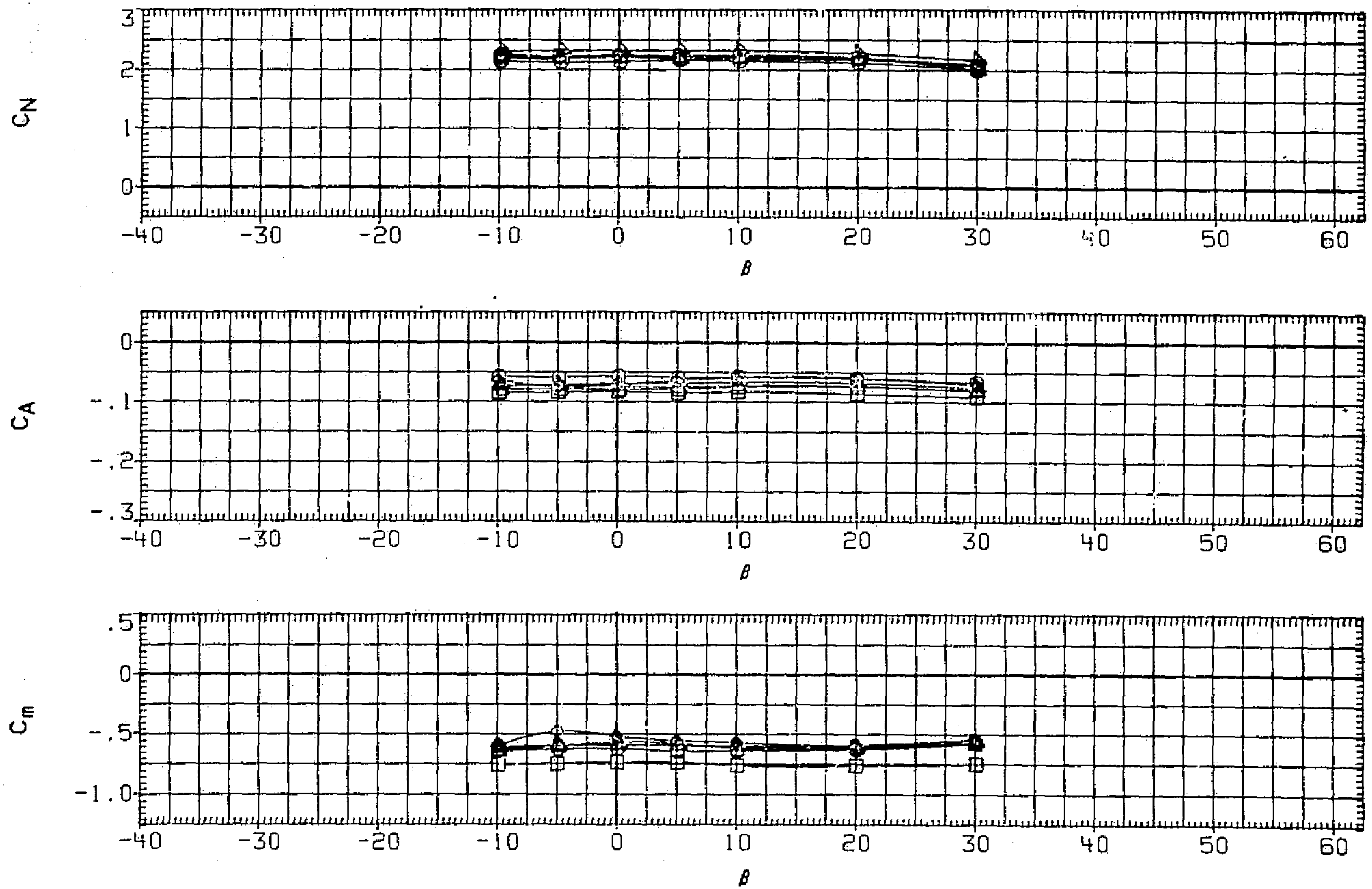

FIG.12 EFFECTS OF VARIOUS STRAKE CONFIGS. ON LONG. AND LAT.-DIRECT. AERO CHARAC.

(E) ALPHA = 80.21

DATA SET	SYMBOL	CONFIGURATION DESCRIPTION	RN
(RDS010)	○	X2 N1 H1 V2 LH7	.200
(RDS013)	□	X2 N1 H1 V2 LH7	2.250
(RDS028)	◇	X2 N1 S11 H1 V2 LH7	.200
(RDS029)	△	X2 N1 S21 H1 V2 LH7	.200
(RDS030)	◺	X2 N1 S31 H1 V2 LH7	.200
(RDS031)	D	X2 N1 S41 H1 V2 LH7	.200

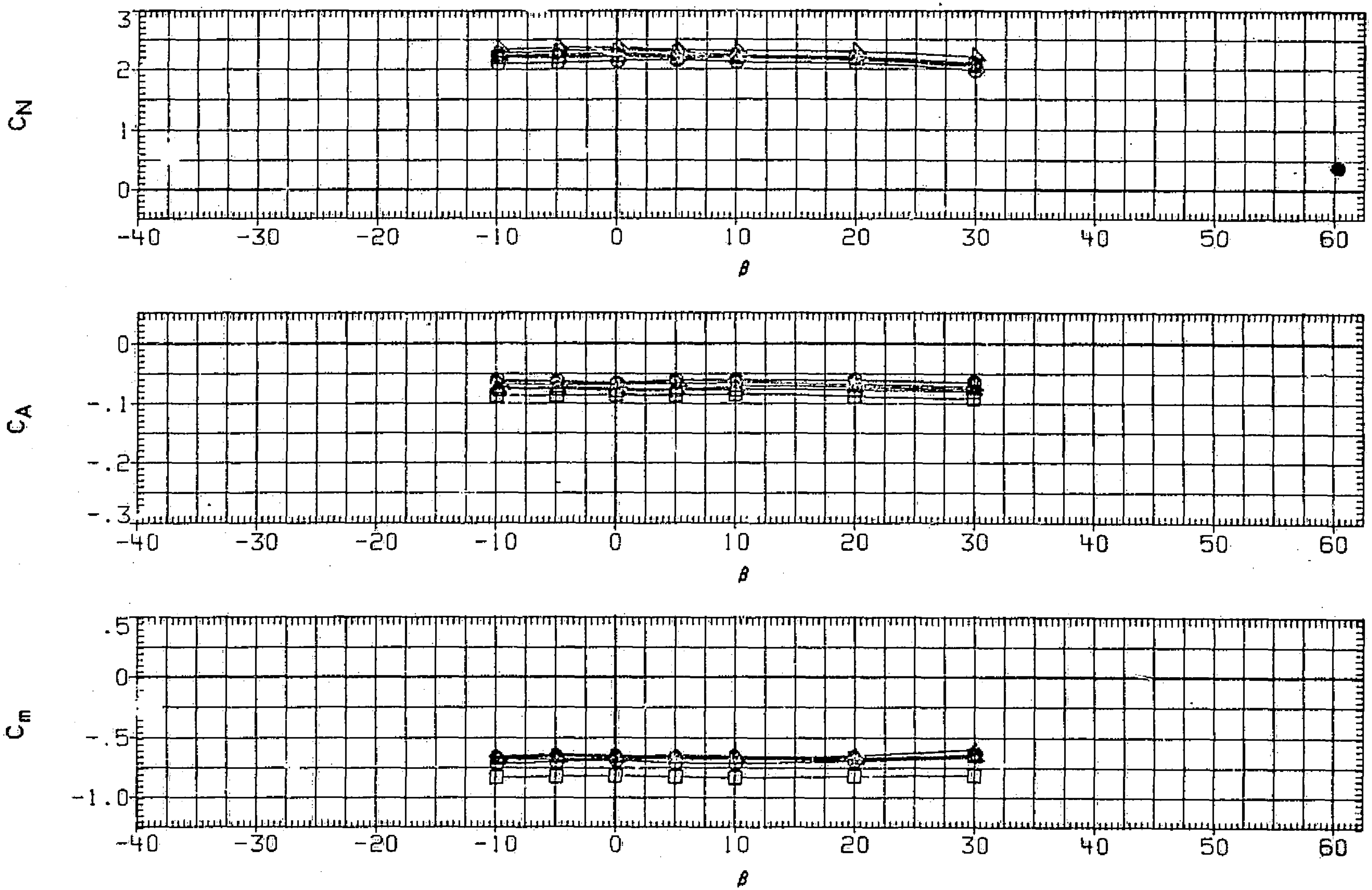

FIG.12 EFFECTS OF VARIOUS STRAKE CONFIGS. ON LONG. AND LAT.-DIRECT. AERO CHARAC.

(F) ALPHA = 89.21

DATA SET	SYMBOL	CONFIGURATION DESCRIPTION	RN
(RDS010)	○	X2 N1 H1 V2 LH7	.200
(RDS013)	□	X2 N1 H1 V2 LH7	2.250
(RDS032)	◇	X2 N1 S51 H1 V2 LH7	.200
(RDS033)	△	X2 N1 S61 H1 V2 LH7	.200
(RDS034)	⊿	X2 N1 S3 H1 V2 LH7	.200
(RDS035)	◺	X2 N1 S4 H1 V2 LH7	.200

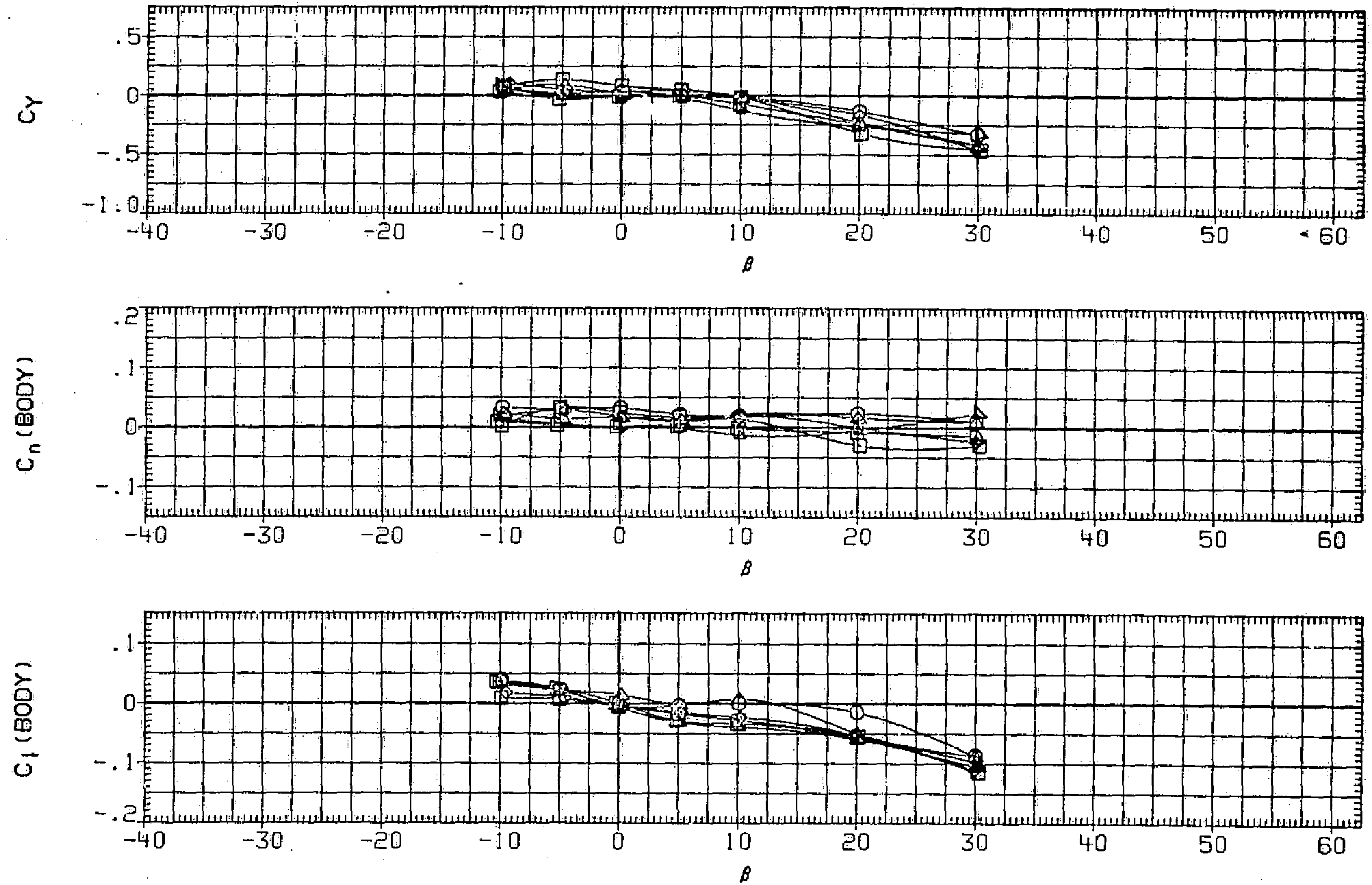

FIG.12 EFFECTS OF VARIOUS STRAKE CONFIGS. ON LONG. AND LAT.-DIRECT. AERO CHARAC.

(A) ALPHA = 40.33

DATA SET	SYMBOL	CONFIGURATION DESCRIPTION	RN
(RDS010)	○	X2 N1 H1 V2 LH7	.200
(RDS013)	□	X2 N1 H1 V2 LH7	2.250
(RDS032)	◇	X2 N1 S51 H1 V2 LH7	.200
(RDS033)	△	X2 N1 S61 H1 V2 LH7	.200
(RDS034)	◺	X2 N1 S3 H1 V2 LH7	.200
(RDS035)	◻	X2 N1 S4 H1 V2 LH7	.200

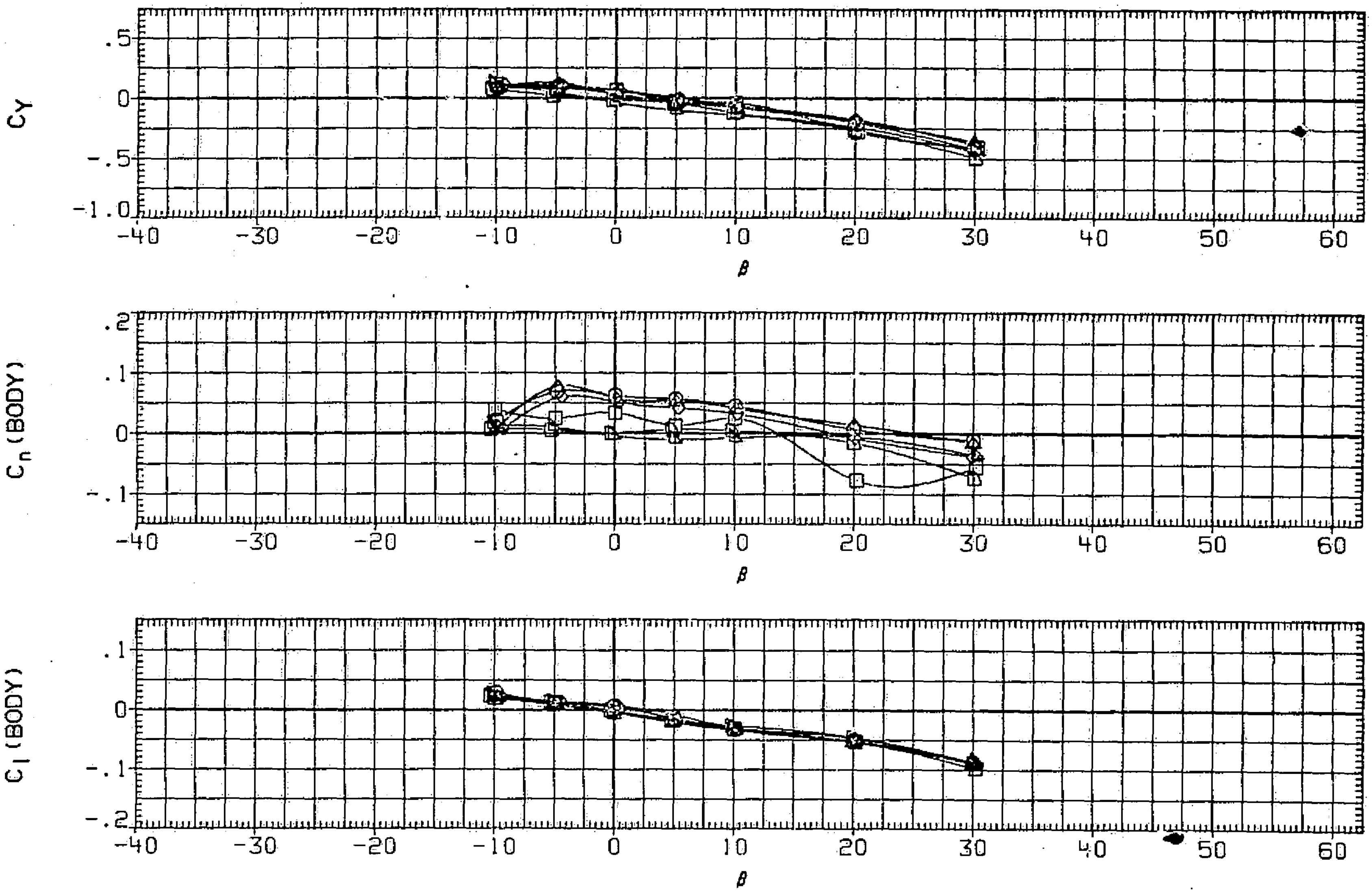

FIG.12 EFFECTS OF VARIOUS STRAKE CONFIGS. ON LONG. AND LAT.-DIRECT. AERO CHARAC.

(B) ALPHA = 50.36

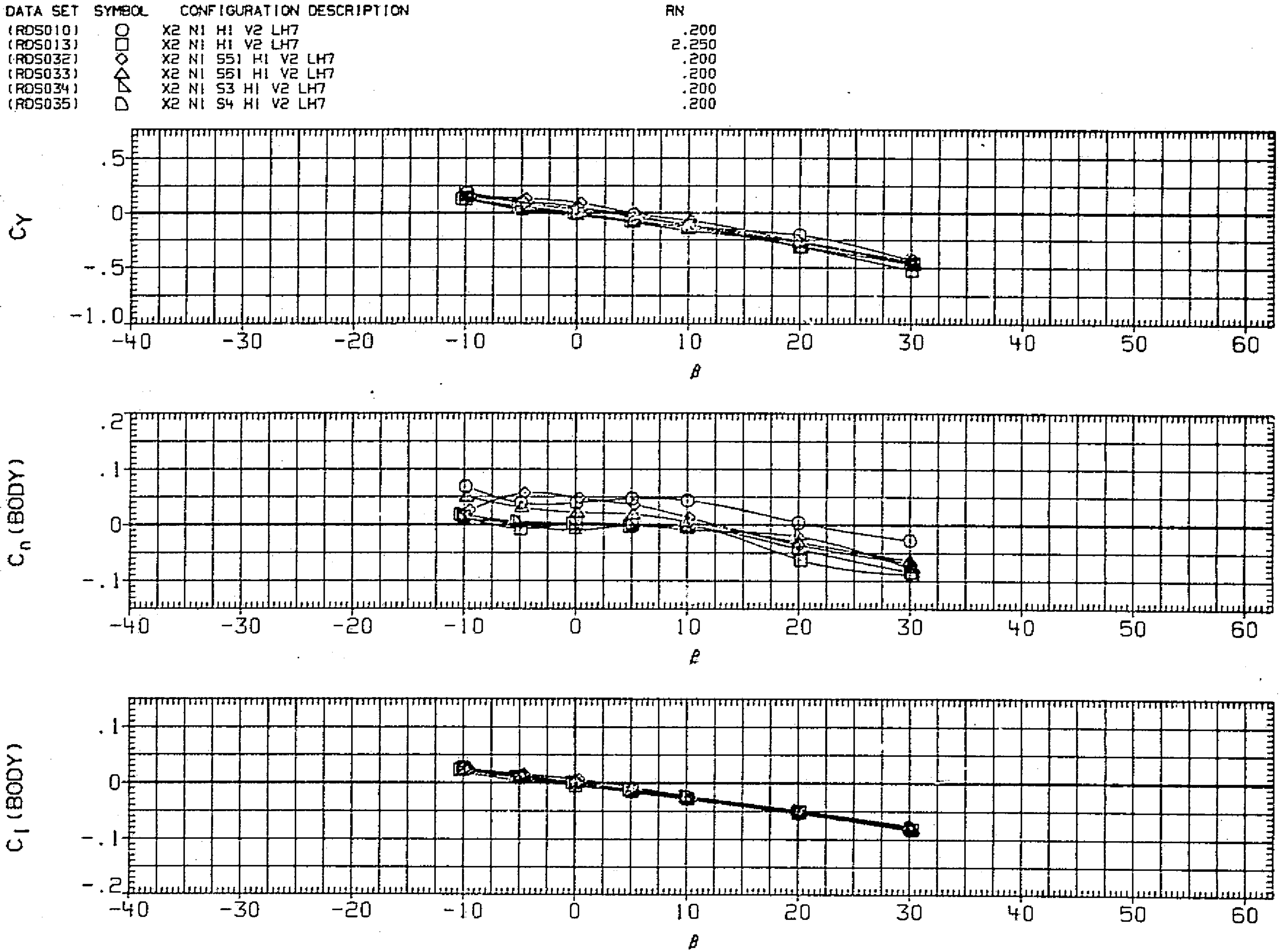

FIG.12 EFFECTS OF VARIOUS STRAKE CONFIGS. ON LONG. AND LAT.-DIRECT. AERO CHARAC.

(C) ALPHA = 60.27

DATA SET	SYMBOL	CONFIGURATION DESCRIPTION	RN
(RDS010)	○	X2 N1 H1 V2 LH7	.200
(RDS013)	□	X2 N1 H1 V2 LH7	2.250
(RDS032)	◇	X2 N1 S51 H1 V2 LH7	.200
(RDS033)	△	X2 N1 S61 H1 V2 LH7	.200
(RDS034)	◺	X2 N1 S3 H1 V2 LH7	.200
(RDS035)	◻	X2 N1 S4 H1 V2 LH7	.200

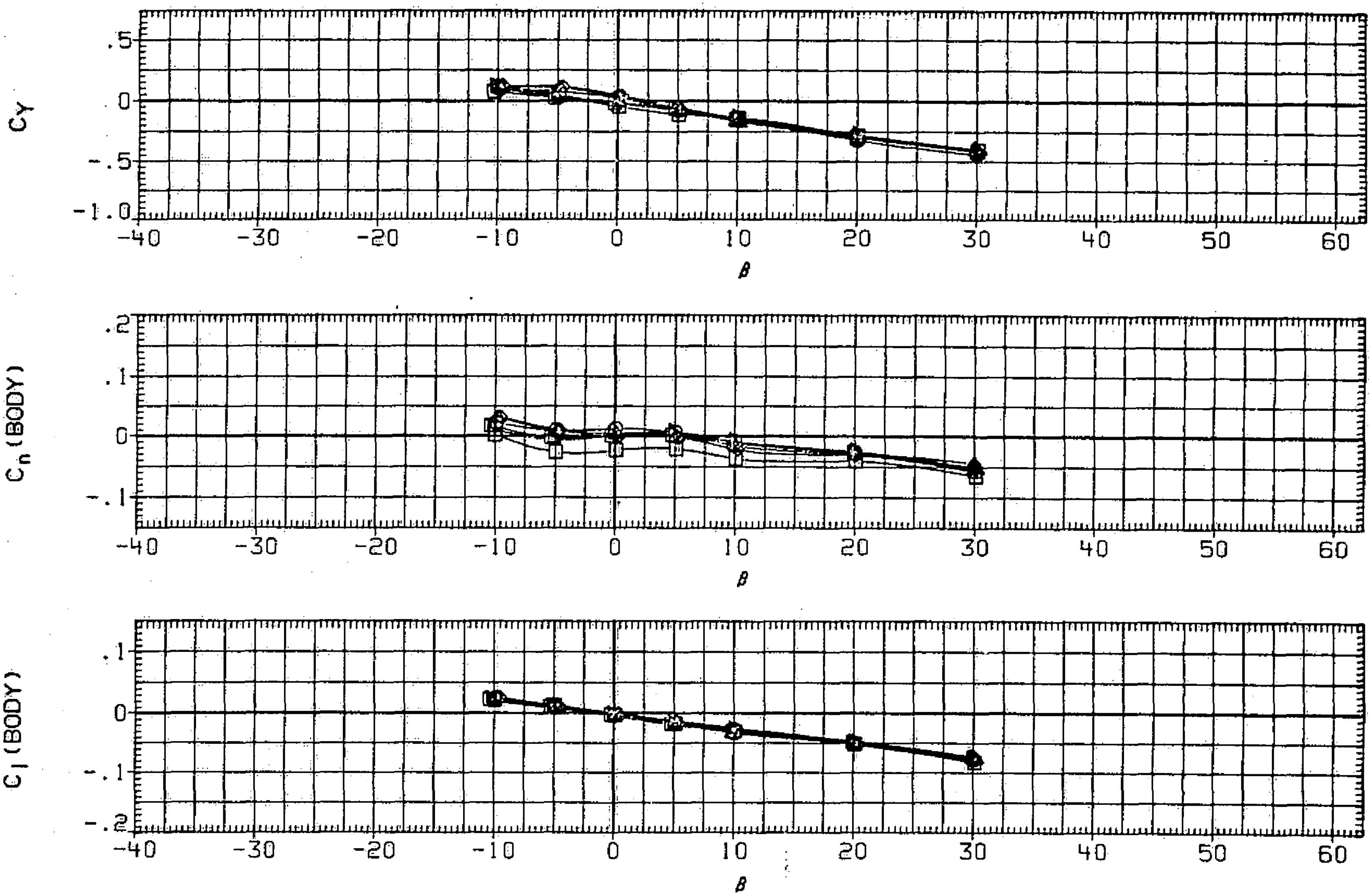

FIG.12 EFFECTS OF VARIOUS STRAKE CONFIGS. ON LONG. AND LAT.-DIRECT. AERO CHARAC.

(D) ALPHA = 70.27

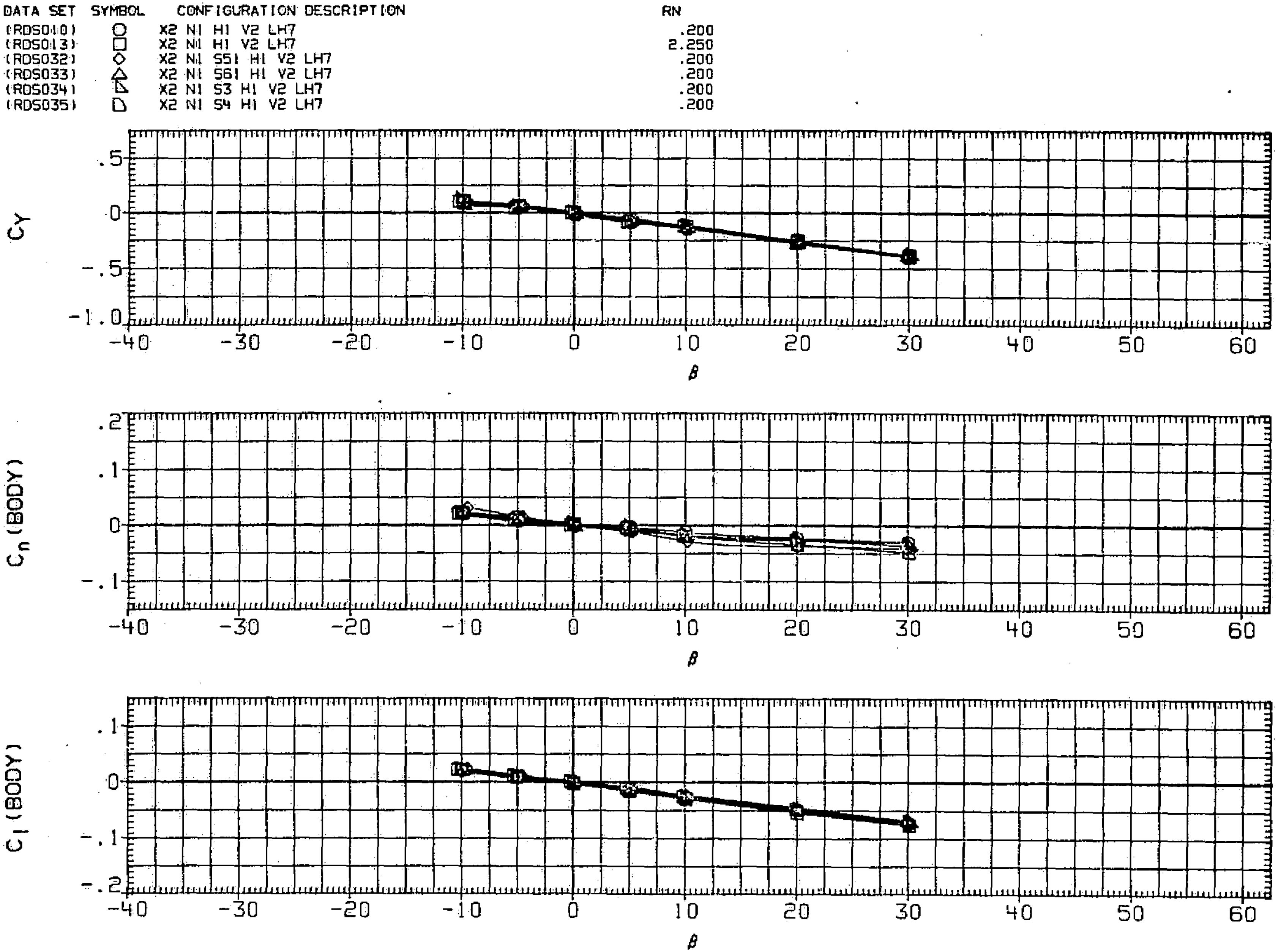

FIG.12 EFFECTS OF VARIOUS STRAKE CONFIGS. ON LONG. AND LAT.-DIRECT. AERO CHARAC.

(E) ALPHA = 80.21

DATA SET	SYMBOL	CONFIGURATION DESCRIPTION	RN
(RDS010)	○	X2 N1 H1 V2 LH7	.200
(RDS013)	□	X2 N1 H1 V2 LH7	2.250
(RDS032)	◇	X2 N1 S51 H1 V2 LH7	.200
(RDS033)	△	X2 N1 S61 H1 V2 LH7	.200
(RDS034)	◺	X2 N1 S3 H1 V2 LH7	.200
(RDS035)	D	X2 N1 S4 H1 V2 LH7	.200

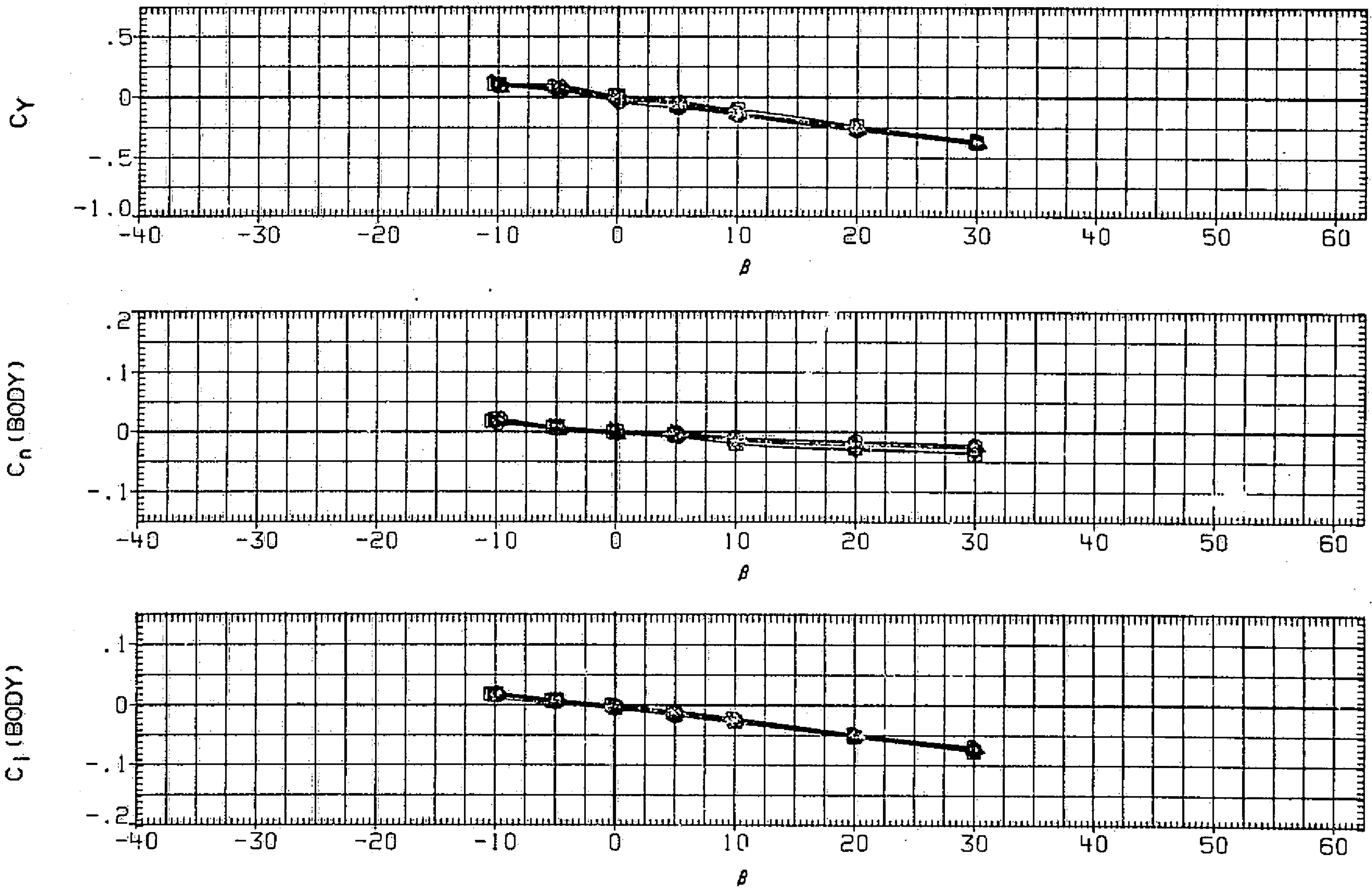

FIG.12 EFFECTS OF VARIOUS STRAKE CONFIGS. ON LONG. AND LAT.-DIRECT. AERO CHARAC.

(F) ALPHA = 89.21

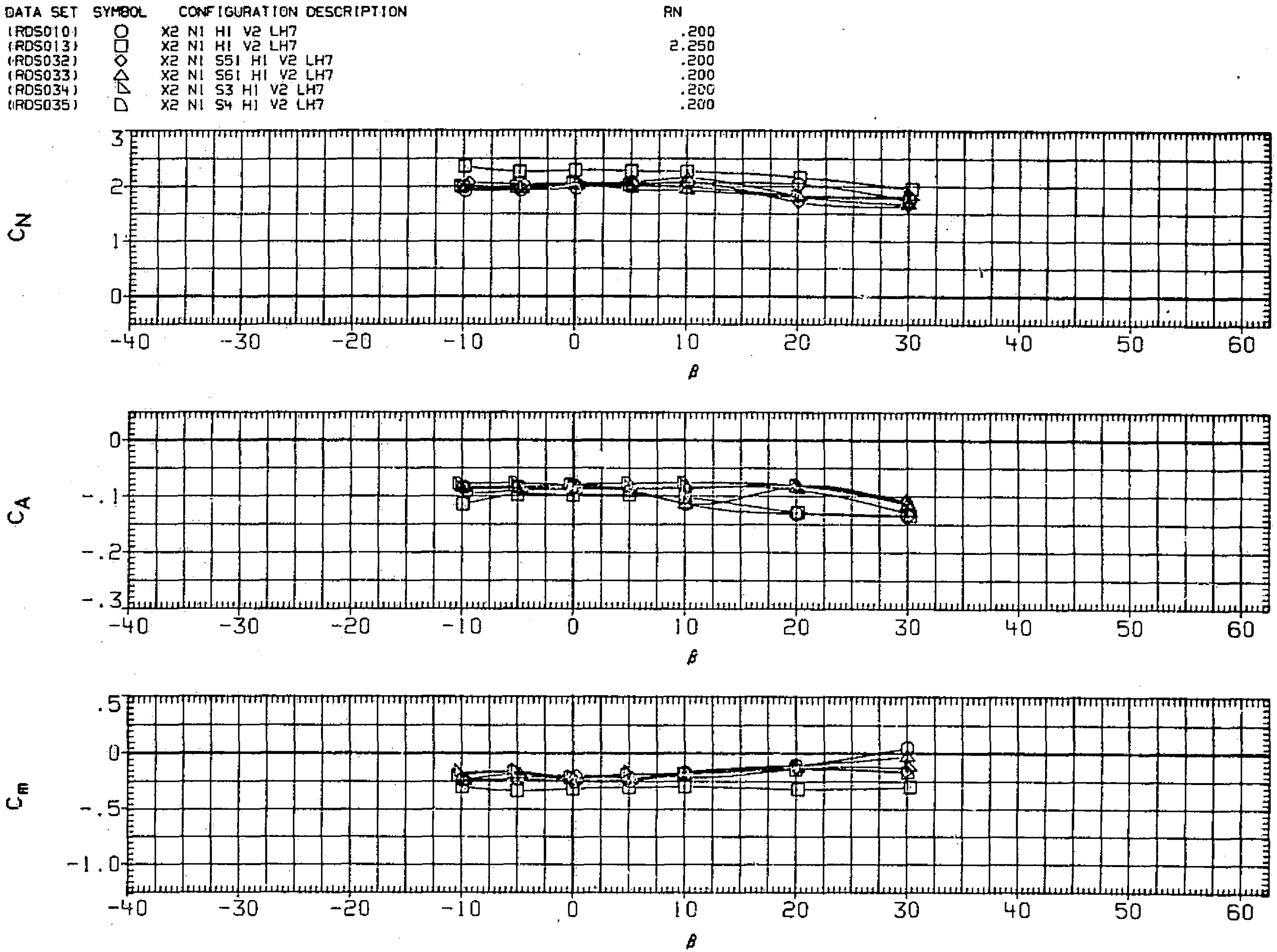

FIG.12 EFFECTS OF VARIOUS STRAKE CONFIGS. ON LONG. AND LAT.-DIRECT. AERO CHARAC.

(A) ALPHA = 40.33

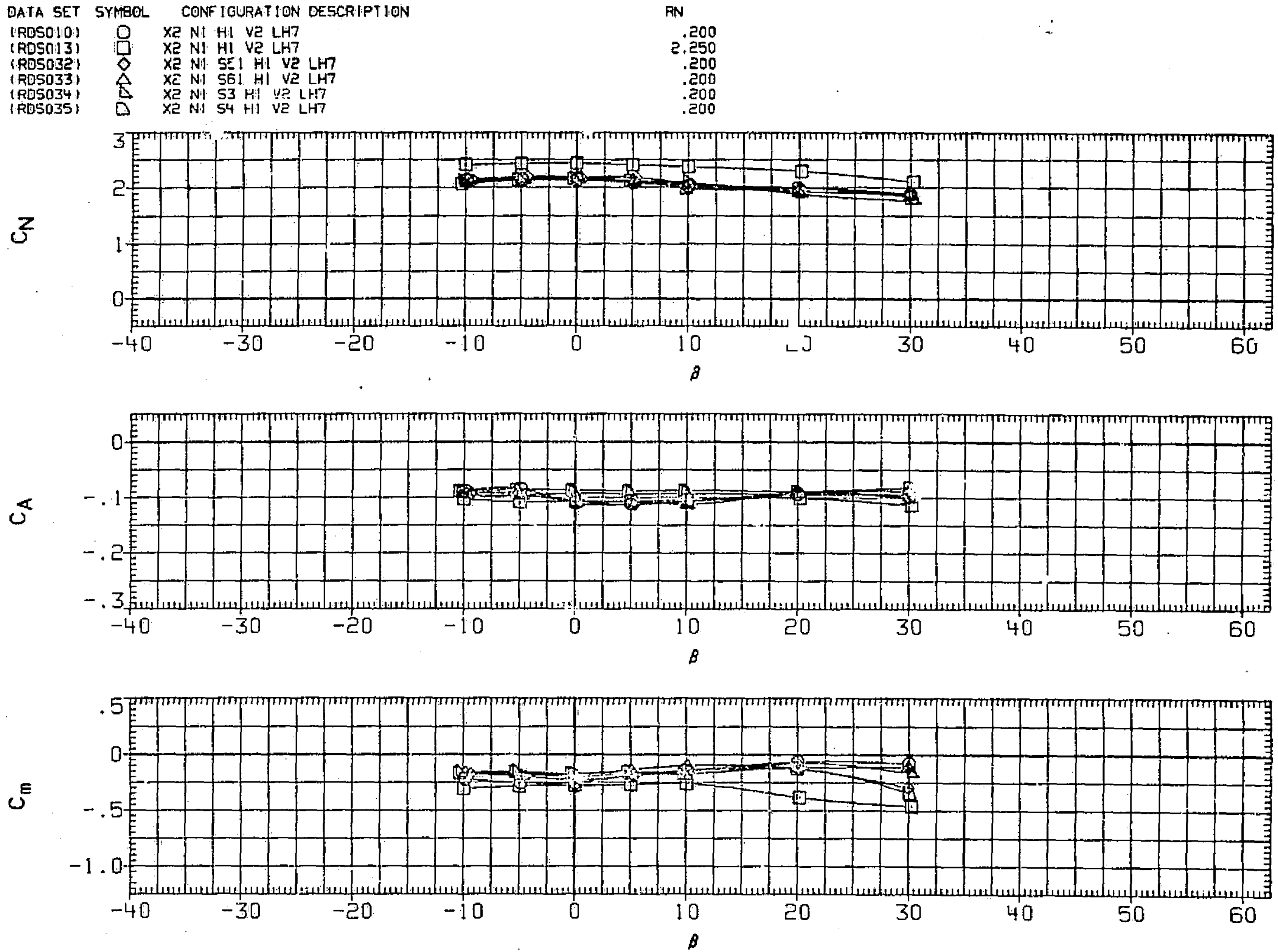

FIG.12 EFFECTS OF VARIOUS STRAKE CONFIGS. ON LONG. AND LAT.-DIRECT. AERO CHARAC.

(B) ALPHA = 50.36

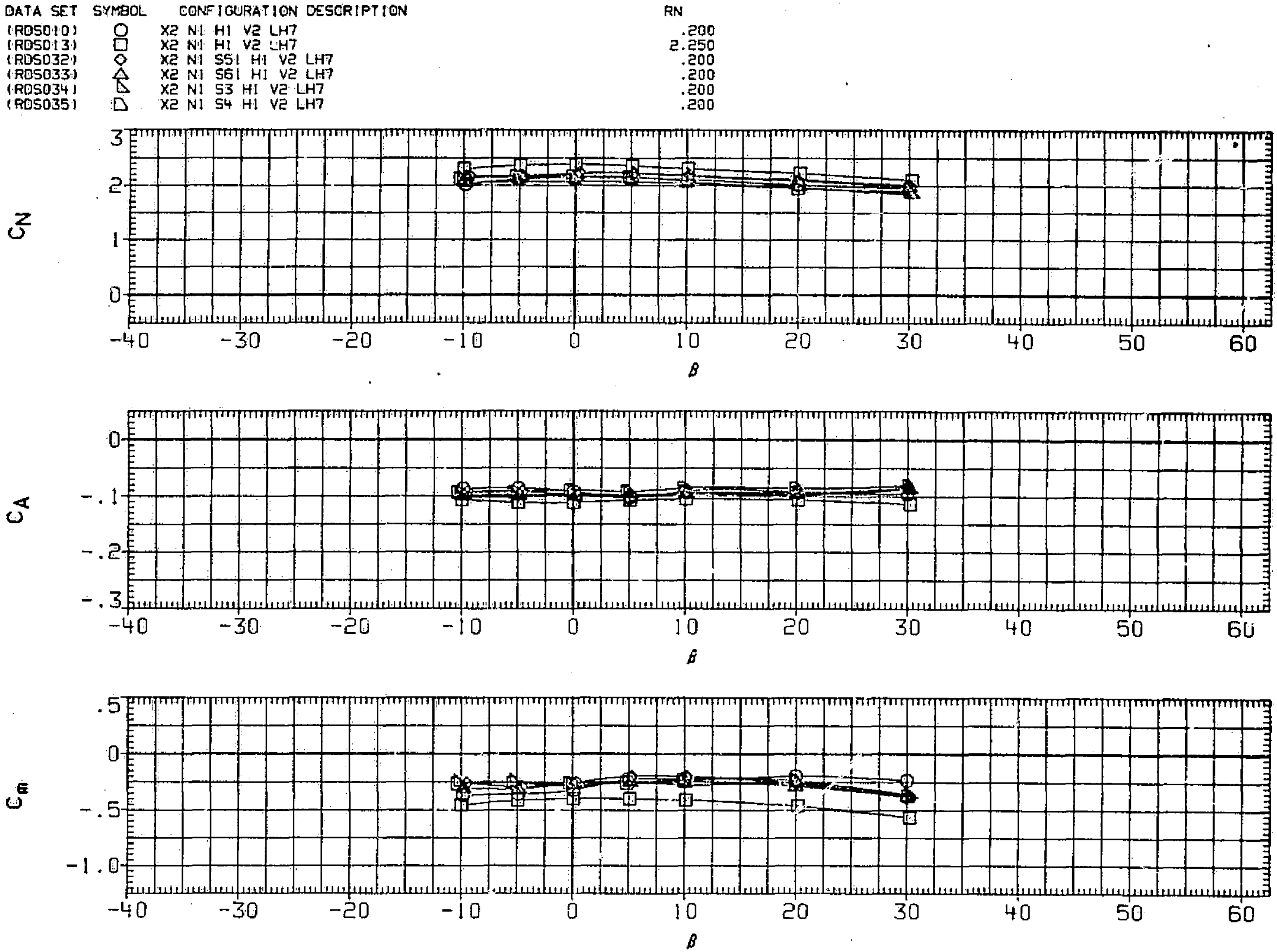

FIG.12 EFFECTS OF VARIOUS STRAKE CONFIGS. ON LONG. AND LAT.-DIRECT. AERO CHARAC.

(C) ALPHA = 60.27

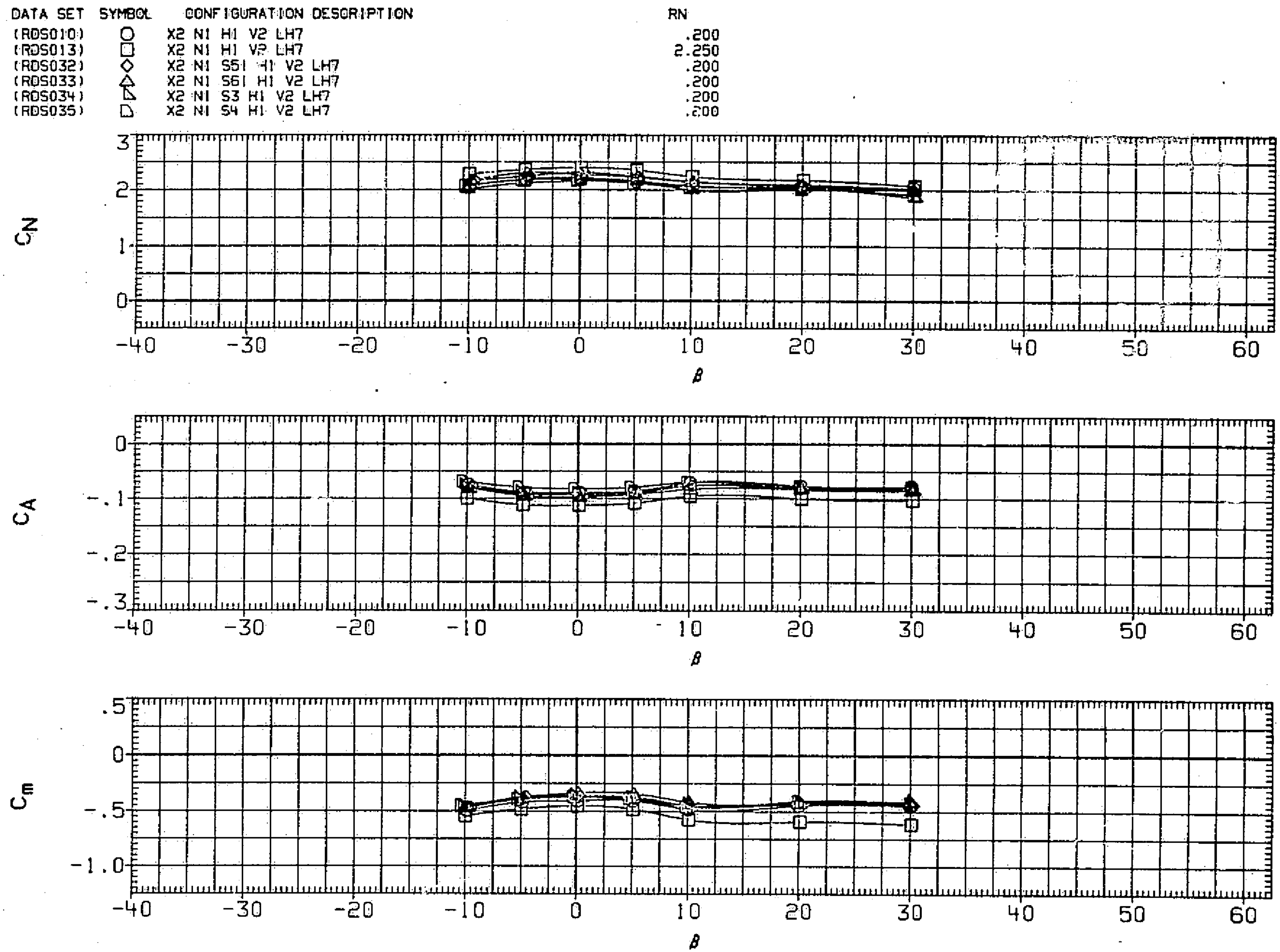

FIG.12 EFFECTS OF VARIOUS STRAKE CONFIGS. ON LONG. AND LAT.-DIRECT. AERO CHARAC.

(D) ALPHA = 70.27

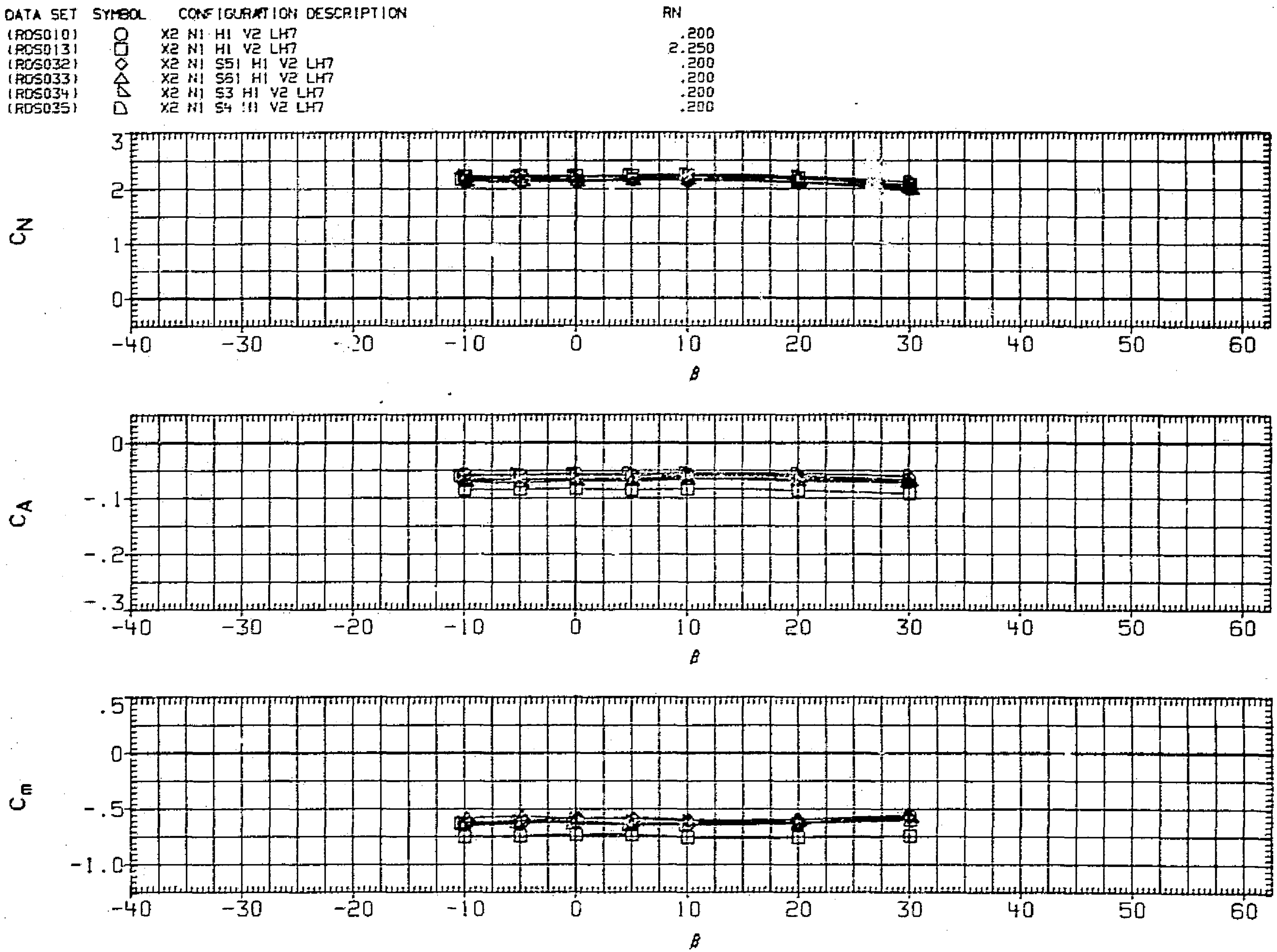

FIG.12 EFFECTS OF VARIOUS STRAKE CONFIGS. ON LONG. AND LAT.-DIRECT. AERO CHARAC.

(E) ALPHA = 80.21

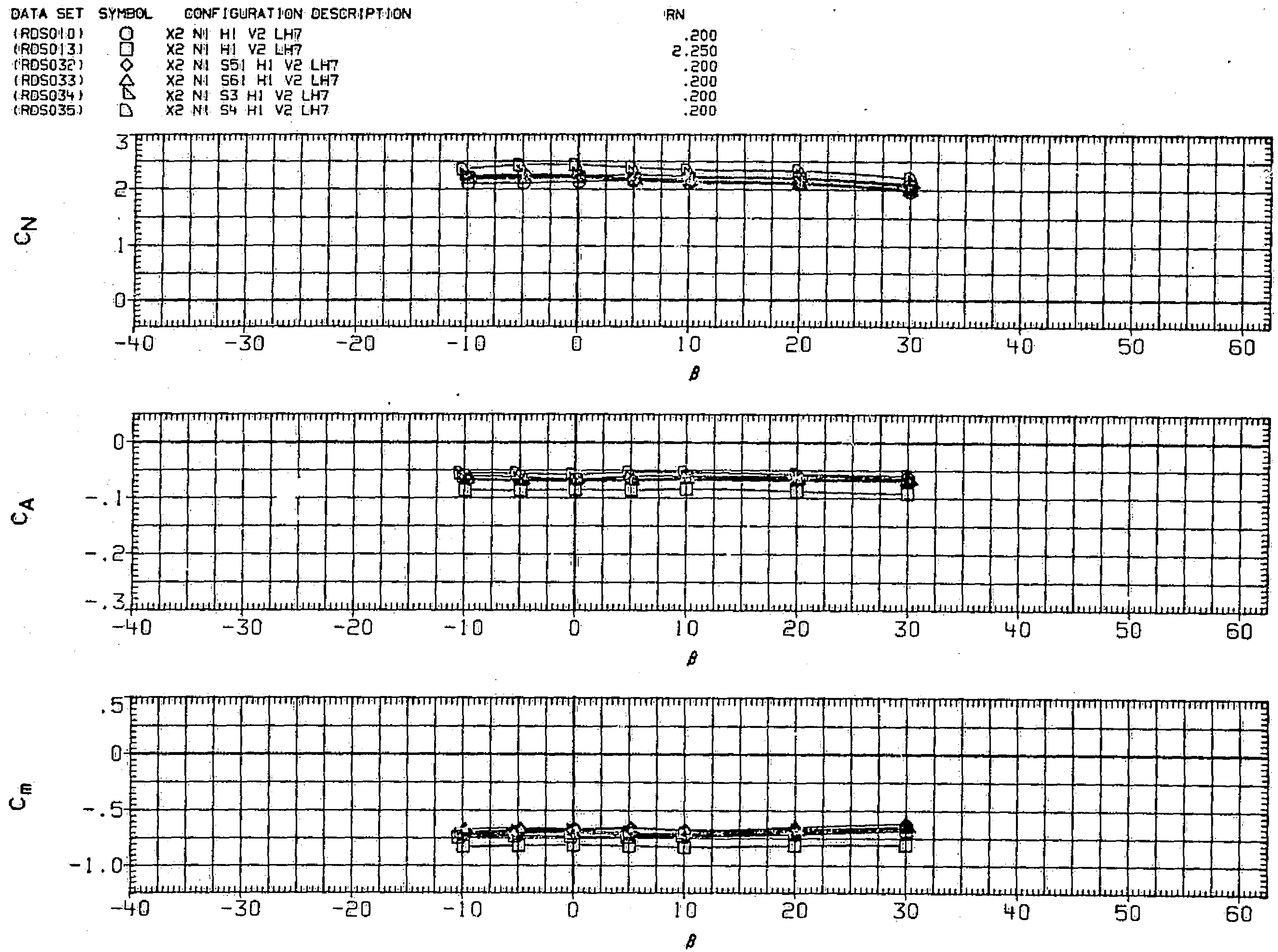

FIG. 12 EFFECTS OF VARIOUS STRAKE CONFIGS. ON LONG. AND LAT.-DIRECT. AERO CHARAC.

(F) ALPHA = 89.21

DATA SET	SYMBOL	CONFIGURATION DESCRIPTION	AIL-L	HOR-L	HOR-R	RN
(DDS049)	○	X1 N3 H1 V2 LH7	.000	.000	.000	.300
(DDS054)	□	X1 N3 H1 V2 LH7	.000	.000	.000	2.250
(RDS066)	◇	X3 N3 I1 S1 H1 V2 LH7	.000	-5.000	-15.000	.300
(DDS068)	△	X3 N3 I1 S1 H1 V2 LH7	.000	-5.000	-15.000	2.250
(RDS090)	◺	X3 N3 I1 S1 A1 H1 V2 LH7	30.000	-5.000	-15.000	.300
(RDS091)	D	X3 N3 I1 S1 A1 H1 V2 LH7	30.000	-5.000	-15.000	2.250

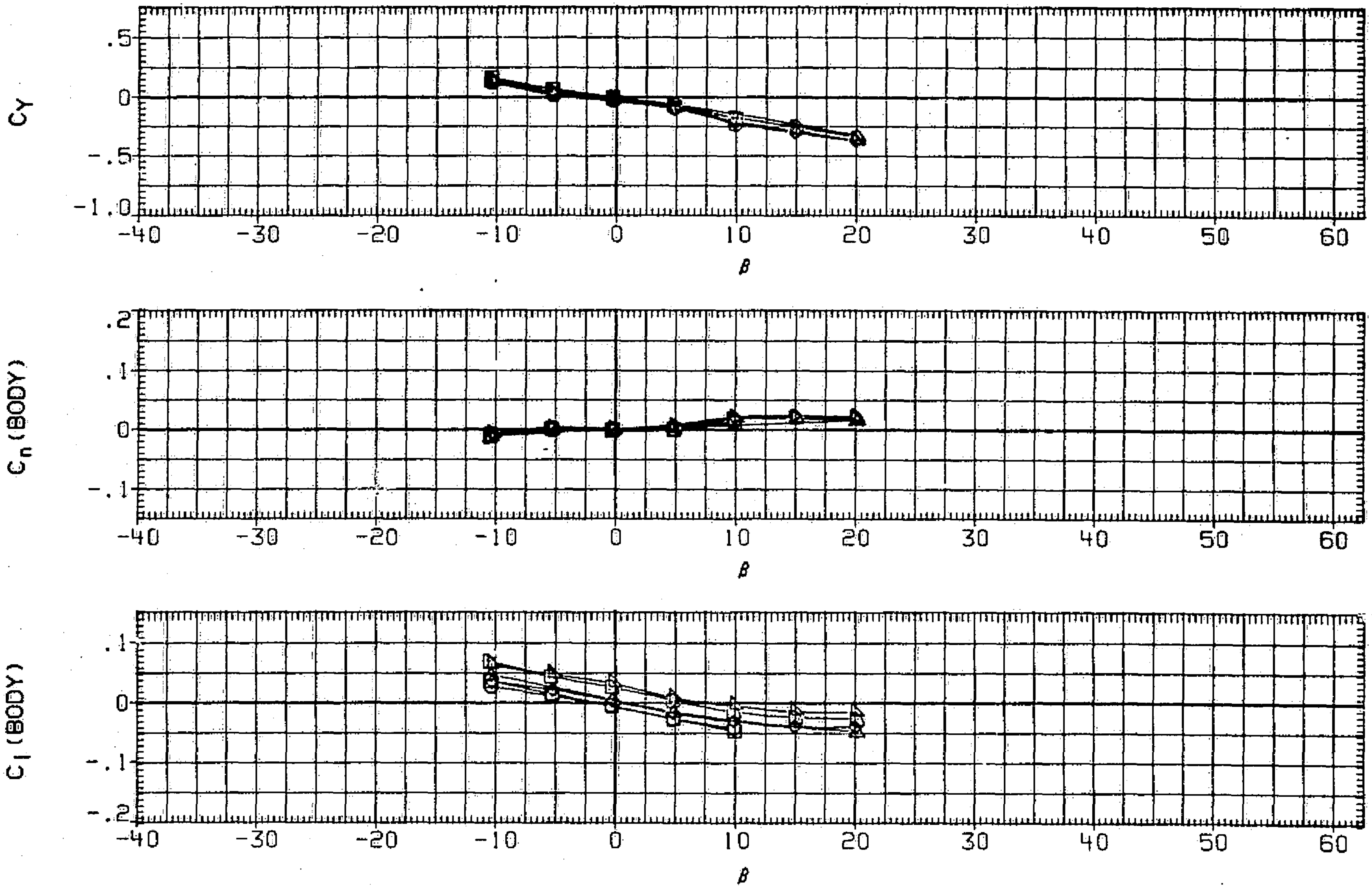

FIG.13 CONTROL DEFLEC. AND REY. NO. EFFECTS ON LAT.-DIR. AERO CHAR.,AIL-R=-AIL-L

(A) ALPHA = 20.27

DATA SET	SYMBOL	CONFIGURATION DESCRIPTION	AIL-L	HOR-L	HOR-R	RN
(RDS087)	○	X3 N3 I1 S1 A1 H1 V2 LH7	30.000	-10.000	-10.000	.300
(DDS089)	□	X3 N3 I1 S1 A1 H1 V2 LH7	30.000	-10.000	-10.000	2.250
(RDS084)	◇	X3 N3 I1 S1 A1 H1 V2 LH7	-30.000	-10.000	-10.000	.300
(DDS086)	△	X3 N3 I1 S1 A1 H1 V2 LH7	-30.000	-10.000	-10.000	2.250

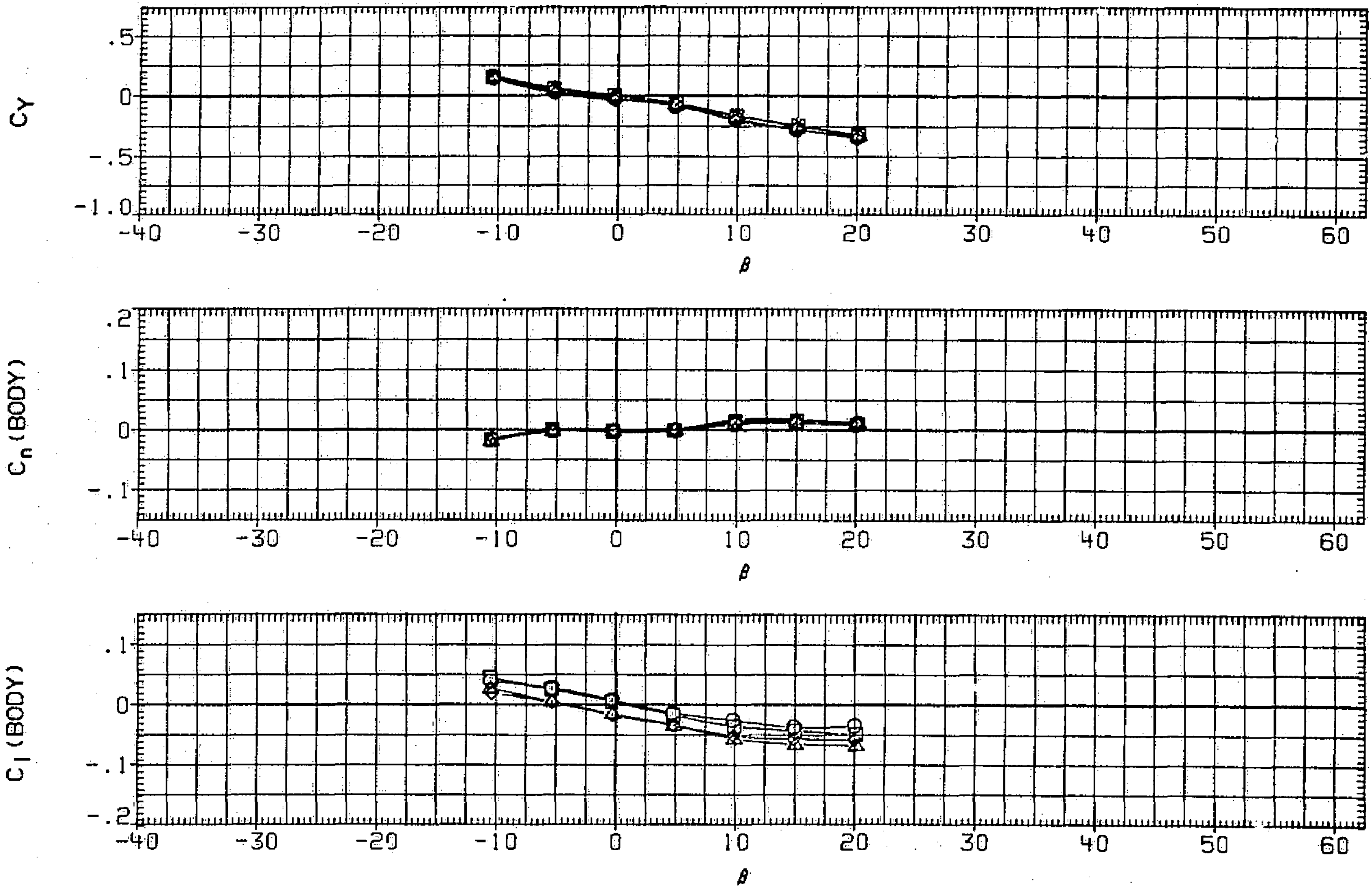

FIG.13 CONTROL DEFLEC. AND REY. NO. EFFECTS ON LAT.-DIR. AERO CHAR., AIL-R=0.0

(A) ALPHA = 20.36

DATA SET	SYMBOL	CONFIGURATION DESCRIPTION	AIL-L	HOR-L	HOR-R	RN
(DDS010)	○	X2 N1 H1 V2 LH7	.000	.000	.000	.200
(DDS013)	□	X2 N1 H1 V2 LH7	.000	.000	.000	2.250
(RDS019)	◇	X2 N1 A1 H1 V2 LH7	30.000	-5.000	-15.000	.200
(RDS020)	△	X2 N1 A1 H1 V2 LH7	30.000	-5.000	-15.000	2.250

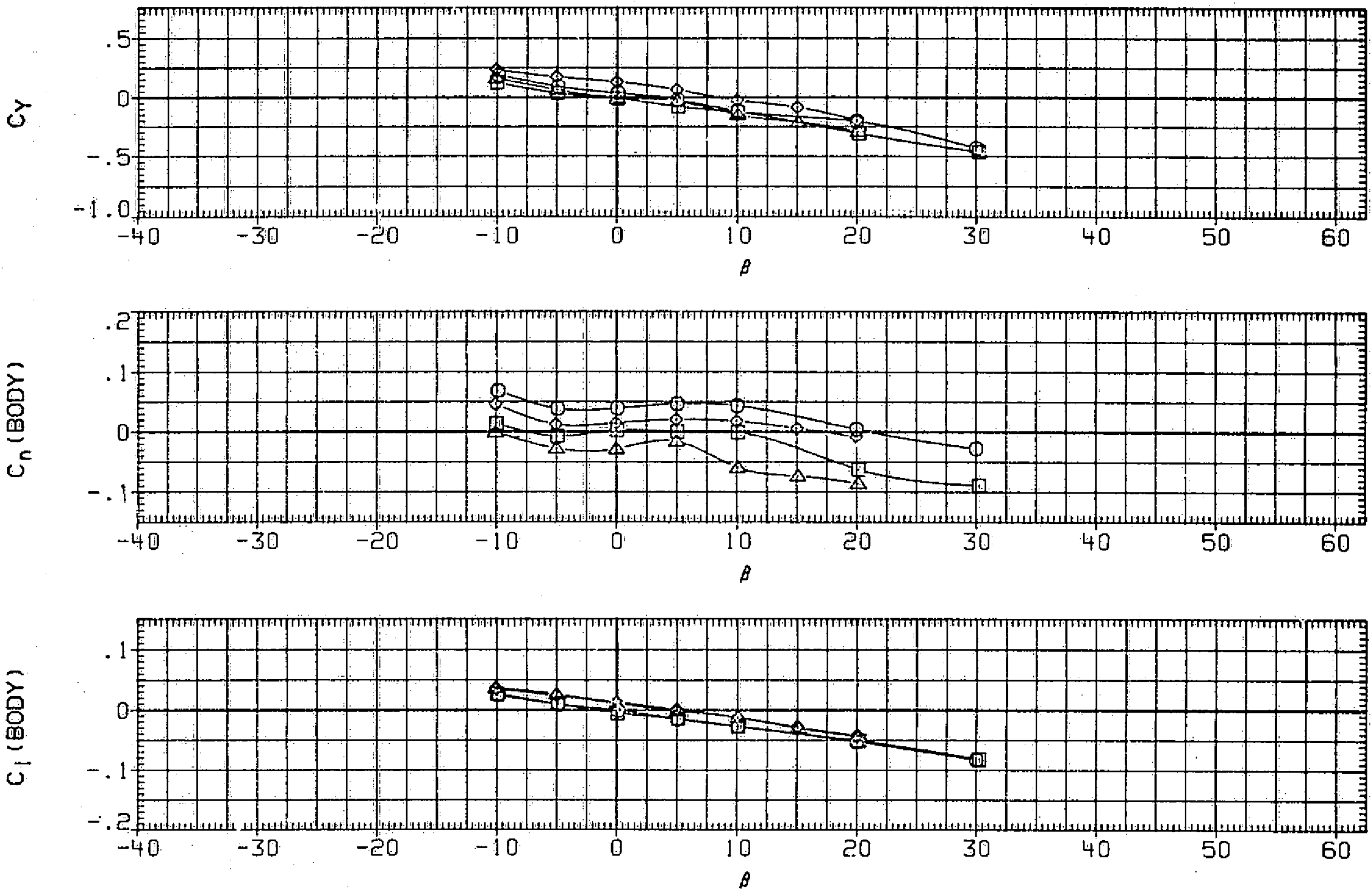

FIG.13 CONTROL DEFLEC. AND REY. NO. EFFECTS ON LAT.-DIR. AERO CHAR.,AIL-R=-AIL-L

(A)ALPHA = 60.27

DATA SET	SYMBOL	CONFIGURATION DESCRIPTION	HOR-L	HOR-R	RN
(RDSP49)	○	A H1 V2 LH7 (A=X1 N3,ALPHA=20. A=X2 N1,ALPHA=60)	.000	.000	.300
(RDSP54)	□	A H1 V2 LH7 (A=X1 N3,ALPHA=20. A=X2 N1,ALPHA=60)	.000	.000	2.250
(RDSP76)	◇	A11S1H1V2LH7 (A=X3N3,ALPHA=20. A=X1N1,ALPHA=60)	-15.000	-15.000	2.250
(RDS074)	△	X3 N3 I1 S1 H1 V2 LH7	-15.000	-15.000	.300
(RDS026)	◺	X1 N1 I1 S1 H1 V2 LH7	-15.000	-15.000	.200

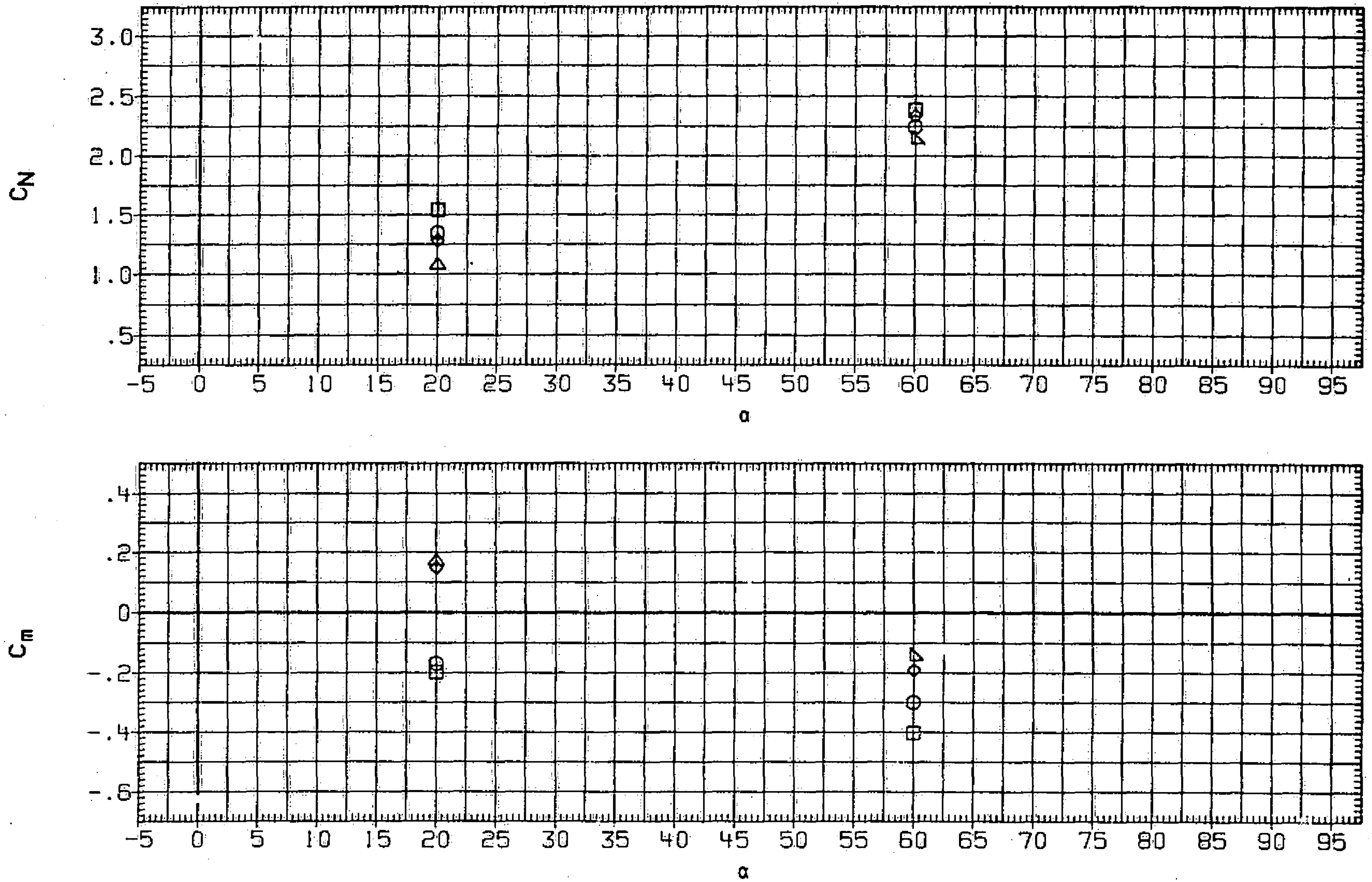

FIG.14 CONTROL DEFLEC. AND REY. NO. EFFECTS ON LONG. AERO CHAR.,AIL-R=AIL-L=0

(A)BETA = .00

DATA SET	SYMBOL	CONFIGURATION DESCRIPTION	HOR-L	HOR-R	RN
(RDSP49)	○	A H1 V2 LH7 (A=X1 N3,ALPHA=20, A=X2 N1,ALPHA=60)	.000	.000	.300
(RDSP54)	□	A H1 V2 LH7 (A=X1 N3,ALPHA=20, A=X2 N1,ALPHA=60)	.000	.000	2.250
(RDSP76)	◇	A1IS1H1V2LH7 (A=X3N3,ALPHA=20, A=X1N1,ALPHA=60)	-15.000	-15.000	2.250
(RDSQ74)	△	X3 N3 I1 S1 H1 V2 LH7	-15.000	-15.000	.300
(RDSQ26)	◺	X1 N1 I1 S1 H1 V2 LH7	-15.000	-15.000	.200

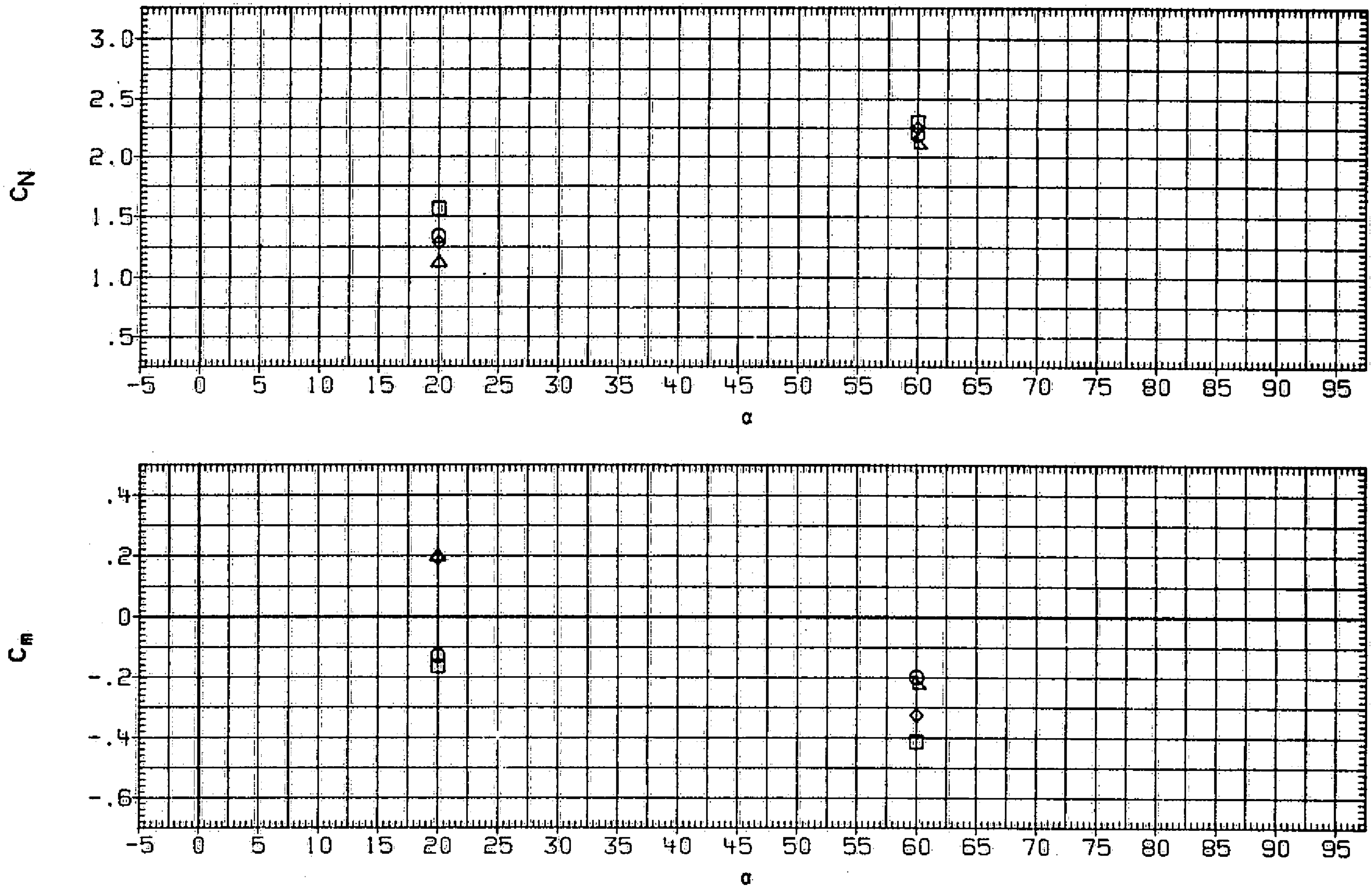

FIG.14 CONTROL DEFLEC. AND REY. NO. EFFECTS ON LONG. AERO CHAR.,AIL-R=AIL-L=0

(B)BETA = 10.00

1. Report No. NASA TM-78438	2. Government Accession No.	3. Recipient's Catalog No.
4. Title and Subtitle LOW-SPEED AERODYNAMIC CHARACTERISTICS OF A 0.08-SCALE YF-17 AIRPLANE MODEL AT HIGH ANGLES OF ATTACK AND SIDESLIP		5. Report Date
		6. Performing Organization Code
7. Author(s) Daniel N. Petroff, Stanley H. Scher, and Carl E. Sutton*		8. Performing Organization Report No. A-7214
		10. Work Unit No. 760-17-01
9. Performing Organization Name and Address NASA Ames Research Center Moffett Field, Calif. 94035		11. Contract or Grant No.
		13. Type of Report and Period Covered Technical Memorandum
12. Sponsoring Agency Name and Address National Aeronautics and Space Administration Washington, D.C. 20546		14. Sponsoring Agency Code

15. Supplementary Notes

*ARO, Inc., Moffett Field, Calif. 94035

16. Abstract

A 0.08-scale model of the YF-17 airplane was tested in the Ames 12-Foot Pressure Wind Tunnel at a Mach number of 0.2 and at Reynolds numbers of 0.2 to 2.3 million based on a fuselage forebody depth of 0.128 m (0.42 ft). Angles of attack ranged from 0° to 90°; the angle of sideslip ranged from -10° to 30°. Data were obtained with and without the nose boom and with several strake configurations; also, data were obtained for various control surface deflections.

Analysis of the results revealed that selected strake configurations adequately provided low Reynolds number simulation of the high Reynolds number characteristics. The addition of the boom in general tended to reduce the Reynolds number effects.

17. Key Words (Suggested by Author(s))		18. Distribution Statement	
Static stability High angle of attack Stall characteristics High Reynolds number		Unlimited STAR Category -02	
19. Security Classif. (of this report) Unclassified	20. Security Classif. (of this page) Unclassified	21. No. of Pages 118	22. Price* $5.50

*For sale by the National Technical Information Service, Springfield, Virginia 22161